



TECHNISCHE UNIVERSITÄT MÜNCHEN  
TUM School of Engineering and Design

**Biological H<sub>2</sub>/CO<sub>2</sub> Methanation in Trickle Bed Reactors –  
Toward Industrial Application**

**Carolina Feickert Fenske**

Vollständiger Abdruck der von der TUM School of Engineering and Design der  
Technischen Universität München zur Erlangung einer

**Doktorin der Ingenieurwissenschaften**

**-Dr.-Ing.-**

genehmigten Dissertation.

*Vorsitz:* apl. Prof. Dr. rer. nat. habil. Brigitte Helmreich

*Prüfer\*innen der Dissertation:*

1. Priv.-Doz. Dr.-Ing. habil. Konrad Koch
2. Prof. Dr. Lars Ottosen
3. Assoc. Prof. Dr. Marika Kokko

Die Dissertation wurde am 23.05.2023 bei der Technischen Universität München  
eingereicht und durch die TUM School of Engineering and Design am 26.09.2023  
angenommen.

## Abstract

The current energy crises caused by the geopolitical dependency on fossil fuels and the climate crises based on increasing greenhouse gas emissions demonstrate the importance of the energy transition based on renewable energy sources. Flexible and long-term energy storage technologies are required to ensure a sustainable and secure power supply based on a high share of volatile renewables. A promising approach is the biological conversion of H<sub>2</sub> and CO<sub>2</sub> into storable CH<sub>4</sub> in trickle bed reactors. Research in trickle bed reactor design and operation increased remarkably in recent years, resulting in a high number of publications. The efficient and on-demand operation could already be proved but was mostly limited on a laboratory scale and sterile conditions. Reactor upscaling and implementation at real application conditions are necessary to assess the potential of trickle bed reactors as energy conversion and storage technology. Therefore, a pilot-scale trickle bed reactor with a reactor volume of 1.2 m<sup>3</sup> was installed at the wastewater treatment plant Garching.

The methanation performance in trickle bed reactors can be improved by approaching the gas flow through the reactor toward plug flow. A gas flow through the reactor approaching plug flow increases the initial feed gas partial pressure and reduces the risk that the feed gases leave the reactor before being converted into CH<sub>4</sub>. Therefore, preliminary gas flow experiments with a step input tracer test were performed before reactor startup to identify reactor design properties and operational conditions that support a gas flow toward plug flow. An important finding of the preliminary gas flow experiments was that the feed gases of H<sub>2</sub> and a CO<sub>2</sub> source were flowing as a gas mixture through the reactor with mutual gas properties. An improved gas flow approaching plug flow was observed when the feed gases were introduced from top-to-bottom and when no trickling was applied. A breakthrough of the gases in the bottom-to-top gas flow direction indicated a channeling or bypass effect. The most evident explanation are gas density differences. While a breakthrough of feed gases is more likely when biological conversion activity is limited, a top-to-bottom gas flow direction is recommended to reduce the risk of a breakthrough. Next to the gas flow conditions, the experiments highlighted a share of stagnant volumes of 19%, while 81% of the entire gas volume was actively flown through.

Aiming for a proof of concept, the pilot-scale trickle bed reactor was inoculated and operated for nearly 450 days, including two extended standby periods. Biogas was used as CO<sub>2</sub> source, which already contained a significant CH<sub>4</sub> content of 63% ± 1% and thus shortened the gas residence time. A constantly decreasing pH level due to volatile fatty

acid accumulation was challenging for a stable methanation performance. When too low pH levels were reached, the methanation process broke down. The volatile fatty acid formation can be explained by  $H_2$  and  $CO_2$  conversion into acetic acid through the homoacetogenesis pathway, organic material degradation, and biomass decay. However, no effect on the pH level is expected if the process liquid buffer capacity is high enough. In contrast, the process liquid dilution with metabolic water constantly decreases the buffer capacity of the process liquid. The most successful pH control strategy was to increase the buffer capacity by adding digester supernatant to maintain an  $NH_4^+$  concentration of over 400 mg/L. During stable methanation, the biogas  $H_2S$  concentration of about 200 ppm was reduced by half, but with increasing gas loads, an artificial sulfur source was required to satisfy the sulfur demand of the methanogens completely. After process optimizations, long-term biogas upgrading with a gas load of  $42.7 \text{ m}^3/(\text{m}^3_{RV}\cdot\text{d})$  resulted in a  $CH_4$  production of  $6.1 \text{ m}^3/(\text{m}^3_{RV}\cdot\text{d})$  with gas grid injection quality ( $CH_4 > 96\%$ ). Taking the inert  $CH_4$  content in the biogas into account, this corresponds to a  $CH_4$  product gas flow rate of  $17 \text{ m}^3/(\text{m}^3_{RV}\cdot\text{d})$ , which lays in the upper range compared to other studies. Furthermore, reducing the artificial nutrient addition without loss in methanation performance demonstrated cost reduction potentials. The results of the pilot-scale reactor operation give evidence that higher gas loads can be applied in the future by promoting gas conversion through the hydrogenotrophic pathway and improved reactor operation.

Based on the results of the pilot-scale study and on peer-reviewed journal articles, a comprehensive state-of-the-art review on the biological methanation in trickle bed reactors was performed to provide an overview of reactor design, process parameters, reactor operation, and recent developments. The review includes essential information that will support the decision-making of scientists and project managers in future projects. Furthermore, research needs were identified to improve the techno-economic performance of trickle bed reactors as promising energy conversion and storage technology.

## Zusammenfassung

Die aktuelle Energiekrise, die durch die geopolitische Abhängigkeit von fossilen Brennstoffen verursacht wurde, als auch die Klimakrise zeigen, wie wichtig der Ausbau erneuerbarer Energiequellen für eine sichere Energieversorgung ist. Um eine nachhaltige und sichere Stromversorgung auf der Grundlage eines hohen Anteils volatiler erneuerbarer Energien zu gewährleisten, sind flexible und langfristige Energiespeichertechnologien erforderlich. Ein vielversprechender Ansatz ist die biologische Umwandlung von  $H_2$  und  $CO_2$  in speicherbares  $CH_4$  in Rieselbettreaktoren. Die Forschung zur biologischen Methanisierung in Rieselbettreaktoren hat in den letzten Jahren stark zugenommen. Der effiziente und bedarfsgerechte Betrieb konnte bereits im Labormaßstab mit bis zu 100 L und unter kontrollierten Laborbedingungen nachgewiesen werden. Um das Potenzial von Rieselbettreaktoren als Energieumwandlungs- und Speichertechnologie besser einzuschätzen, ist eine Skalierung des Reaktors in den nächstgrößeren Maßstab und die Untersuchung der Einsatzfähigkeit des Reaktors unter realen Anwendungsbedingungen erforderlich. Daher wurde auf der Kläranlage Garching ein Rieselbettreaktor im Pilotmaßstab mit einem Reaktorvolumen von  $1.2\text{ m}^3$  installiert.

Die Methanisierungsleistung in Rieselbettreaktoren kann verbessert werden, indem der Gasstrom durch den Reaktor in Richtung Pfropfenströmung gelenkt wird. Ein Gasstrom durch den Reaktor, der sich dem Pfropfenstrom annähert, erhöht den  $H_2$  und  $CO_2$  Partialdruck am Gaseingang und verringert das Risiko, dass die Eduktgase den Reaktor verlassen, bevor sie in  $CH_4$  umgewandelt werden. Deshalb wurden vor der Inbetriebnahme des Pilotreaktors Gasströmungsexperimente durchgeführt, die die physikalischen Reaktoreigenschaften ermitteln und Betriebsbedingungen untersuchen können, die einen Gasdurchfluss in Richtung Pfropfenströmung unterstützen. Die Durchführung der Gasströmungsexperimente vor der Inokulation des Reaktors hat sich als einfache und effiziente Methode zur Nachbildung der reaktor spezifischen Strömungsdynamik gezeigt. Die Experimente wurden mit unbehandelten Füllkörpern durchgeführt, um eine biologische Gasumwandlung zu vermeiden, die den Vergleich der Kurvenverläufe verhindern würde. Eine wichtige Erkenntnis aus den rein physikalischen Gasströmungsexperimenten war, dass die Eduktgase aus  $H_2$  und einer  $CO_2$ -Quelle als Gasmisch mit gemeinsamen Gaseigenschaften durch den Reaktor strömten. Eine verbesserte Gasströmung wurde beobachtet, wenn die Gase von oben nach unten eingeleitet wurden und die Berieselung der Prozessflüssigkeit auf ein notwendiges Minimum reduziert wurde. Ein Durchbruch der Gase wurde erfasst, wenn die Gasströmung von unten nach oben entgegen der Berieselungsrichtung verlief. Der frühe

Durchbruch der Eduktgase im Gasausgang deutet auf einen Kanalisierungs- oder Bypass-Effekt aufgrund von Gasdichteunterschieden hin. Ein Durchbruch der Eduktgase tritt wahrscheinlich nur ein, wenn die Umwandlungskapazität der methanogenen Archaeen ausgeschöpft ist. Um das Risiko eines Durchbruchs zu verringern, wird das Einleiten der Eduktgase von oben nach unten empfohlen. Weiterhin konnten durch die Gasdurchflusseexperimente Reaktor spezifische Eigenschaften wie der Anteil stagnierender Volumina von 19% also auch des aktiv durchströmten Gasvolumens von 81% bestimmt werden.

Um das Konzept der biologischen Methanisierung in Rieselbettreaktoren im Pilotmaßstab zu demonstrieren, wurde der Rieselbettreaktor auf der Kläranlage Garching mit Faulschlamm inokuliert und fast 450 Tage lang betrieben, einschließlich zweier Stillstandsphasen. Als CO<sub>2</sub>-Quelle wurde Biogas verwendet, das bereits einen signifikanten CH<sub>4</sub>-Gehalt von 63% ± 1% aufwies und somit die Gasverweilzeit verkürzte. Ein kontinuierlich sinkender pH-Wert aufgrund der Akkumulation organischer Säuren stellte eine große Herausforderung für eine stabile Methanisierungsleistung dar. Wenn zu niedrige pH-Werte erreicht wurden, brach der Methanisierungsprozess zusammen. Die Bildung organischer Säuren kann durch die Umwandlung von H<sub>2</sub> und CO<sub>2</sub> in Essigsäure durch die Homoacetogenese als auch durch den Abbau von organischem Material und Biomasse Zerfall erklärt werden. Solange die Pufferkapazität der Prozessflüssigkeit hoch genug ist, sind keine erheblichen Änderungen des pH-Wertes zu erwarten. Allerdings führte die Verdünnung der Prozessflüssigkeit mit metabolischem Wasser zu einer Verringerung der Pufferkapazität. Die Erhöhung der Pufferkapazität durch Zugabe von Faulschlammzentrifugat mit dem Ziel einer NH<sub>4</sub><sup>+</sup> Konzentration von über 400 mg/L hat sich als erfolgreichste Strategie zur pH-Stabilisierung herausgestellt.

Zudem deuten die Ergebnisse darauf hin, dass der H<sub>2</sub>S Anteil im Biogas mit etwa 200 ppm als Schwefelquelle von den Mikroorganismen genutzt wurde, und somit der notwendige Aufwand zur finalen Aufreinigung des Produktgases vor der Gasnetzeinspeisung reduziert werden kann. Mit steigender Gaslast war aber die Zudosierung einer künstlichen Schwefelquelle erforderlich, um den Schwefelbedarf der Methanogenen vollständig zu decken. Nach Prozessoptimierungen konnte eine stabile Biogasaufbereitung von über zwei Wochen mit einer Gaslast von 42.7 m<sup>3</sup>/(m<sup>3</sup><sub>RV</sub>·d) erreicht werden, die in eine CH<sub>4</sub>-Produktion von 6 m<sup>3</sup>/(m<sup>3</sup><sub>RV</sub>·d) und Gasnetz-Einspeisequalität (CH<sub>4</sub> > 96%) resultierte. Das entspricht mit Berücksichtigung des inerten CH<sub>4</sub>-Anteils im Biogas einem CH<sub>4</sub>-Produktgasdurchfluss von 17 m<sup>3</sup>/(m<sup>3</sup><sub>RV</sub>·d), was im Vergleich zu anderen Studien im oberen Bereich liegt. Darüber hinaus zeigte die Reduzierung der künstlichen Nährstoffzugabe ohne Verlust der Methanisierungsleistung Kostensenkungspotenziale auf. Durch Maßnahmen, die eine Gasumwandlung über die hydrogenotrophe Methanogenese verstärken z.B. durch die Anreicherung von

hydrogenothrophen Methanogenen, wird ein höherer möglicher Gaslasteneinsatz erwartet, wodurch die CH<sub>4</sub>-Produktionsrate weiter gesteigert werden kann.

Auf der Grundlage der Ergebnisse der Pilotstudie und von Fachzeitschriftenartikeln wurde eine umfassende Zusammenfassung über den Stand der Technik, die neusten Entwicklungen und notwenige Forschungsschwerpunkte erstellt. Die zusammengefassten Informationen und die daraus gewonnenen Erkenntnisse liefern eine wichtige Grundlage, die die Entscheidungsfindung in zukünftigen Projekten unterstützen kann. Der Betrieb im Pilotmaßstab als auch jüngste Entwicklungen in der Technik demonstrieren das große Potential von Rieselbettreaktoren, um als Energieumwandlungs- und Speicherungstechnologie eingesetzt zu werden.

## **Danksagung**

Diese Arbeit wäre ohne die großartige Unterstützung von Kollegen, Freunden und meiner Familie nicht möglich gewesen. Deshalb möchte ich allen Menschen, die mich auf diesem Weg begleitet, mich unterstützt und mich immer wieder ermutigt haben, meine tiefe Dankbarkeit aussprechen.

Ein ganz besonderer Dank geht an meinen Betreuer, Doktorvater und eisernen Konkurrenten um den Fahrradpokal PD Dr.-Ing. habil. Konrad Koch. Vielen Dank Konrad, für deine stetige Unterstützung, deine ehrliche Art, die vielen Ratschläge und vor allem die Aufmunterung während herausfordernder Phasen, die mir immer wieder viel Kraft gegeben haben. Dass du dir immer die Zeit für Gespräche, Feedback und Diskussionen nimmst, mir aber auch die Gestaltungsfreiheit im Projekt gegeben hast, hat mich während des Projektes sehr motiviert.

Auch bei meinem Mentor und Co-Author Dietmar Strübing möchte ich mich ganz herzlich für das wertvolle Feedback und die hilfreichen Gespräche bedanken, die mich über den Tellerrand schauen lassen und mich in meinem Vorhaben bestärkt haben.

Die Durchführung dieses Dissertationsprojektes wäre vor allem nicht ohne die unermüdliche Unterstützung und Beratung von Hubert Moosrainer möglich gewesen. Herzlichen Dank Hubert! Du hast mir nicht nur gezeigt wie ich Pumpen repariere und Sensoren verkable, sondern auch jeden Morgen, wenn ich zu dir in die Werkstatt gekommen bin, die Sonne aufgehen lassen. Auch dir Maximilian Damberger möchte ich ganz besonders danken für deine Hilfe und motivierenden Worte, die mir während der letzten Phasen des Reaktorbetriebes sehr geholfen haben.

Als Anlagenbauer hat vor allem Steffen Wiegland die Realisierung des Projektes maßgeblich unterstützt, wofür ich mich herzlich bedanken möchte. Dabei geht auch ein besonderer Dank an das Team der Kläranlage Garching, wo wir den Pilotreaktor installieren und betreiben durften. Für die Finanzierung des Projektes möchte ich mich bei dem Bayerischen Staatsministerium für Wirtschaft, Landesentwicklung und Energie (StMWi) bedanken. Außerdem möchte ich mich bei unseren Projektpartnern Bernhard Munk und Michael Leuhn von der Bayerischen Landesanstalt für Landwirtschaft für die Durchführung der molekularbiologischen Analysen und für die hilfreichen Gespräche bedanken.

Ganz besonders möchte ich mich bei Franz Kirzeder, Francesco Fianelli, Yasin Md, Amelie Heimann, Nil Guereli, Dominik Kugler, Julian Straub, Meenakshi Prasad und

Ömer Kart für ihren Engagement und Einsatz während ihrer Masterarbeiten und Semesterarbeiten bedanken. Die Zusammenarbeit mit euch hat mir viel Freude bereitet und ohne eure Unterstützung wäre die Realisierung dieses Dissertationsprojektes nicht möglich gewesen.

Außerdem möchte ich meiner Prüfungskommission Assoc. Prof. Dr. Marika Kokko und Prof. Dr. Lars Ottosen ganz herzlich für die Unterstützung und das wertvolle Feedback zu den Untersuchungsschwerpunkten und Hypothesen bedanken. Ein großes Dankeschön geht auch an Prof. Dr.-Ing. Jörg E. Drewes und Apl. Prof. Dr. rer. nat. habil. Brigitte Helmreich, die mir die Promotion am Lehrstuhl ermöglicht haben.

Ganz herzlich möchte ich mich bei all meinen Kollegen und Freunden am Lehrstuhl für Siedlungswasserwirtschaft für die wirklich schöne Zeit bedanken. Ein ganz besonderer Dank geht an Myriam Reif. Du hast mir nicht nur im Labor mit Rat und Tat zur Seite gestanden, sondern hast mir mit deiner Herzlichkeit, weltoffenen Art und den vielen Kochsessions mit Stinsi und Co. viel Freude bereitet. Ganz besonders möchte ich mich bei Jonas Aniol, den besten Bürokollegen, Emil Bein und Philipp Stinshoff bedanken. Vielen Dank euch für eure unermüdlichen Aufmunterungen, fachlichen Ratschläge, spontanen Einsätze an den Reaktoren und Experimenten und für die lustigen Gespräche. Außerdem möchte ich mich bei Susanne Wießler für das Engagement am Lehrstuhl, für die Hilfe bei der Bürokratie und für die liebe Art bedanken. Vielen Dank auch an Dr. Oliver Knoop, Wolfgang Schröder, Uschi Wallentits, Heidi Mayrhofer und das gesamte Laborteam für eure Hilfsbereitschaft und eure Unterstützung im Labor.

Ein riesengroßer Dank gilt meiner Familie und meinen Freunden, die mich während allen Phasen ermutigt und unterstützt haben. Danke Paco für deine unendliche Unterstützung, dass du mir immer wieder Mut gemacht und Kraft gegeben hast.



# Contents

<b>Abstract</b>	<b>I</b>
<b>Zusammenfassung</b>	<b>III</b>
<b>Danksagung</b>	<b>VI</b>
<b>1. Introduction</b>	<b>1</b>
<b>2. Background</b>	<b>4</b>
2.1 Renewable energy generation	4
2.2 Energy conversion and storage technologies	6
2.3 Power-to-X	7
2.3.1 Hydrogen generation	7
2.3.1.1 Dynamic operation	8
2.3.1.2 Economic assessment	9
2.3.1.3 Prerequisites and byproducts	10
2.3.1.4 H <sub>2</sub> application	11
2.3.2 H <sub>2</sub> and CO <sub>2</sub> methanation	11
2.3.2.1 Catalytic methanation	12
2.3.2.2 Biological methanation	13
2.3.3 Power-to-X projects	18
<b>3. Research significance and hypotheses</b>	<b>20</b>
3.1 Research objective #1	20
3.2 Research objective #2	21
3.3 Research objective #3	23
<b>4. Preliminary gas flow experiments identify improved gas flow conditions in a pilot-scale trickle bed reactor for H<sub>2</sub> and CO<sub>2</sub> biological methanation</b>	<b>25</b>
4.1 Abstract	27
4.2 Introduction	27
4.3 Material and methods	29
4.3.1 Reactor setup	29
4.3.2 Design of gas flow experiment	31
4.4 Results and discussion	33
4.4.1 Effect of gas flow direction on the gas flow behavior	35
4.4.2 Physical effect of trickling on the gas flow behavior	39
4.4.3 Effect of dead volumes on the gas residence	40

---

4.5	Conclusion	42
4.6	Acknowledgements	42
<b>5.</b>	<b>Biogas upgrading in a pilot-scale trickle bed reactor – Long-term biological methanation under real application conditions</b>	<b>43</b>
5.1	Abstract	45
5.2	Introduction	45
5.3	Material and Methods	47
5.3.1	Reactor setup and system integration into the wastewater treatment plant	47
5.3.2	Inoculation and operating conditions	49
5.3.3	Monitoring and experimental analysis	50
5.4	Results and discussion	52
5.4.1	Reactor start-up and technical challenges	54
5.4.2	pH control measures	55
5.4.2.1	Increasing the sulfur concentration	56
5.4.2.2	Changing the H <sub>2</sub> /CO <sub>2</sub> feed gas ratio	58
5.4.2.3	Increasing the ammonium concentration in the trickling medium	59
5.4.3	Reduction of nutrient addition	61
5.4.4	Biofilm formation	62
5.4.5	Methanation performance and future perspectives	63
5.5	Conclusion	64
5.6	Acknowledgements	65
<b>6.</b>	<b>Biological methanation in trickle bed reactors - A critical review</b>	<b>66</b>
6.1	Abstract	67
6.2	Introduction	67
6.3	The trickle bed reactor concept	69
6.3.1	Reactor set-up	69
6.3.2	Process parameters	71
6.3.2.1	Temperature	71
6.3.2.2	Pressure	72
6.3.2.3	Co and CO <sub>2</sub> sources	72
6.3.2.4	Gas supply	74
6.3.2.5	Metabolic water production	75
6.3.2.6	pH level and VFA production	75
6.3.2.7	pH control	77
6.3.2.8	Redox potential	77
6.3.2.9	Trickling	78
6.3.2.10	Nutrient management	80
6.3.2.11	Microbiology	84

---

6.3.2.12 Biofilm formation	86
6.3.3 Reactor operation	88
6.3.3.1 Inoculation	88
6.3.3.2 Reactor performance	89
6.3.3.3 Dynamic operation	91
6.4 Research needs and future direction	93
6.5 Conclusion	96
6.6 Acknowledgements	97
<b>7. Research outcomes and conclusions</b>	<b>98</b>
<b>8. Outlook and future research needs</b>	<b>101</b>
<b>9. Appendix</b>	<b>106</b>
9.1 List of publications	106
9.2 List of supervised student theses	107
9.3 Supplementary information for Chapter 4	108
9.4 Supplementary information for Chapter 5	112
9.5 Supplementary information for Chapter 6	113
<b>References</b>	<b>114</b>

# 1. Introduction

With the target to reduce the effect of global warming and geopolitical dependency on fossil fuels, renewable energies are to become the most important energy source in the future. The European Commission aims to increase the share of renewable energy in the EU's energy mix to over 40% by 2030 and to become climate neutral by 2050 [1]. Particularly installations of wind and solar power plants are needed to be increased significantly to cover the future global energy demand, which is still rising. The challenge of wind and solar power is their fluctuating and weather-dependent availability, that cannot be adjusted properly to the energy demand. Thus, already now renewable electricity is curtailed to avoid instabilities in the vulnerable electrical grid [2]. To ensure a sustainable and secure power supply based on a high share of volatile renewables, long-term and demand-driven energy storage technologies are needed. Well researched storage technologies, such as pumped hydropower plants, and batteries, can balance short-term fluctuations, but their storage capacity is limited [3].

A promising storage approach is the Power-to-X concept. Electrical energy that is generated when energy production exceeds the energy demand can be converted into storable chemical energy, such as  $H_2$  and  $CH_4$ . The synthetically produced gas can be fed into the existing natural gas grid, where it can be stored over a period from minutes to months. However, due to the chemical properties of  $H_2$ , its injection into the natural gas grid is limited in most countries with  $H_2$  concentrations in the gas grid of 0-12% maximum [4].  $CH_4$  has a higher energy density (10 kWh/m<sup>3</sup> for  $CH_4$  vs. 3 kWh/m<sup>3</sup> for  $H_2$ ) and can be injected into the natural gas grid without restrictions, as the natural gas infrastructure is designed for  $CH_4$  storage. Compared to pumped hydropower plants and batteries the storage capacity of existing natural gas grids is remarkably high. The European gas grid for example, has a storage capacity of about 1,100 TWh [5].

Within the Power-to-Methane approach,  $H_2$  is generated through water electrolysis by using renewable electricity. Afterward,  $H_2$  is synthesized in combination with a carbon source into storable  $CH_4$  (Figure 1-1).

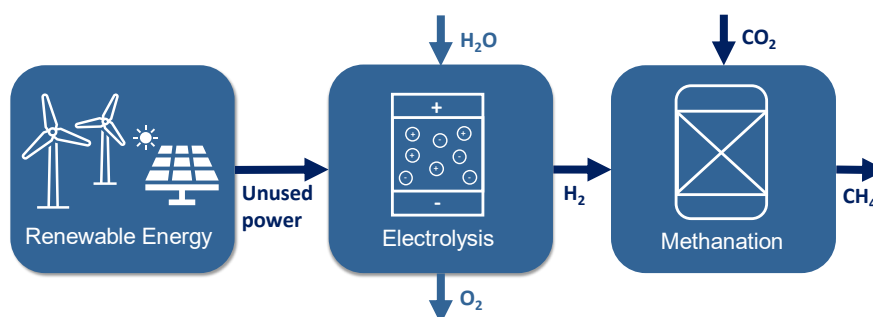


**Figure 1-1:** Simplified scheme of the Power-to-Methane concept.

$H_2$  and  $CO_2$  methanation can be performed through the chemical catalytic pathway or the biological pathway. The gas conversion in catalytic reactors is performed by metal catalysts, while biological reactors use anaerobic microorganisms belonging to the genera of methanogenic archaea. Catalytic methanation takes place at temperatures between  $250\text{ }^\circ\text{C}$  and  $700\text{ }^\circ\text{C}$  and pressures up to 100 bar [6, 7]. Biological methanation is performed at temperatures between  $35\text{ }^\circ\text{C}$  to  $75\text{ }^\circ\text{C}$  and mostly at ambient pressure, which allows a simple reactor operation and results in comparable low parasitic energy consumption [8]. Furthermore, the mild temperatures enable a facilitated and more efficient dynamic operation of the reactor on demand. In catalytic reactors, high temperature gradients during start-up and shut-down cause sintering and inactivation of metal catalysts. Another important advantage of biological methanation is the high tolerance of methanogenic microorganisms toward impurities in the feed gas, thus rendering gas pretreatment unnecessary.

The limiting step in biological reactors is the poor  $H_2$  gas-to-liquid mass transfer [9] and the slow kinetic of methanogens [10], which results in lower volumetric  $CH_4$  production rates compared to the catalytic methanation. Among various reactor designs, trickle bed reactors (TBRs) were identified to show an improved phase boundary interface for mass transfer. In contrast to liquid-filled reactor configurations, the active volume in TBRs is gas-filled, which enables independent control of the superficial gas velocity [11]. TBRs are typically designed to enable plug flow conditions, which ensures a high initial partial pressure of the feed gases, and provide a fixed packing bed with a high specific surface area [11, 12]. Furthermore, methanogenic microorganisms are immobilized in a biofilm on the packing bed surface, which allows improved gas transfer interface [11].

In the past years, research on the biological methanation in TBRs increased significantly, but technology readiness was mostly demonstrated on laboratory scale with reactor sizes of up to 100 L and/or operation at sterile conditions. Technology upscaling under real environmental conditions on a pilot-scale is the necessary step to identify the TBR potential for energy conversion and storage.

A promising CO<sub>2</sub> source is biogas, which can be upgraded directly at the point of origin. Biological methanation converts CO<sub>2</sub> to generate additional CH<sub>4</sub> instead of removing CO<sub>2</sub>, as performed in established biogas upgrading facilities. Thus, within the framework of this dissertation the potential of TBRs was demonstrated by the installation of a pilot-scale reactor on a wastewater treatment plant (WWTP) to upgrade the local biogas to synthetic natural gas with gas grid injection quality.

## 2. Background

To understand the need for energy conversion and storage technologies, such as the biological methanation in TBRs, this section provides an overview of the topic's background. Starting with the current situation of renewable energy generation, a summary of different energy conversion and storage technologies is followed.

### 2.1 Renewable energy generation

Energy generation is one of the main contributors to global warming, and the demand for energy is still increasing. Between 2009 and 2019, the final energy consumption grew by 19%. [13] A transition toward a renewable energy-based system and increased energy efficiency are irremissible to meet global targets of CO<sub>2</sub> emission reduction. However, the share of renewable energy in global energy generation is low, and fossil fuels cover most of the energy demand so far. In 2019, renewables met about 11.7% of the global final energy consumption, while the share of renewable energy is very uneven among the heating and cooling, transport, and power sector (Figure 2-1). The percentage of renewables is the highest in the power sector, where hydropower, followed by solar and wind power, contributes to significant renewable energy generation. [13]

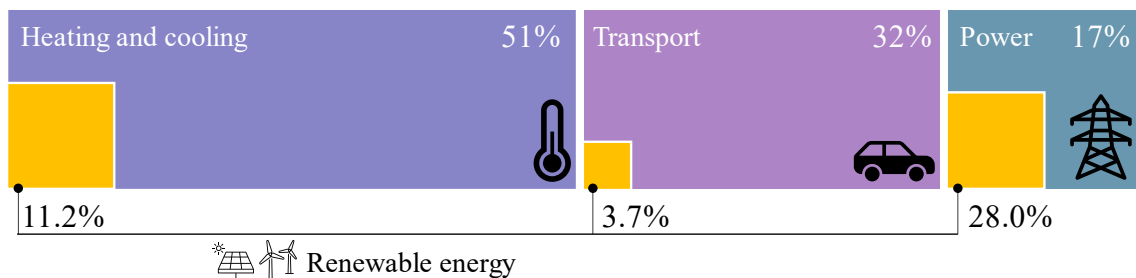


**Figure 2-1:** Sector-depending contribution of renewable energy in the global energy consumption in 2019 adapted from REN21 [13].

In order to advance geopolitical energy independence and meet climate objectives, the European Commission has the target to cover at least 40% of the EU's energy mix with renewable energy by 2030 and become climate neutral by 2050 [1]. Several countries, such as Iceland, Norway, and Sweden, already cover more than 50% of their total final energy consumption with renewable energy [13]. Furthermore, the share of renewable energy in the European energy mix, particularly in electricity generation, increased constantly over the past years. Exemplary Figure 2-2 shows the increase in renewable energy generation in Germany. As indicated in the figure, mainly wind and solar power contribute to renewable electricity generation. Costs for solar power have

decreased clearly over the past decades and already fell below costs for coal- or gas-fired power plants in most countries [14].

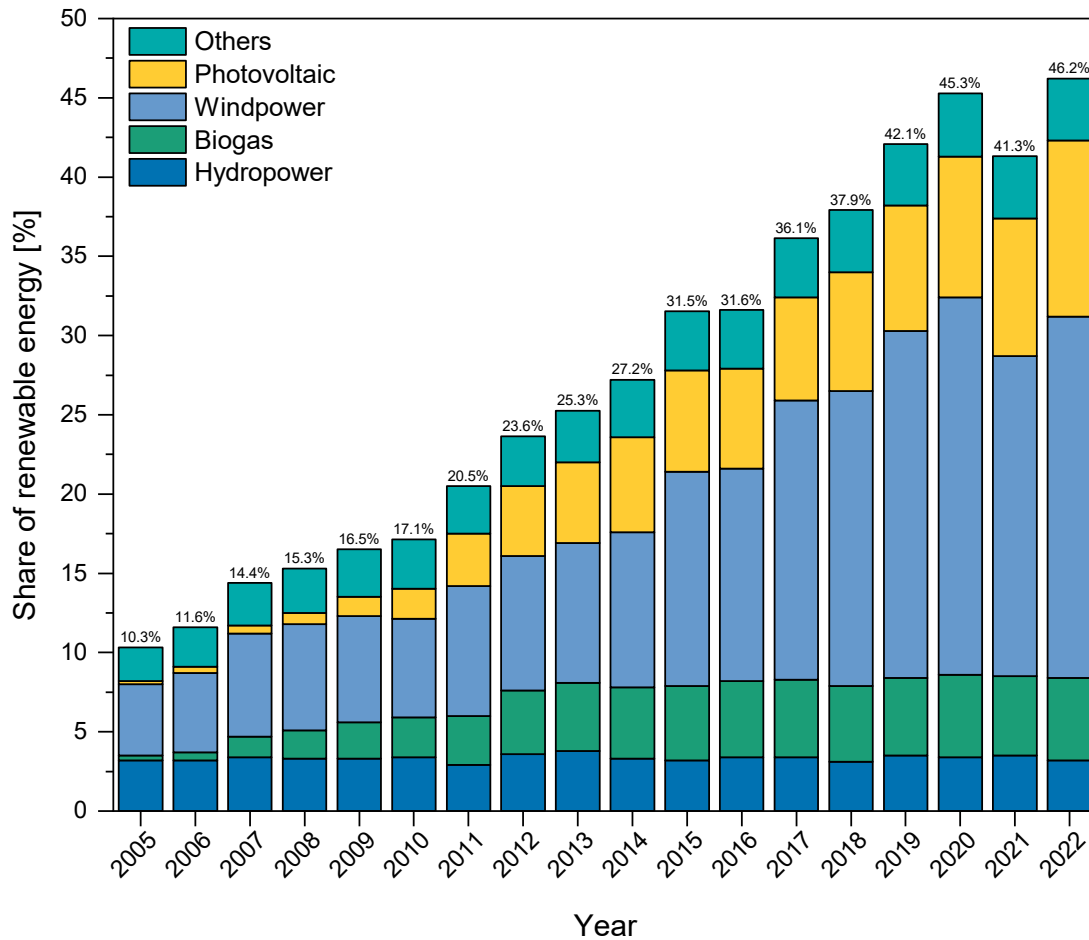


**Figure 2-2:** Share of renewable energy sources in the gross electricity generation in Germany based on the data from German Federal Network Agency [15].

A big challenge of weather-dependent energy sources, such as solar and wind power, is their fluctuating and intermittent operation. Thus, energy supply by renewable sources cannot be appropriately adjusted to the energy demand. Furthermore, exceeding the energy demand leads to an instability of the electric grid. In 2019, around 2.8% of the renewable electricity produced in Germany was curtailed from the electrical grid, corresponding to 6.5 TWh [2]. The electric energy that is generated when energy production exceeds the energy demand can be saved in energy storage systems to balance the vulnerable electrical grid. Energy conversion and storage technologies are essential drivers for the energy transition based on renewable sources, ensuring a sustainable and secure energy supply.



## 2.2 Energy conversion and storage technologies

To support the energy transition based on renewable energy sources, flexible and demand-oriented energy storage technologies are required. The suitability of energy conversion and storage technologies depends on the storage capacity and discharge time (Figure 2-3). Standard storage technologies include pumped hydropower plants, batteries, flywheels, and compressed air energy storage. Pumped hydropower plants and batteries are well-researched technologies. Pumped hydropower plants are very effective storage technologies applied in many countries to balance short-term fluctuations in the electric grid. [16] The global pumped hydropower storage capability in 2020 was about 8.5 TWh and is expected to increase to over 11.7 TWh by 2026 [17]. With a worldwide low installed capacity of about 16 GW in 2021, batteries are typically applied for short-term (hour-day) grid balancing [16]. Other technologies, such as chemical energy carriers, are more suitable for long-term storage.

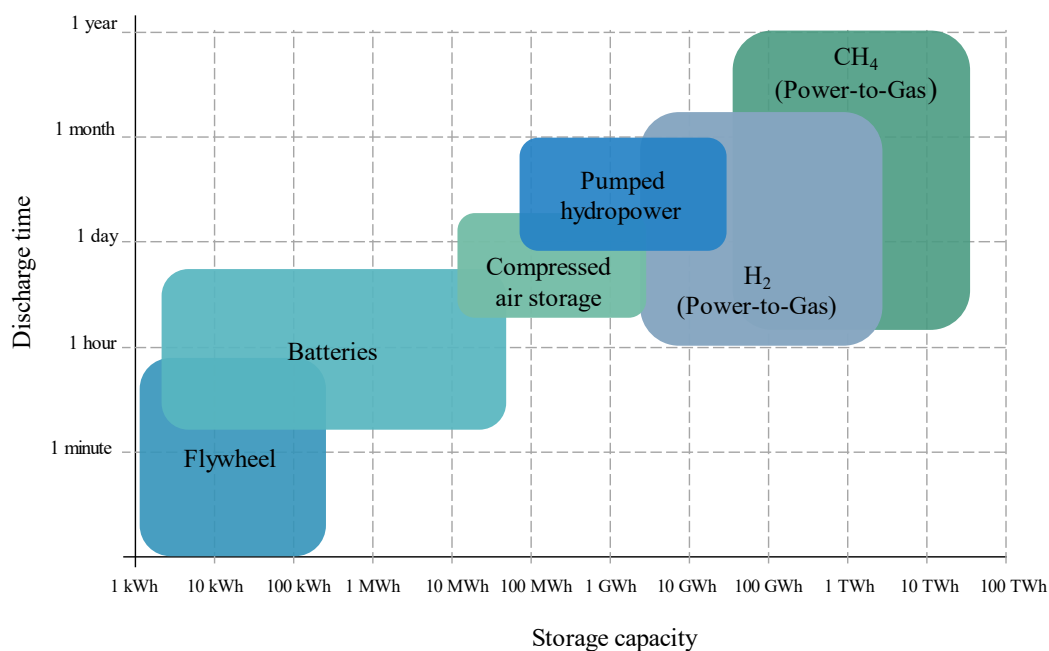


**Figure 2-3:** Comparison of energy storage technologies depending on the discharge time and storage capacity (adapted from Schaaf et al. [3]).

Compared to natural gas grids, the storage capacity of pumped hydropower plants and batteries is very low. The European gas grid, for example, has a storage capacity of about 1,100 TWh [5], where natural gas can be flexibly stored from minutes to months. The natural gas in the gas grid is mainly CH<sub>4</sub>. Higher hydrocarbons, e.g., ethane, propane, and butane, increase the calorific value, while inert components, such as CO<sub>2</sub> and N<sub>2</sub>, reduce the calorific value of the natural gas [18]. The gas grid injection in many countries is restricted to national standards and regulations. Synthetic natural gas that is produced from coal, biomass, or the methanation of CO and CO<sub>2</sub> can be injected into the gas grid

when specific gas qualities are ensured. Typically, a lower and upper Wobbe index defines the gas quality in the gas grid. H<sub>2</sub> and CO<sub>2</sub> concentrations in the natural gas grid are limited in many countries with thresholds of 0-12% and 1-8%, respectively. [4]

## 2.3 Power-to-X

Power-to-X describes the conversion of renewable electric energy into storable energy carriers. The Power-to-X technology is based on H<sub>2</sub> generation through water electrolysis, which can be further processed in combination with a carbon source into chemicals, such as CH<sub>4</sub>, methanol, formic acid, formaldehyde, and alkanes [19]. Power-to-Gas includes the electric energy conversion into gas fuels, while Power-to-Liquid specifies the production of liquid fuels [20].

### 2.3.1 Hydrogen generation

Most H<sub>2</sub> is still produced through steam CH<sub>4</sub> reforming, using natural gas or other fossil fuels [19]. About 76% of the H<sub>2</sub> is generated from natural gas, 23% from coal, and less than 0.7% from renewable energy and fossil fuel plants equipped with carbon capture usage and storage [21]. A side product of this high-temperature process is CO, which reduces the gas quality. For the sustainable production of H<sub>2</sub>, water electrolysis operated with unused renewable electricity produces high-purity H<sub>2</sub> by splitting water into H<sub>2</sub> and O<sub>2</sub> (Eq. (2.1)).



However, only about 0.1% of global H<sub>2</sub> production is generated by water electrolysis [21]. To increase this number, electrolysis efficiency and costs need to be improved.

The three leading electrolysis technologies are alkaline electrolysis, polymer electrolyte membrane/proton exchange membrane (PEM) electrolysis, and solid oxide electrolysis. They are classified depending on the electrolyte (Figure 2-4). The suitability of an electrolyzer highly depends on the framework requirements of the project. An overview of the electrolyzer parameters is provided in Table 2-1.

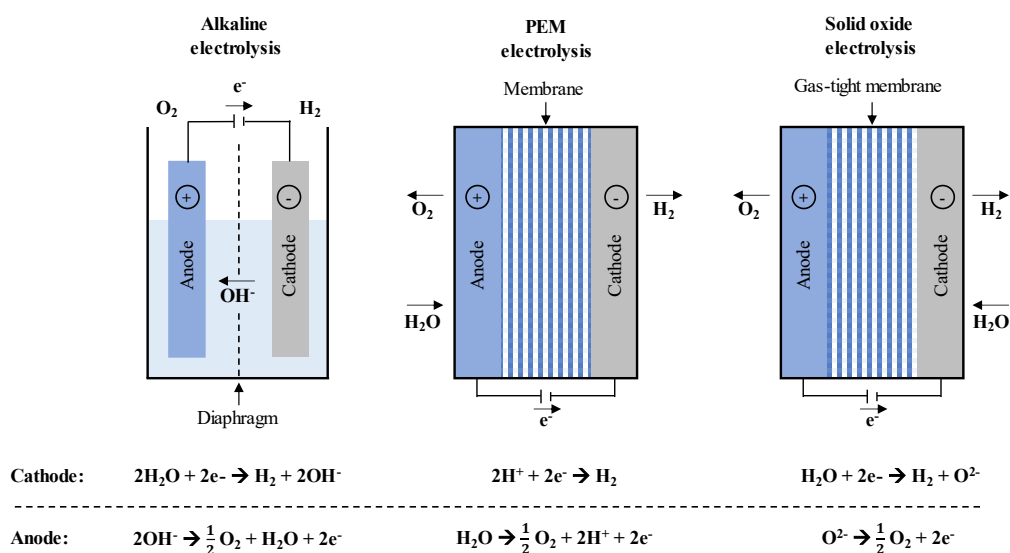


**Figure 2-4:** Electrolysis technologies adopted from Rego de Vasconcelos and Lavoie [19].

Alkaline electrolysis is the most mature and reliable technology, already commercially available for decades on a large scale of up to 6 MW of single-stack capacities [22]. Alkaline electrolysis uses an electrolyte solution, e.g., NaOH or KOH, which requires recovery and recycling [21]. PEM electrolysis is also applied commercially in comparable lower-scale systems, and solid oxide electrolysis is still in the development stage [19]. Alkaline and PEM electrolysis operate at lower temperatures (50-80 °C) [23] compared to solid oxide electrolysis, which works at temperatures between 900-1,000 °C [22, 24]. Thus, solid oxide electrolysis is specified as high-temperature electrolysis. Increasing temperatures improve kinetics and thermodynamics, enabling high power-to-H<sub>2</sub> efficiency for solid oxide electrolysis [22]. However, material instability is a major challenge of high heat applications [19]. Alkaline and PEM electrolyzers achieve up to 82% voltage efficiencies and solid oxide electrolyzers even up to 86% [25]. A high H<sub>2</sub> purity can be obtained for both electrolyzers, with up to 99.9% in the alkaline electrolysis and up to 99.99% in the PEM electrolysis [22].

### 2.3.1.1 Dynamic operation

The dynamic operation of the electrolyzer units is an important consideration if the application of water electrolysis for grid balancing services is targeted. Alkaline electrolysis needs a minimum load of 10-40% of the nominal H<sub>2</sub> production. [22] No minimum load requirements were reported for low-pressure PEM electrolyzers, while for short periods, even overloads are possible with up to 160% of design capacity [21]. With a range of -100 to 100%, solid oxide electrolysis can operate with high load variations and even in reverse mode to reproduce electricity. When maintaining the nominal

temperature, the load can be changed in alkaline and PEM electrolysis to stabilize power grids within seconds. Hot and pressurized standbys are possible within seconds for PEM electrolysis, 1-5 min for alkaline electrolysis, and 15 min for solid oxide electrolysis. Furthermore, PEM electrolysis is the most flexible technology regarding cold standbys. 5-10 min are required to heat up PEM electrolyzers and about 1-2 h for alkaline electrolysis. [22] Due to the high operating temperature in solid oxide electrolysis, hours are usually required to heat up the electrolysis unit. Therefore, cold standbys are very energy-consuming and not economically reasonable [22, 26]. The heat-up time depends on boundary conditions, such as the nominal temperature, electrolyzer size, design, thermal capacity, current density, and cold standby duration. Thus, the time to heat up an electrolyzer unit varies highly in the literature.

### 2.3.1.2 Economic assessment

Water electrolysis costs decreased significantly in the last years [27]. With investment costs of 800-1,500 €/kW in 2017 and maintenance costs of 2-3% of the annual investment costs, alkaline electrolysis has the lowest capital and operational costs [22], resulting from lower material costs and technology commercialization [21]. PEM electrolysis is more expensive because of the high costs of membrane materials and electrode catalysts (platinum, iridium) [21]. The investment costs lay between 1,400-2,100 €/kW and maintenance costs of 3-5% of the annual investment costs [22]. Solid oxide electrolysis has the highest costs of about 3570 €/kW in 2017 [27]. As solid oxide electrolysis is still in the pre-commercial phase, cost estimations and predictions are highly uncertain [22]. The investment costs are expected to decrease, among others, due to improvements in efficiency, manufacturing, and technology commercialization. Investment costs for alkaline and PEM electrolysis were predicted to fall below 500 €/kW and solid oxide electrolysis to 535 €/kW in 2050 [27]. Possible cost reduction potentials are higher cell areas, less share of noble metal in electrodes, and alternative membrane materials [22].

The electrolyzer plant and stack lifetime are important considerations in assessing the economic feasibility of the electrolyzer. Alkaline and PEM electrolysis showed plant lifetimes of about 20 years [22]. The stack efficiency decreases over time due to voltage degradation, but the reported lifetime varies highly in the literature. The highest stack lifetime is expected for alkaline electrolysis with up to 90,000 h, followed by solid oxide electrolysis with up to 40,000 h, and PEM electrolysis with up to 20,000 h until the cell stack needs replacement [25]. Higher current densities and temperatures impact stack degradation. Load cycling was reported not to considerably affect the lifetime of PEM and solid oxide electrolysis. However, more research on parameters influencing the stack and plant lifetime and strategies to improve the lifetime is required. [22]

**Table 2-1:** Overview of water electrolysis technologies specifications adopted from Buttler and Spliethoff [22], David et al. [28], Borge-Diez et al. [25], and Rego de Vasconcelos and Lavoie [19].

		<b>Alkaline electrolysis</b>	<b>PEM electrolysis</b>	<b>Solid oxide electrolysis</b>
Status		Commercial	Commercial	Prototype
Cell temperature	°C	60–80	50–80	900–1,000
Cell pressure	bar	10–30	20–50	1–15
H <sub>2</sub> purity	%	>99.8	99.999	-
Current density	A/cm <sup>2</sup>	0.25–0.45	1.0–2.0	0.3–1.0
Cell voltage	V	1.8–2.4	1.8–2.2	0.95–1.3
Voltage efficiency	%	62–82	67–82	81–86
Load capacity	%	25–100	0–100	–100/+100
Cold start-up time		15min – 2 h	5–10 min	hours
Warm start-up time		1–5 min	<10 s	15 min
Stack lifetime	h	<90,000	<20,000	<40,000
System lifetime	years	20-30	10-20	-
Investment costs	€/kW	800–1,500	1,400–2,100	> 2,000
Maintenance costs (% of investment costs per year)	%	2–3	3–5	-

### 2.3.1.3 Prerequisites and byproducts

A prerequisite for the electrolysis operation is the accessibility to high-quality water. Theoretically, about 0.8 L of water is required to generate 1 m<sup>3</sup> of H<sub>2</sub>, which is in reality higher [29]. This can become a challenge in water-stressed areas. Water impurities, such as cations, anions, and organic and inert compounds, can cause severe damage of electrolyzers and other installations. Thus, water intended to be used in electrolyzer units usually needs to be purified before its application. Water quality thresholds can vary depending on the electrolysis technology and manufacturer specifications. Typically, electrical conductivity is limited to 1 µS/cm, and total organic carbon to 50 µg/L. Tap water is widely used for electrolysis and is usually purified by reverse osmosis, typically employed as a first purification step. If other water sources are used, additional pre-treatment, e.g., activated carbon adsorption, before purification might be necessary. [30]

O<sub>2</sub> is produced as a by-product in water electrolysis. Per kg of H<sub>2</sub>, about 8 kg of O<sub>2</sub> is generated. To improve economic performance, O<sub>2</sub> can be further applied in the aeration process of the WWTP, in the methane combustion unit, in the healthcare sector, or for

industrial operations. [21] The excess heat energy generated during the electrolysis can be further used.

#### 2.3.1.4 H<sub>2</sub> application

Since 1975, the global demand for H<sub>2</sub> is steadily increasing. The majority is used for oil refining and NH<sub>3</sub> production, whereas the latter is mainly applied as fertilizer. In 2018 about 73.9 million tons of pure H<sub>2</sub> was produced, of which 52% was used for refining, 43% for NH<sub>3</sub> production, and 6% for other purposes. Further, 45 million tons of H<sub>2</sub>, supplied as a gas mixture, is used for CH<sub>3</sub>OH and steel production. [21]

There is potential to use H<sub>2</sub> in the power, and transport sector, such as for shipping and aviation [21]. Furthermore, H<sub>2</sub> can be injected into the existing natural gas network, but the H<sub>2</sub> properties challenge its usage. H<sub>2</sub> is highly flammable and has a small molecular size, wherefore H<sub>2</sub> diffuses through most types of materials, which makes H<sub>2</sub> storage and transport difficult. Thus, injection of H<sub>2</sub> into the natural gas grid is usually limited to country-specific thresholds, varying between 0-12% [4]. Due to the low energy density of H<sub>2</sub> (3 kWh/m<sup>3</sup> vs. 10 kWh/m<sup>3</sup> for CH<sub>4</sub> at STP), it is typically compressed or liquified for transportation and storage purposes. For example, utilizing H<sub>2</sub> as fuel for transportation requires compressing H<sub>2</sub> up to 500 bar and fueling into the car tank up to 900 bar [31]. H<sub>2</sub> transportation and storage costs might be threefold the costs of H<sub>2</sub> production [21]. Thus, using H<sub>2</sub> onsite and on-demand reduces the costs considerably. Alternatively, H<sub>2</sub> can be converted in a subsequent step to chemical energy carriers with an improved storage capacity, such as CH<sub>4</sub>.

#### 2.3.2 H<sub>2</sub> and CO<sub>2</sub> methanation

CO<sub>2</sub> is a major contributor to global warming. By utilizing CO<sub>2</sub> sources to convert CO<sub>2</sub> into CH<sub>4</sub>, CO<sub>2</sub> is temporarily captured. CH<sub>4</sub> has a considerably higher energy density. Furthermore, due to the high storage capacity of the gas grid, natural gas can be stored for minutes to months.

The chemical conversion of H<sub>2</sub> and CO<sub>2</sub> into CH<sub>4</sub> is an exothermic reaction (Eq. 2.2), which releases 165 kJ/mol, while 889 kJ/mol of the total 1,054 kJ/mol are bound in CH<sub>4</sub>. Consequently, plenty of 84% remains in the methane. Aiming for high CH<sub>4</sub> concentrations in the product gas is challenging as high H<sub>2</sub> and CO<sub>2</sub> conversion rates are required (Figure 2-5). For example, an H<sub>2</sub> and CO<sub>2</sub> conversion of 99% results only in a CH<sub>4</sub> concentration of 95% [18].



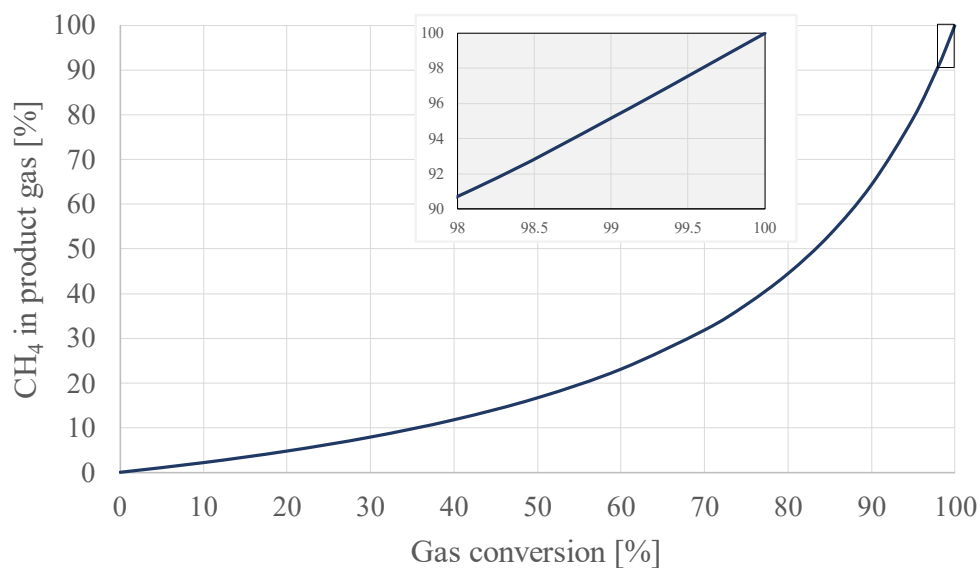


**Figure 2-5:** Relationship between the biological H<sub>2</sub> and CO<sub>2</sub> conversion and the corresponding CH<sub>4</sub> concentration in the product gas (adopted from Götzt et al. [18]).

There are two principal pathways of the H<sub>2</sub> and CO<sub>2</sub> conversion into CH<sub>4</sub>; the catalytic and the biological process. Catalytic methanation uses metal catalysts for gas conversion, known as the Sabatier process. In biological reactors, anaerobic microorganisms (methanogens) of the genera archaea are responsible for gas conversion. Both pathways demonstrated the ability to produce high-quality product gas, meeting the gas grid injection requirements. Which methanation pathway is the most suitable depends on the system boundary conditions, such as gas load, feed gas quality or the need for dynamic operation.

To date, catalytic and biological methanation costs are still very high, but substantial reductions with technology development and commercialization are expected. A cost reduction for catalytic methanation of about 67% with 800 €/kW in 2017 to 130-400 €/kW in 2050 and biological methanation of about 75% with 1200 €/kW in 2017 to 300 €/kW in 2050 were predicted [27]. However, due to limited large-scale projects, cost calculations and prediction, particularly for biological methanation, are highly uncertain.

### 2.3.2.1 Catalytic methanation

Catalytic methanation is a well-known process that has been investigated for decades [18]. Catalytic methanation reactors operate at temperatures between 200-700 °C and at pressures of up to 100 bar [18]. The high temperatures and pressures enable comparable high gas conversion rates that result in high CH<sub>4</sub> production rates. Furthermore, catalytic methanation reactors reach an average efficiency of 80-85% [25]. Ni is the most applied catalyst because of its low material cost, abundance, and activity. However, nickel is

deactivated at high temperatures, which is why other metal catalysts are sometimes preferred, e.g., Fe, Ru, Rh, and Co. [18, 25].

Various reactor configurations were reported in the literature [32]. Steady-state reactor concepts are the adiabatic fixed-bed, the fluidized-bed, the three-phase, and the structured reactor [18]. The last two reactor configurations are still in the development stage. A detailed description of the different reactor configurations is provided by Götz et al. [18]. Due to the heat generated during the exothermic methanation process, temperature control is the most challenging parameter in catalytic reactors. Too high temperatures and temperature gradients can result in catalyst sintering and cracking, which reduces the catalyst's lifetime or even deactivate the catalysts [18]. Depending on the reactor concept and operation mode, more or less temperature control is required.

Fixed bed reactors in different variations are most applied in projects around the world [33]. Due to adiabatic fixed-bed reactors' poor heat transfer capacity, they are often constructed in series with intercooling. Structured-type reactors, such as monolith or honeycomb reactors, are constructed in a way to support the heat transfer of the fixed-bed [18, 25]. A challenge of the metallic structure is the complicated replacement of deactivated catalysts. More effective heat removal is achieved in fluidized and three-phase reactors. [18]. However, application on a large scale was only rarely reported.

A major drawback of catalytic methanation due to the high operating temperatures is the limited capacity for dynamic operation. Changing the gas load results in high-temperature variations, which can damage the catalyst. Catalytic reactors typically require a minimum gas load of 10-40%, depending on the reactor configuration. In order to enable a quick restart and avoid the formation of Ni carbonyls, only hot standbys or standbys with a temperature above 200 °C should be applied. Isothermal reactors are expected to stabilize the temperature better, but investigations on the dynamic operation are scarce. [18] Another challenge of catalytic methanation is that impurities in the feed gas, such as sulfur compounds or higher hydrocarbons, can deactivate the metal catalysts [18]. Thus, gas pretreatment is typically applied to ensure high-purity feed gas.

### **2.3.2.2 Biological methanation**

Biological reactors are operated at temperatures between 5 and 122 °C and mostly ambient pressure [18]. Also biological methanation reach high conversion efficiencies of up to 83.2% [34]. H<sub>2</sub> and CO<sub>2</sub> conversion is performed by anaerobic microorganisms of the genera archaea. The process is known from the last step in the anaerobic degradation of anaerobic digesters (Figure 2-6).



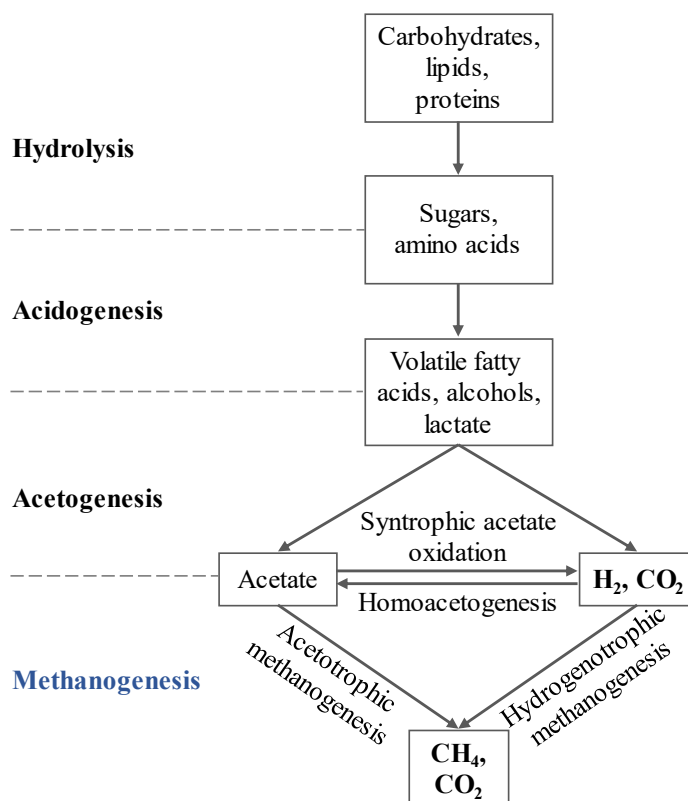


**Figure 2-6:** Key stages in the anaerobic degradation process. Modified from Strübing [35] and based on information of Logroño et al. [36].

Adding H<sub>2</sub> directly into the biogas digester is also possible, which is defined as in-situ biological methanation. In anaerobic digesters many microorganisms are involved in the four-step degradation of organic material [18]. With the aim to upgrade biogas, in-situ methanation reduces the requirement for constructing an additional reactor, which lowers investment costs [18]. However, adding external H<sub>2</sub> leads to an increased H<sub>2</sub> partial pressure, which affects the pH level and can deteriorate the acidogenesis and acetogenesis pathways. Increasing pH levels in in-situ methanation reactors shift the NH<sub>4</sub><sup>+</sup>/NH<sub>3</sub>-equilibrium toward NH<sub>3</sub>, which has inhibitory effects on the anaerobic digestion process. [35] The key parameter in anaerobic digesters is the organic loading rate, which limits the in-situ methanation potential. Furthermore, the H<sub>2</sub> partial pressure influences the microbial community composition and thus, the H<sub>2</sub> conversion pathways. [37] In ex-situ biological reactors, process conditions (e.g., temperature, pH level, nutrient addition) can be better adjusted to the requirements of the methanogens [18]. Furthermore, higher H<sub>2</sub> partial pressures can be applied without disturbing other microbial pathways, which improves the gas-liquid mass transfer. Thus, in-situ biogas upgrading is typically limited, achieving lower CH<sub>4</sub> concentrations than ex-situ methanation reactors [37].

In contrast to catalytic reactors, methanogenic microorganisms have a high tolerance against impurities in the feed gas. Even small concentrations of O<sub>2</sub> were identified to have no impact on the methanation process. [18] Other components, such as sulfur compounds, are even expected to be partially removed by microorganisms [38]. Furthermore, the mild temperature conditions of biological reactors allow a facilitated dynamic operation with fewer energy losses, particularly for cold standbys. The capacity for load changes only depends on the performance of the methanogenic microorganisms and does not damage costly catalyst materials. The limiting factor in biological methanation is the low H<sub>2</sub> gas-liquid mass transfer, which results in comparable low gas conversion rates. Thus, biological reactors are constructed with much greater reactor sizes than catalytic reactors at the same gas flow. The volumetric H<sub>2</sub> gas-liquid mass transfer  $R_{H_2}$  is described in Eq. (2.3), where  $k_{La}$  is the volumetric mass transfer coefficient,  $H_{H_2,cp}$  the H<sub>2</sub> Henry's law constant,  $p_{H_2,G}$  the H<sub>2</sub> partial pressure in the gas phase, and  $c_{H_2,L}$  the H<sub>2</sub> concentration in the liquid phase.

$$R_{H_2} = k_{La} \cdot (H_{H_2,cp} \cdot p_{H_2,G} - c_{H_2,L}) \quad \text{Eq. (2.3)}$$

The H<sub>2</sub> partial pressure can be increased by higher operational pressures or by expanding the H<sub>2</sub> share in the feed gas. Furthermore, the H<sub>2</sub> partial pressure can be elevated locally by approaching a gas flow toward plug flow. The reactor configuration and operational strategies highly influence the transfer between H<sub>2</sub> and methanogenic archaea. The volumetric mass transfer coefficient  $k_{La}$  can be increased with a reactor design that provides a phase boundary interface [11].

### Reactor configurations

The most common reactor configurations applied for biological methanation are the TBR, the continuous stirred tank reactor (CSTR), and the (hollow fiber) membrane reactor (Figure 2-7). The first investigations and upscaling projects started with the CSTR. The microorganisms in CSTRs are suspended in the liquid, and the feed gas is introduced into the liquid phase forming bubbles [4]. Mechanical agitation and stirring are applied to decrease the gas bubble size and enhance the feed gas distribution. Thus, suspended methanogens can better convert the feed gas. The gas-liquid mass transfer is expected to increase with higher angular velocities resulting in enhanced feed gas conversion rates [39]. However, the energy consumption for mixing is relatively high and will even increase with reactor upscaling [11, 18, 40]. About 10% of the overall energy input is required for mixing in CSTRs [35, 39].

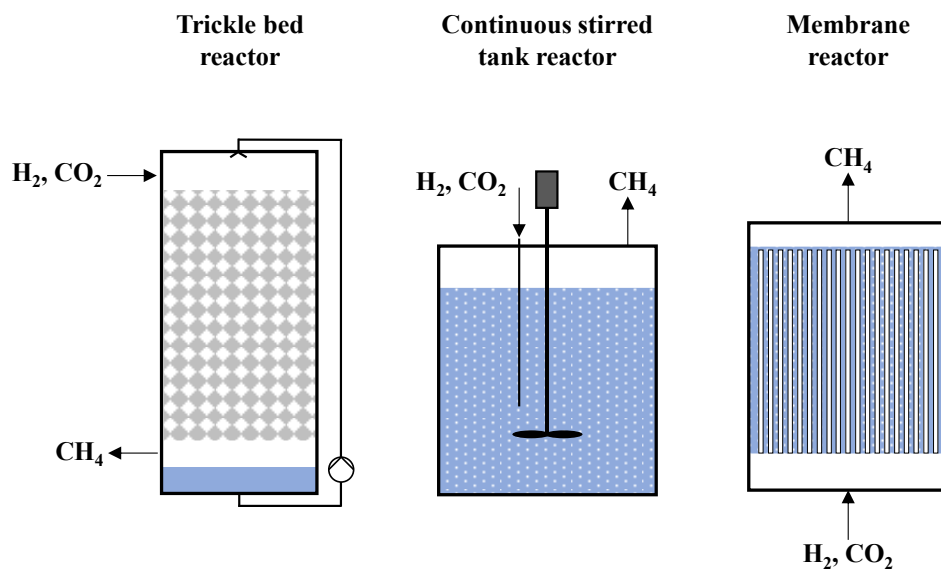


**Figure 2-7:** Commonly applied reactor configurations in the biological methanation (adopted from Thema et al. [4]).

TBRs and membrane reactors are biofilm-based processes and require less energy for operation. Biological methanation in membrane reactors is the most recent development. In membrane reactors, membranes are submerged in a liquid phase. The microorganisms are immobilized in a biofilm on top of the membranes, which convert the feed gases when diffusing through the membrane. Thus, no feed gas bubbles arise when methanogens convert the passing feed gases entirely. [4]

Due to an improved gas-liquid mass transfer, TBRs have gained a high research interest in recent years. While investigations in biological methanation started with CSTRs, most projects now focus on TBRs [27]. The concept of the TBRs applying biological methanation can be already found in the 1990s by Kimmel et al. [41] but intensified research started after the publication of Burkhardt and Busch [12], resulting in a high number of publications on this topic.

TBRs are gas-filled cylindrical columns packed with biocarrier material in a packing bed. The process liquid is stored in a reservoir at the bottom of the reactor and trickled over the packing bed to provide essential nutrients to the microorganisms, which are immobilized on the packing bed surface. A packing bed with a high volumetric surface area is often preferred to give a prominent place where microorganisms can immobilize and get in contact with the feed gas. Unlike liquid-filled reactor configurations, the gas-filled TBRs allow independent control of the superficial gas velocity [11]. Since the feed gas is not introduced into the liquid phase, no energy-intensive mixing or pressurized gas supply is required. In addition, a high height-to-diameter ratio of the reactor allows

approaching plug flow conditions, which can further improve methanation performance by increasing the local feed gas partial pressure  $p_{G}$  at the gas entrance.

### **Application potentials**

Biogas is probably the most suitable  $\text{CO}_2$  source for biological methanation. Biogas typically contains 50-70%  $\text{CH}_4$ , 30-50%  $\text{CO}_2$ , and minor amounts of  $\text{N}_2$  (0-3%), water vapor (5-10%),  $\text{O}_2$  (0-1%),  $\text{H}_2\text{S}$  (0-10,000 ppm),  $\text{NH}_3$  (0-200  $\text{mg}/\text{m}^3$ ), and siloxanes (0-41  $\text{mg}/\text{m}^3$ ) [18, 42]. Biogas is typically upgraded by well-established technologies, e.g., water scrubbing, pressure swing adsorption, membrane, and cryogenic separation. While these technologies are applied to remove the  $\text{CO}_2$  content in biogas and other trace compounds to obtain a biomethane with gas grid injection quality, biological methanation can benefit from the  $\text{CO}_2$  content by its conversion in combination with  $\text{H}_2$ . A case study in Denmark performed by Nashmin Elyasi et al. [43] showed that biological  $\text{H}_2$  and  $\text{CO}_2$  methanation could be an economical alternative to water scrubbing. However, cost predictions are still highly uncertain but are expected to decrease with commercialization and further development of the technology.

As demonstrated in several studies, raw biogas can be applied in biological methanation systems without pretreatment due to the robustness of methanogenic microorganisms toward impurities. With  $\text{H}_2\text{S}$  concentrations in the biogas of up to 3000 ppm, no negative effects on the methanation performance of methanogens were reported [44, 45]. Due to the highly corrosive nature of  $\text{H}_2\text{S}$ , most countries have stringent  $\text{H}_2\text{S}$  limits of 2-20 ppm for gas grid injection [4]. By applying biological methanation, even a reduction of  $\text{H}_2\text{S}$  is reasonable, as methanogens require sulfur as a nutrient [46]. The  $\text{CH}_4$  content in biogas flows as inert gas through the reactor. A  $\text{CH}_4$  concentration in biogas between 50-70% increases the gas load by 20-47%, reducing the gas residence time and lowering the feed gas pressure. Thus, larger reactor volumes are required to generate the same  $\text{CH}_4$  production rate as in pure  $\text{CO}_2$  operated reactors. [35]

Biogas production sites like WWTPs and biogas plants have a high potential for integrating biological methanation. WWTPs and biogas plants offer resources that can be applied for reactor inoculation and nutrient supply. The electricity generation from biogas in Germany was highly promoted, resulting in a strong expansion between 2005 and 2012 (Figure 2-8). About 9,600 biogas plants in Germany generate an electrical output of more than 5,600 MW [47]. According to the German Federal Network Agency [15], 30.2 TWh gross electricity from biogas originating from biogas plants, WWTPs, and landfill were produced in 2022. About 5.4% of German electricity consumption is covered by biogas [47]. Applying biological methanation for upgrading biogas instead of conventional upgrading technologies or combined heat and power plants can additionally generate

about 12.1 TWh biomethane when assuming an average CO<sub>2</sub> concentration of 40% in biogas.

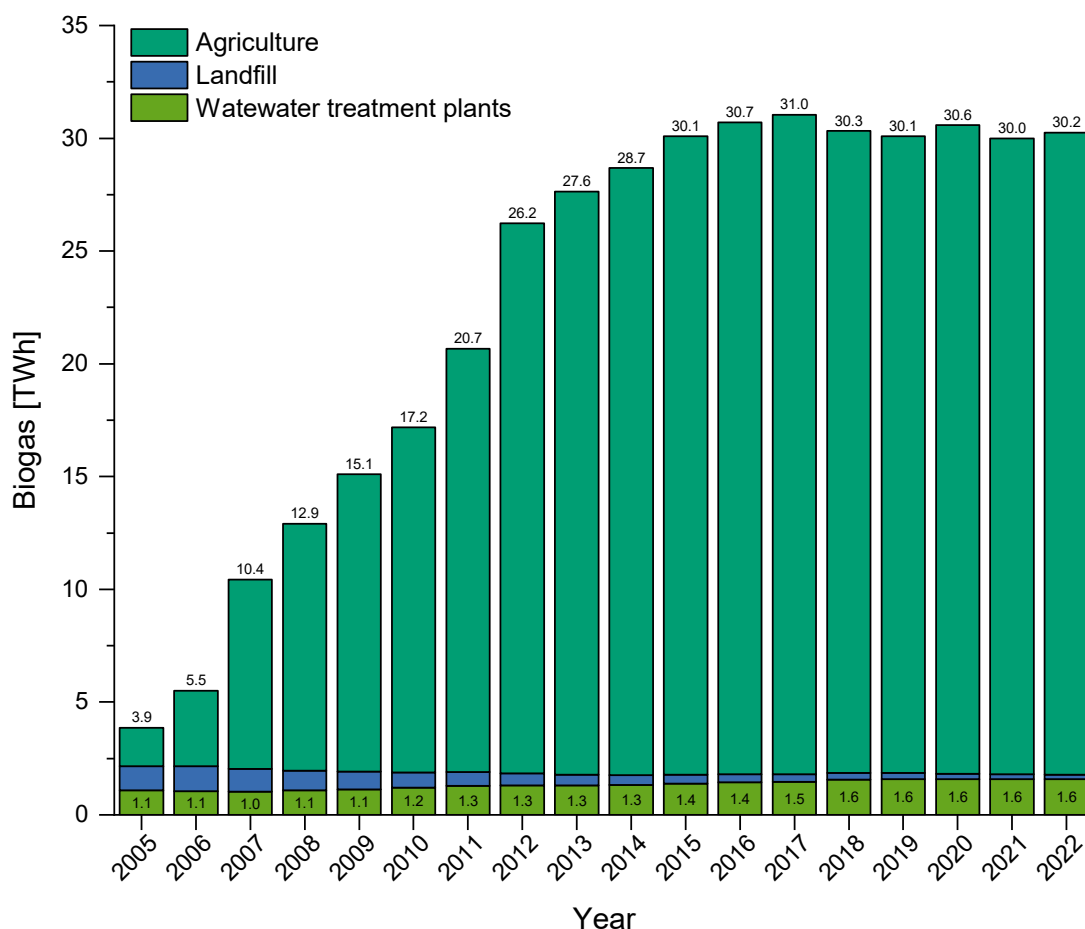


**Figure 2-8:** Gross electricity generation from biogas in Germany from 2005 until 2022 based on the data from German Federal Network Agency [15].

### 2.3.3 Power-to-X projects

Research in the Power-to-X technology is already performed for several decades. Since 2010, the number of Power-to-X projects increased highly. Most projects are in Europe, especially Germany, although interest in the technology is extending [32]. Particularly countries with extensive solar resources are expanding their plans for green H<sub>2</sub> production [25]. The majority of Power-to-X projects were constructed at a laboratory or demonstration scale with plant capacities below 1 MW. So far, the focus of Power-to-X projects was mainly set on water electrolysis and catalytic methanation. [32]

While commercialization started with alkaline electrolysis, most recent projects focused on PEM electrolysis due to its better dynamic operation [32] and only few projects investigated solid oxide electrolysis [27]. Enbridge Gas Inc., in partnership with Cummins Inc., currently operates a 2.5 MW PEM electrolyzer in Ontario, Canada, with

a total plant capacity of 5 MW [48, 49]. In 2021, Air Liquide inaugurated a 20 MW PEM system with four 5 MW electrolyzer units in Bécancour, Canada [50]. Furthermore, within the Normand'Hy project, Air Liquide S.A. is planning to build a 200 MW facility with 5 MW PEM electrolyzer units from Siemens Energy by 2025 in Port-Jérôme, France [51]. A few projects were already performed with solid oxide electrolysis. Within the GrInHy2.0 project, Salzgitter AG and the electrolysis manufacturer Sunfire constructed a 0.72 MW solid oxide electrolyzer in Salzgitter, Germany. According to the operators, the electrolyzer has been operating since 2019 and is the largest solid oxide electrolyzer in the world. [52]

Most working groups of Power-to-X projects, including a methanation step, do not provide detailed information on the reactor type [27]. Catalytic methanation projects mostly applied fixed bed reactors [33], followed by fluidized bed, multi-channel, honeycomb, and packed bed reactors [27]. Biological methanation projects are mostly limited to a power capacity below 1.0 MW, with TBRs being the most applied reactor technology, followed by CSTRs [27]. The Limeco Power-to-Gas plant based on biological methanation was constructed on an industrial scale in Dietikon, Switzerland, by Hitachi Zosen Inova Schmack GmbH and inaugurated in 2022. Electricity generated from waste incineration is used in a PEM electrolysis plant of 2.5 MW capacity. Biogas from the local WWTP is upgraded in a 50 m<sup>3</sup> methanation reactor, but the reactor configuration was not stated. [53, 54] Current information on other existing or planned biological methanation plants reported by Thema et al. [27] and Zavarkó et al. [53] was only limited available and poorly traceable.

### 3. Research significance and hypotheses

This dissertation's core objective was to construct and operate a pilot-scale trickle bed reactor (TBR) under real industrial conditions to identify the TBR potential as an energy conversion and storage technology. This was realized by constructing a TBR with 0.8 m<sup>3</sup> reaction volume installed on the wastewater treatment plant (WWTP) in Garching. Three main research objectives are proposed to improve the methanation performance further and assess the pilot-scale TBR potential.

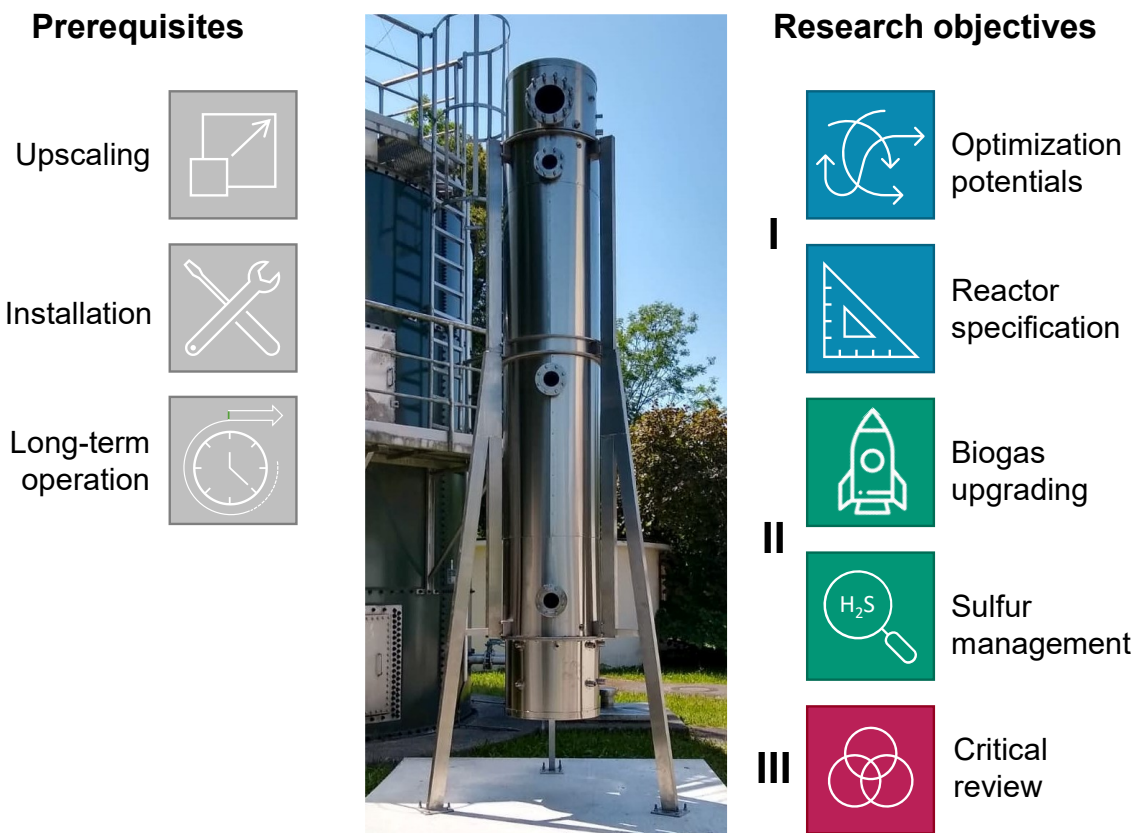


**Figure 3-1:** An overview of prerequisites to enable the investigations of the research objectives.

#### 3.1 Research objective #1

**Applying gas flow experiments in a TBR to identify operational conditions that support plug flow and elucidate optimization potentials in reactor design.**

The methanation performance in TBRs can be improved by approaching the gas flow through the reactor toward plug flow. In an ideal plug flow reactor, all fluid elements in the same cross-section of the tubular reactor have the same gas residence time (GRT)

[55]. A gas flow approaching plug flow conditions maintains a high partial pressure of the feed gases at the gas entrance, which improves the local gas-liquid mass transfer. Furthermore, disruptive gas flow patterns, such as back-mixing, channeling, or bypassing, are reduced. Disruptive gas flow patterns increase the probability that feed gas leaves the TBR without conversion due to short residence time [56]. An increasing height-to-diameter ratio can achieve better plug flow conditions [39]. However, other reactor design properties, such as protruding objects and operational parameters, are expected to influence the gas flow through the reactor, too. Thus, within the first research objective, the pilot-scale reactor was used to identify constructional and operational conditions that support plug flow. A simple and convenient method to receive information on the gas flow behavior is the application of preliminary gas flow experiments, such as tracer tests. Furthermore, gas flow experiments provide information about reactor-specific properties, such as stagnant gas volumes. Within research objective #1, preliminary gas flow experiments using a step input tracer test in a pilot-scale TBR were performed to test hypothesis #1.

***Hypothesis #1:** Operating TBRs with a top-to-bottom gas flow and with a minimized trickling rate achieve flow conditions closest to plug flow.*

Hypothesis #1 is elaborated within Chapter 4. Performing gas flow experiments already in a pilot-scale reactor is expected to better approximate the results for industrial implementations, as smaller reactor volumes can cause measurement uncertainties due to scaling effects. Furthermore, the constructional properties and operating conditions were chosen based on the settings of TBRs for biological methanation, allowing the transfer of the gas flow experiment results. Gas flow experiments were designed to simulate reactor restart conditions after a standby period. Thus, step input tracer tests used a mixture of H<sub>2</sub> and a CO<sub>2</sub> source as feed gases, which displaced the CH<sub>4</sub> inside the reactor. The experiments were repeated two times (n=3) to enable statistical significance. The investigations resulted in **Paper I**.

**Paper I:** *Feickert Fenske, Carolina; Md, Yasin; Strübing, Dietmar; Koch, Konrad (2023): Preliminary gas flow experiments identify improved gas flow conditions in a pilot-scale trickle bed reactor for H<sub>2</sub> and CO<sub>2</sub> biological methanation. In Bioresource Technology 371, p. 128648. DOI: <https://doi.org/10.1016/j.biortech.2023.128648>*

## **3.2 Research objective #2**

**Biogas upgrading in a pilot-scale TBR - Demonstrating the system upscaling and integration under the real field of application.**



The target of research objective #2 is the upscaling of the TBR as energy conversion technology to a pilot-scale level. The research on TBRs has gained increasing interest in recent years, but the startup and operation were mostly performed on a lab-scale level with reactor sizes of below 100 L and in a controlled laboratory environment. Furthermore, most studies used pure CO<sub>2</sub>, but only few studies applied real biogas as CO<sub>2</sub> source in TBRs [57–59]. Raw biogas consists of about 50-70% CH<sub>4</sub>, 30-50% CO<sub>2</sub>, and trace concentrations of impurities, such as H<sub>2</sub>S, NH<sub>3</sub>, and moisture. The high tolerance of methanogenic microorganisms toward impurities makes biological methanation an ideal biogas upgrading technology. However, considering the inert CH<sub>4</sub> content in biogas, TBRs might not reach the same volumetric CH<sub>4</sub> production rate as during the operation with pure CO<sub>2</sub> due to a reduced GRT. Therefore, hypothesis #2.1 targets to achieve a CH<sub>4</sub> production rate in the pilot-scale TBR comparable to previously studied biological methanation reactors but applying biogas as a CO<sub>2</sub> source of over 2 m<sup>3</sup>/(m<sup>3</sup><sub>Reaction volume</sub>·d) with gas grid injection qualities (CH<sub>4</sub> > 96%).

***Hypothesis #2.1:*** *A TBR on a pilot-scale level can upgrade real biogas of a WWTP to gas grid injection qualities (CH<sub>4</sub> > 96%) with CH<sub>4</sub> production rates at full load comparable to previously studied biological methanation reactors applying biogas as a CO<sub>2</sub> source (> 2 m<sup>3</sup>/(m<sup>3</sup><sub>Reaction volume</sub>·d)).*

An essential element for the metabolism of methanogenic archaea is sulfur [46]. The H<sub>2</sub>S present in biogas could be partially used by methanogens as a sulfur source, reducing the H<sub>2</sub>S concentration in the product gas. This would be beneficial as, due to the highly corrosive properties of H<sub>2</sub>S, limitations for gas grid injection are quite strict. Still, none of the studies that applied biogas as CO<sub>2</sub> source investigated the potential of methanogenic archaea to reduce the disturbing H<sub>2</sub>S concentration in the biogas for downstream processes while being consumed by the microorganisms as a sulfur source. Therefore, hypothesis #2.2 suggests that the H<sub>2</sub>S in biogas can be reduced by methanogens while maintaining a sulfur source for their metabolism.

***Hypothesis #2.2:*** *The application of TBRs for biogas upgrading is beneficial to reduce the H<sub>2</sub>S concentration in the product gas (< 100 ppm) and maintain a sulfur source for methanogenic archaea.*

Hypotheses #2.1 and #2.2 are addressed within Chapter 5. To research hypotheses #2.1 and #2.2, the pilot-scale reactor was inoculated with anaerobic sludge of the local digester. The gas load of biogas and H<sub>2</sub> was gradually increased and adjusted according to the desired product gas concentrations. No additional sulfur source was added during hypothesis #2.2 testing to observe if H<sub>2</sub>S can be supplied as the only sulfur source.

The investigations of hypotheses #2.1 and #2.2 resulted in **Paper II**.

**Paper II:** *Feickert Fenske, Carolina; Kirzeder, Franz; Strübing, Dietmar; Koch, Konrad (2023): Biogas upgrading in a pilot-scale trickle bed reactor – Long-term biological methanation under real application conditions. Bioresource Technology 376, p. 128868. DOI: <https://doi.org/10.1016/j.biortech.2023.128868>*

### **3.3 Research objective #3**

**Providing an overview of TBR design and operation for biological methanation and concluding future research needs.**

Since the publications from Burkhardt and Busch [12] in 2013 and Burkhardt et al. [60] in 2015, research on the biological methanation of H<sub>2</sub> and CO<sub>2</sub> in TBRs has received increasing attention. Several review articles provide comprehensive information on biological methanation [40] and biological biogas upgrading [42], but only Sposob et al. [61] published a review article about biological methanation in TBRs. However, since the release of the review article, many new studies about TBRs have been published, and several studies have not been considered in the review article [59, 62–66]. Thus, research objective #3 complement the review of Sposob et al. [61] and give an updated overview of the current status of TBR design and operation. Furthermore, the review compares research article results and presents comparison values to adjust process conditions better. It is expected to support the decision-making for reactor design and operation in future projects and improve the methanation performance.

***Research objective #3:** Providing an overview of TBR design and operation for biological methanation and concluding future research needs.*

Research objective #3 is elaborated within Chapter 6: Within the scope of this study, 35 original research articles researching the biological methanation in TBRs, were reviewed and summarized. Furthermore, the review was supplemented with important information from additional relevant articles. The literature review performed for research objective #3 resulted in the submitted **Paper III**.

**Paper III:** *Feickert Fenske, Carolina; Strübing, Dietmar; Koch, Konrad (2023): Biological methanation in trickle bed reactors - A critical review. Bioresource Technology 385, p. 129383. DOI: <https://doi.org/10.1016/j.biortech.2023.129383>*

The overall summary of the structure of the cumulative dissertation with the corresponding chapters, underlying research objectives and hypotheses, and elaborated publications is provided in Table 3-1.

**Table 3-1:** Dissertation structure summarizing research objectives, hypotheses, and corresponding publications.

Chapter	Research objectives	Hypotheses	Publications
4	Applying gas flow experiments in a TBR to identify operational conditions that support plug flow and elucidate optimization potentials in reactor design.	<b>#1:</b> Operating TBRs with a top-to-bottom gas flow and with a minimized trickling rate achieve flow conditions closest to plug flow.	<b>Paper I</b> Feickert Fenske, C.; Md, Y.; Strübing, D.; Koch, K. (2023), <i>Bioresource Technology</i> , 371, 128648.
5	Biogas upgrading in a pilot-scale TBR - Demonstrating the system upscaling and integration under the real field of application.	<p><b>#2.1:</b> A TBR on a pilot-scale level can upgrade real biogas of a WWTP to gas grid injection qualities (<math>\text{CH}_4 &gt; 96\%</math>) with <math>\text{CH}_4</math> production rates at full load comparable to previously studied biological methanation reactors applying biogas as a <math>\text{CO}_2</math> source (<math>&gt; 2 \text{ m}^3/(\text{m}^3_{\text{Reaction volume}} \cdot \text{d})</math>).</p> <p><b>#2.2:</b> The application of TBRs for biogas upgrading is beneficial to reduce the <math>\text{H}_2\text{S}</math> concentration in the product gas (<math>&lt; 100 \text{ ppm}</math>) and maintain a sulfur source for methanogenic archaea.</p>	<b>Paper II</b> Feickert Fenske, C.; Kirzeder, F.; Strübing, D.; Koch, K. (2023), <i>Bioresource Technology</i> , 376, 128868.
6	Providing an overview of TBR design and operation for biological methanation and concluding future research needs.		<b>Paper III</b> Feickert Fenske, C.; Strübing, D.; Koch, K. (2023), <i>Bioresource Technology</i> 385, 129383.

#### 4. Preliminary gas flow experiments identify improved gas flow conditions in a pilot-scale trickle bed reactor for H<sub>2</sub> and CO<sub>2</sub> biological methanation

With the aim to improve the methanation performance in trickle bed reactors (TBRs) by approaching the gas flow through the reactor toward plug flow, this study tested hypothesis #1.

***Hypothesis #1:** Operating TBRs with a top-to-bottom gas flow and with a minimized trickling rate achieve flow conditions closest to plug flow.*

The first step in this study included planning, constructing, and installing of a TBR with 1 m<sup>3</sup> gas volume at the wastewater treatment plant (WWTP) Garching. Preliminary gas flow experiments with a step input tracer test were performed with the pilot-scale reactor to test hypothesis #1. Before every experiment, the reactor was flushed with CH<sub>4</sub> to mimic restart conditions after extended standby periods. The gas flow experiments elucidated an improved gas flow approaching plug flow when the feed gases of H<sub>2</sub> and a CO<sub>2</sub> source (pure CO<sub>2</sub> and biogas) were introduced from top-to-bottom and when no trickling was applied. An early breakthrough of the feed gases in the reverse direction indicated a channeling or bypassing effect. As the experiments showed that the feed gases were already mixed before entering the reactor and did not separate when flowing through the reactor, the most evident explanation for the breakthrough in the bottom-to-top gas flow direction are density differences between the CH<sub>4</sub> and the lighter feed gases that tend to flow up. While a breakthrough of feed gases is more likely when biological conversion activity is limited, a top-to-bottom gas flow direction is recommended to reduce the risk of a breakthrough. Trickling affected the gas flow to a lesser extent, but with a relatively low hydraulic loading of 0.64 m<sup>3</sup>/(m<sup>2</sup>·h), the effect will likely increase with higher trickling rates. Thus, the tested ***hypothesis #1 can be accepted.***

The gas flow experiments further elucidated the share of unused and stagnant zones, which was identified in the experiments with biogas as CO<sub>2</sub> source to be 19% of the gas volume. The results of the gas flow experiments were published in **Paper I**.

---

This chapter has been published with some editorial changes as follows:

*Feickert Fenske, Carolina; Md, Yasin; Strübing, Dietmar; Koch, Konrad (2023): Preliminary gas flow experiments identify improved gas flow conditions in a pilot-scale*

*trickle bed reactor for H<sub>2</sub> and CO<sub>2</sub> biological methanation. In Bioresource Technology 371, p. 128648. DOI: <https://doi.org/10.1016/j.biortech.2023.128648>*

Author contributions: Carolina Feickert Fenske and Konrad Koch conceptualized the research objective. Yasin Md and Carolina Feickert Fenske conducted the preliminary gas flow experiments. Carolina Feickert Fenske prepared and analyzed the raw data and accomplished the visualization in Origin. Afterward, Konrad Koch and Carolina Feickert Fenske interpreted and discussed the results of the gas flow experiments. Carolina Feickert Fenske wrote the original manuscript, which was later reviewed and edited by Dietmar Strübing and Konrad Koch. All authors approved the final version of the manuscript.

## 4.1 Abstract

Biological methanation of H<sub>2</sub> and CO<sub>2</sub> is a potential energy conversion technology that can support the energy transition based on renewable sources. The methanation performance in trickle bed reactors can be improved by approaching the gas flow through the reactor toward plug flow. Through preliminary gas flow experiments without biological conversion, this study investigated operational and constructional conditions that enhance plug flow in a pilot-scale trickle bed reactor with 1 m<sup>3</sup> gas volume. An improved gas flow was observed when the feed gas was applied in a top-to-bottom direction and when the process liquid was not trickled through the packing bed. Furthermore, the gas flow experiments identified reactor-specific properties, such as unused or dead volumes. Applying gas flow experiments prior to reactor start-up is recommended as a simple and convenient method to identify individual reactor properties and optimization potentials for higher methanation performance.

## 4.2 Introduction

To provide a sustainable and secure power supply based on high shares of volatile renewable energy, long-term and on-demand energy storage technologies are required to stabilize the electricity grid in times of energy overproduction and demand. The existing natural gas grid comprises a huge energy storage potential. Within the Power-to-Gas approach, surplus electrical energy is converted into H<sub>2</sub> by water electrolyzes first. However, the introduction of H<sub>2</sub> into the gas grid is limited depending on national regulations due to safety and economic constraints. Going one step beyond, H<sub>2</sub> can be converted together with a CO<sub>2</sub> source to storable CH<sub>4</sub> ( $4 \text{ H}_2 + \text{CO}_2 \rightarrow \text{CH}_4 + 2 \text{ H}_2\text{O}$ ) through the chemical catalytic or the biological pathway. In biological reactors H<sub>2</sub> and CO<sub>2</sub> are converted by anaerobic microorganisms belonging to the genera of methanogenic archaea. A potential CO<sub>2</sub> source is raw biogas that is typically composed of 50-70% CH<sub>4</sub>, 30-50% CO<sub>2</sub>, and trace amounts of other compounds, such as H<sub>2</sub>S. The methanogenic microorganisms applied in the biological methanation have a high tolerance toward impurities in the feed gas (i.e., H<sub>2</sub>S), reducing the requirements for the pretreatment of the gas. Furthermore, the methanation process in biological reactors is performed at atmospheric pressure and temperatures in the mesophilic or thermophilic range, which allows a simple reactor application and results in comparable low energy requirements for the reactor operation. A major challenge in the biological pathway is the low H<sub>2</sub> gas-to-liquid mass transfer due to the low solubility of H<sub>2</sub> in water. TBRs were identified to improve the mass transfer by a fixed packing bed, providing a high surface area per reactor volume [12]. In contrast to other reactors, the active volume, where the methanation process takes place, is gas-filled. A process liquid serving as a source of

nutrients, but initially also containing most of the methanogenic microorganisms, is trickled over the packing bed aiming for a biofilm formation on the biofilm carriers.

In order to integrate TBRs on an industrial level and to be competitive with other energy conversion concepts, the CH<sub>4</sub> production rate must be increased. One approach to further improve the TBR performance is to optimize the gas flow toward plug flow. In an ideal plug flow reactor, all fluid elements in the same cross-section of the tubular reactor have the same gas residence time (GRT) [55]. Channeling and bypassing effects increase the probability that feed gas leaves the TBR without conversion due to a too short residence time [56]. Furthermore, plug flow conditions maintain a high initial partial pressure of H<sub>2</sub> and CO<sub>2</sub>, supporting the local gas liquid mass transfer. TBRs are constructed with high height-to-diameter ratios to support plug flow [39], but the knowledge about the influence of operational conditions on the gas flow in TBRs for biological methanation is still limited. An approach to elucidate the hydrodynamic interactions in TBRs is the modeling of the fluid flows by computational fluid dynamics (CFD). Such a model was developed by Markthaler et al. [67] and further improved by Markthaler et al. [68]. The advanced model allows the simulation of the gas flow at different gas and liquid residence times, but only few conclusions about reactor operation to improve the methanation performance were drawn.

A simple and convenient method is the application of gas flow experiments, such as tracer tests, which should exclude gas conversion [56]. Gas flow experiment results describe the flow behavior in the reactor at specific operational conditions and provide information about reactor-specific properties, such as dead gas volumes. To the authors' best knowledge, there is no single study yet that has investigated the influence of specific operational conditions on the gas flow behavior of TBRs for biological methanation applying gas flow experiments, such as the tracer test.

The gas flow behavior through the reactor is dependent on the reactor design (e.g., reactor dimensions, geometry, packing bed) and operational parameters (e.g., inlet gas flow rate, temperature, gas mixture). The constructional properties and operating conditions of the reactor in this study were chosen according to settings of TBRs in recently published lab-scale studies [11, 57, 58]. Therefore, it is expected that the main findings of these experiments are generally applicable to other TBRs, too.

The influence of the gas flow direction, flowing downward or upward, on the reactor performance has gained increasing research interest. On a laboratory and pilot-scale, feed gases were introduced into the reactor either from top-to-bottom in a co-current flow direction to the trickling liquid flow [41, 44, 62, 64, 69, 70], from bottom-to-top in a counter-current flow direction to the trickling liquid flow [11, 57] or directly into the

liquid phase [7]. Porté et al. [71] studied the performance of two identical constructed reactors in both flow directions and did not find significant differences in CH<sub>4</sub> production and concentration depending on the flow direction. Next to the gas flow direction, from top-to-bottom or bottom-to-top, the influence of the CO<sub>2</sub> source (pure CO<sub>2</sub> or biogas) and the effect of the process liquid trickling on the gas flow were investigated.

The aim of this study was to conduct preliminary gas flow experiments without biological conversion to collect comparable and repeatable results of operational conditions that support plug flow and identify reactor properties for constructional optimization.

### 4.3 Material and methods

The TBR at pilot-scale was installed by RMEnergy Umweltverfahrenstechnik GmbH (Langenbach, Germany) at the WWTP in Garching (Germany).

#### 4.3.1 Reactor setup

The jacketed TBR was made of stainless steel and had a total length of 4.5 m and an inner diameter of 0.6 m. The reactor was designed with a height-to-diameter ratio of 7.5 to support plug flow conditions. The volume of the trickling liquid in the reservoir at the bottom of the reactor had a minimum filling level of 55 L and a maximum level of 100 L. For the gas flow experiments, water was used as a process liquid to avoid biological conversion of the gases. The total volume of the process liquid used in the experiments was 66 L. The reactor was filled randomly with Hel-X biocarriers of the type HXF12KLL (Christian Stöhr GmbH & Co. Elektro- und Kunststoffwaren KG, Marktrodach, Germany) with a filling length of 3.5 m. A porous stainless-steel plate was integrated to hold the packing bed above the reservoir. The biocarrier were 12 mm long and had a diameter of 12 mm. The specific surface area of the biofilm carriers was 859 m<sup>2</sup>/m<sup>3</sup>. The trickle bed (3.5 m height and 0.6 m diameter) was packed with 0.193 m<sup>3</sup> of biofilm carriers ( $V_P$  in Table 4-1). The filling was performed uniformly with a homogeneous packing density of 160 kg/m<sup>3</sup>. The reactor dimensions are specified in Figure 4-1. The respective volumes were defined and calculated according to Thema et al. [4] and are listed in Table 4-1.

To maintain a constant temperature of 55 °C throughout the reactor, water was circulated through the heating jacket. A thermostat (Vaillant Deutschland GmbH & Co. KG, Remscheid, Germany) controlled the heated water to the required temperature of 55 °C. In addition, the reactor and pipes were thermally insulated to ensure a constant temperature through the reactor.



The gas flow rate at the reactor outlet was measured by a drum-type gas counter (TG20, Dr.-Ing. RITTER Apparatebau GmbH & Co. KG, Bochum, Germany) and the gas concentrations were monitored by a gas analyzer (AwiFLEX Cool+XL, AWITE Bioenergie GmbH, Langenbach, Germany). The gas analyzer was calibrated shortly before the gas flow experiments. Deviations in the gas concentration of  $\pm 1.8\%$  were quoted by the gas analyzer manufacturer at the time the experiments were conducted (i.e., after one year of the device delivery). A temperature sensor outlet (Endress+Hauser GmbH + Co. KG, Weil am Rhein, Germany) was installed at the top of the reactor, at the bottom, and in the gas. Pressure sensors (Endress+Hauser GmbH + Co. KG, Weil am Rhein, Germany) were installed at the top of the reactor and in the gas outlet. Temperature and pressure were monitored and recorded continuously during the experiments.

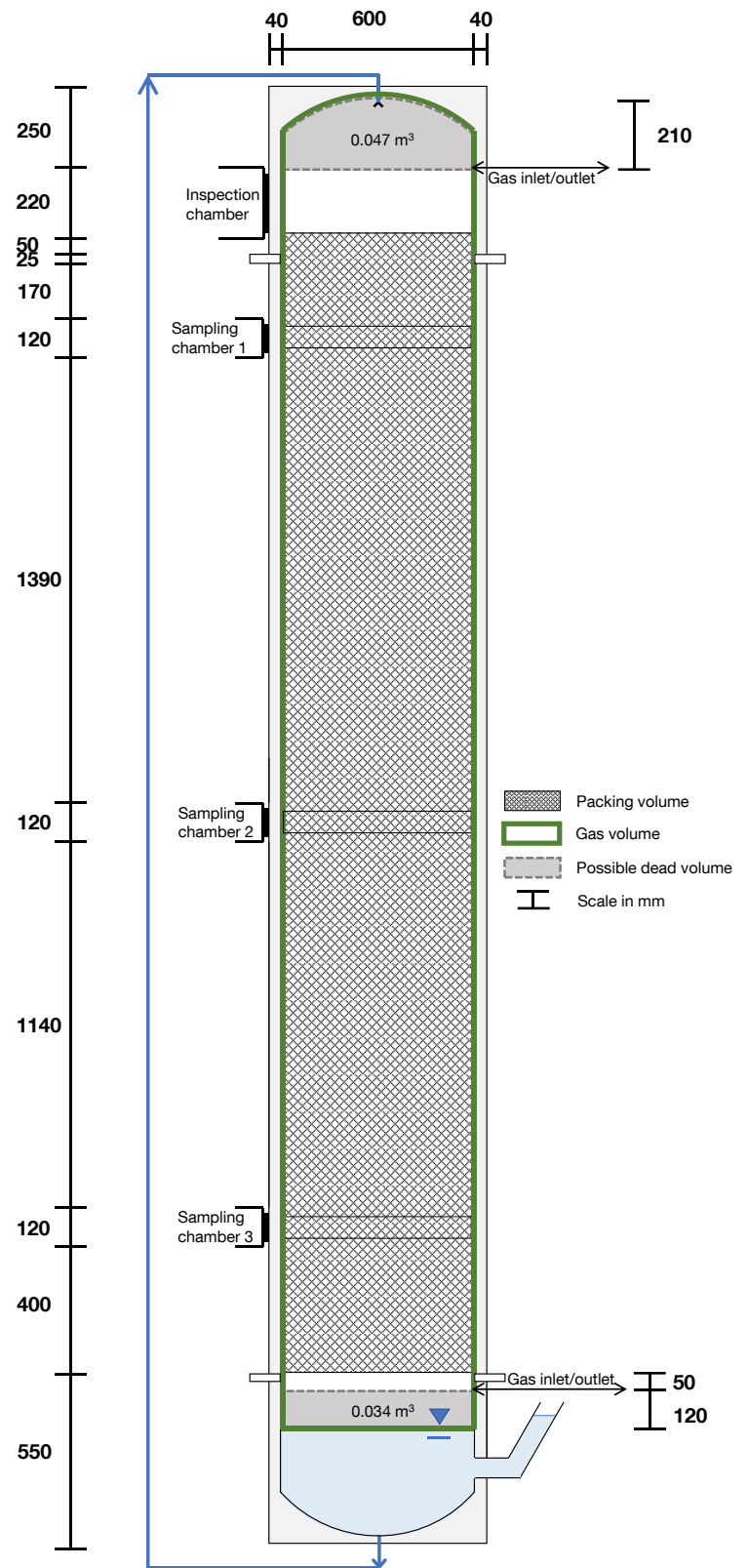


**Figure 4-1:** Dimensions and design of the experimental reactor in mm.

**Table 4-1:** Reactor, liquid, packing and gas volume of the experimental reactor.

	Volume [m <sup>3</sup> ]	Composition [%]
Reactor volume V <sub>R</sub>	1.241	100
Liquid volume V <sub>L</sub>	0.066	5
Packing volume V <sub>P</sub>	0.193	16
Gas volume V <sub>G</sub>	0.982	79

### 4.3.2 Design of gas flow experiment

A step input tracer test was performed to elucidate the hydrodynamics inside the reactor. This method applies a fluid at a specific flow rate and substitutes the flow with another fluid at the same gas flow rate [55]. Before every experiment, the reactor was flushed with CH<sub>4</sub> (Air Liquide Deutschland GmbH, Düsseldorf, Germany; ≥ 99.5 mol %) to mimic restart conditions after a longer standby period. The experiments were conducted with a step input flow of H<sub>2</sub> (Air Liquide Deutschland GmbH, Düsseldorf, Germany; ≥ 99.5 mol %) in combination with a CO<sub>2</sub> source (pure CO<sub>2</sub> (Air Liquide Deutschland GmbH, Düsseldorf, Germany; ≥ 99.7%) or biogas) and performed three times under the same conditions (n = 3). The biogas originating from the full-scale mesophilic digester of the WWTP was obtained from the gas storage tank with a gas composition of 63 ± 1% CH<sub>4</sub>, 37 ± 1% CO<sub>2</sub> and < 200 ppm H<sub>2</sub>S on average.

The H<sub>2</sub> to CO<sub>2</sub> ratio was set to the stoichiometric ratio of 4:1 according to the operational conditions for biological methanation. Because CH<sub>4</sub> was already present in the biogas, the inflow gas composition for the experiments with biogas resulted in a feed gas composition of 59% H<sub>2</sub>, 15% CO<sub>2</sub>, and 26% CH<sub>4</sub>. The mass flow controllers (SmartTrak®100, Sierra Instruments, Monterey, CA, USA) were set for all experiments to the same volumetric inlet gas flow rate Q, which was calculated according to the conditions in the reactor with 55 °C and 1.027 atm (the slightly elevated pressure is caused by the drum-type gas counter used to quantify the product gas) to 1.17 m<sup>3</sup>/h. Both gas streams were merged into a stainless-steel pipe (Ø 2 cm), leading to the reactor. Therefore, the feed gases were already mixed prior to the reactor injection, which resulted in merged gas properties, such as the gas density at the set experimental conditions listed in Table 4-2.

**Table 4-2:** Gas density of H<sub>2</sub>, CO<sub>2</sub>, CH<sub>4</sub> and the mixed feed gas according to the gas compositions at 55°C and the operating pressure of 1.027 atm.

	Density at 55°C [kg/m <sup>3</sup> ]
H <sub>2</sub>	0.077
CO <sub>2</sub>	1.678
CH <sub>4</sub>	0.612
Pure CO <sub>2</sub> experiments: <b>80% H<sub>2</sub> and 20% CO<sub>2</sub></b>	0.397
Biogas experiments: <b>59% H<sub>2</sub>, 15% CO<sub>2</sub> and 26% CH<sub>4</sub></b>	0.456

Experiments with and without trickling were conducted to investigate the impact of trickling on the gas flow. The trickling was achieved by pumping the water of the reservoir to the reactor top with a pulsing flow regime by a membrane pump (NF300, KNF DAC GmbH, Hamburg, Germany) and passing the-water through an axial-flow full cone nozzle (Lechler GmbH, Metzingen, Germany) at a trickling rate of 180 L/h. In all experiments, the reactor was filled with 66 L of water and trickling was applied 30 minutes before the experimental start to ensure wetting of the packing material.

The gas flow to either the top or the bottom of the reactor was designed flexibly to allow for the change of the gas flow direction. The pipes were arranged at the same reactor side and welded with the inner reactor wall (positions and dimensions are illustrated in Figure 4-1).

With a reactor gas volume  $V_G$  of 0.982 m<sup>3</sup>, the theoretical GRT  $\tau$  was calculated to be 50 minutes ( $\tau = \frac{V_G}{Q} = 50.4$  min). The mean GRT  $\bar{t}$  was calculated by the integration of the concentration curve of the outlet gas and determination of the time at the maximum concentration as described in Levenspiel (2012). An overview of the gas flow experiments with the specific operational conditions is provided in Table 4-3. To support the determination between the experiments, the identification codes from Table 4-3 were used in figures and tables.

**Table 4-3:** Overview of gas flow experiments.

Experiment	CO <sub>2</sub>	Biogas	Top-to-bottom	Bottom-to-top	Trickling
T-B_CO <sub>2</sub> _nT	x		x		
B-T_CO <sub>2</sub> _nT	x			x	
T-B_CO <sub>2</sub> _T	x		x		x
B-T_CO <sub>2</sub> _T	x			x	x
T-B_Biogas_nT		x	x		
B-T_Biogas_nT		x		x	
T-B_Biogas_T		x	x		x
B-T_Biogas_T		x		x	

#### 4.4 Results and discussion

The present study investigated the gas flow behavior in a pilot-scale TBR by simulating restart conditions at different reactor operations. Gas flow conditions approaching plug flow are desired as the gas flow with a uniform velocity profile across the radius reduces axial mixing, channeling, and bypassing effects, which limit the reactor performance. Figure 4-2 and Figure 4-3 show the curve progression of H<sub>2</sub>, CO<sub>2</sub>, and CH<sub>4</sub> of the experiments with pure CO<sub>2</sub> and no trickling performed in triplicate as an example to visualize the results of the experiments. The curve progressions of the remaining experiments are visualized in the appendix in Chapter 9.3. The slope length of the curves was defined in the experiment as the time in minutes required to reach a concentration from < 1% to > 98% for H<sub>2</sub> and CO<sub>2</sub> and from > 99% to < 1% for CH<sub>4</sub> of their respective maximum concentration. As the comparison of the curve progressions is relative to each other, the ranges have been identified as the most appropriate for the comparison of the curve progressions. The maximum gas concentrations have not been normalized to 100% to avoid data manipulation. To evaluate the difference between the slope length, a test of significance by a one-way ANOVA (analysis of variance) with post-hoc Tukey HSD (honestly significant difference) was performed using an online application available at [https://astatsa.com/OneWay\\_Anova\\_with\\_TukeyHSD/](https://astatsa.com/OneWay_Anova_with_TukeyHSD/). The results for the slope length correlation of H<sub>2</sub> are listed in Table 4-4, while those for CO<sub>2</sub> and CH<sub>4</sub> can be found in the appendix in Table 9-1 and Table 9-2.

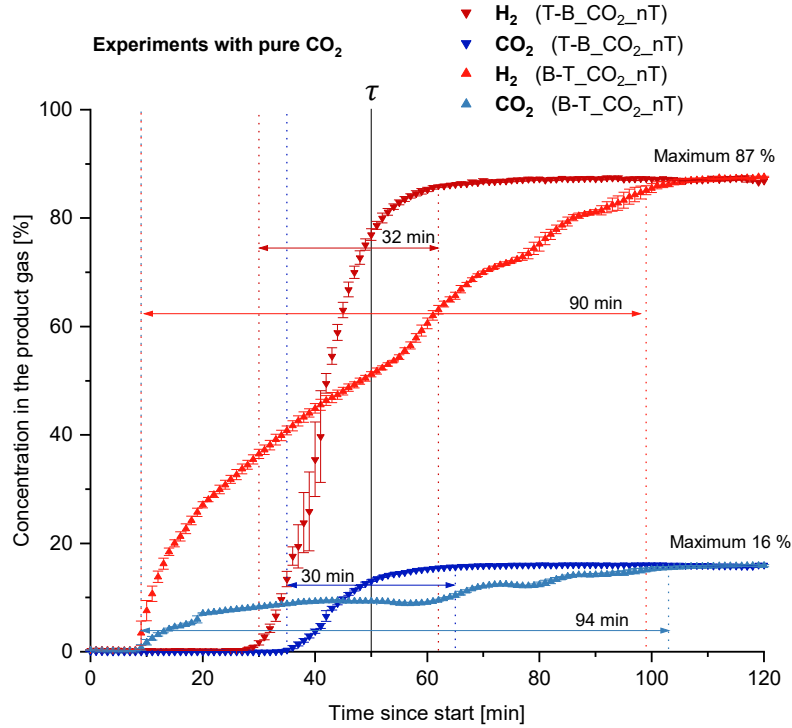


**Figure 4-2:** Curve progression of H<sub>2</sub> and CO<sub>2</sub> (mean ± standard deviation) in the experiments with pure CO<sub>2</sub> and no trickling conducted in three trials (n=3).

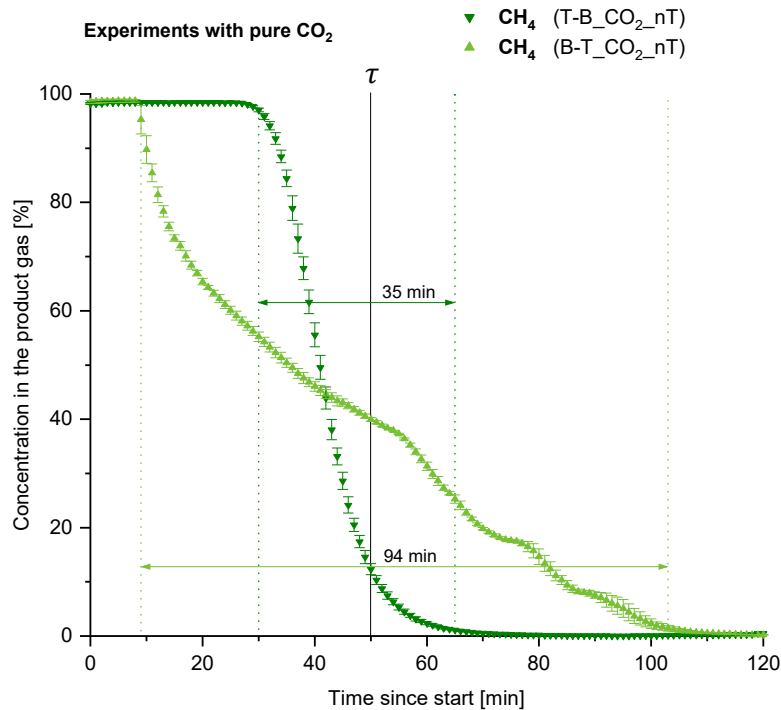


**Figure 4-3:** Curve progression of CH<sub>4</sub> (mean ± standard deviation) in the experiments with pure CO<sub>2</sub> and no trickling conducted in three trials (n=3).

**Table 4-4:** Test of significance by a one-way ANOVA with post-hoc Tukey HSD of the H<sub>2</sub> slope lengths for pure CO<sub>2</sub> (above) and biogas as CO<sub>2</sub> source (below) at a significance level of 5% and 1%, respectively.

	T-B_CO <sub>2</sub> _nT	B-T_CO <sub>2</sub> _nT	T-B_CO <sub>2</sub> _T	B-T_CO <sub>2</sub> _T
T-B_CO <sub>2</sub> _nT		0.001 **	0.001 **	0.001 **
B-T_CO <sub>2</sub> _nT			0.001 **	0.900
T-B_CO <sub>2</sub> _T				0.001 **

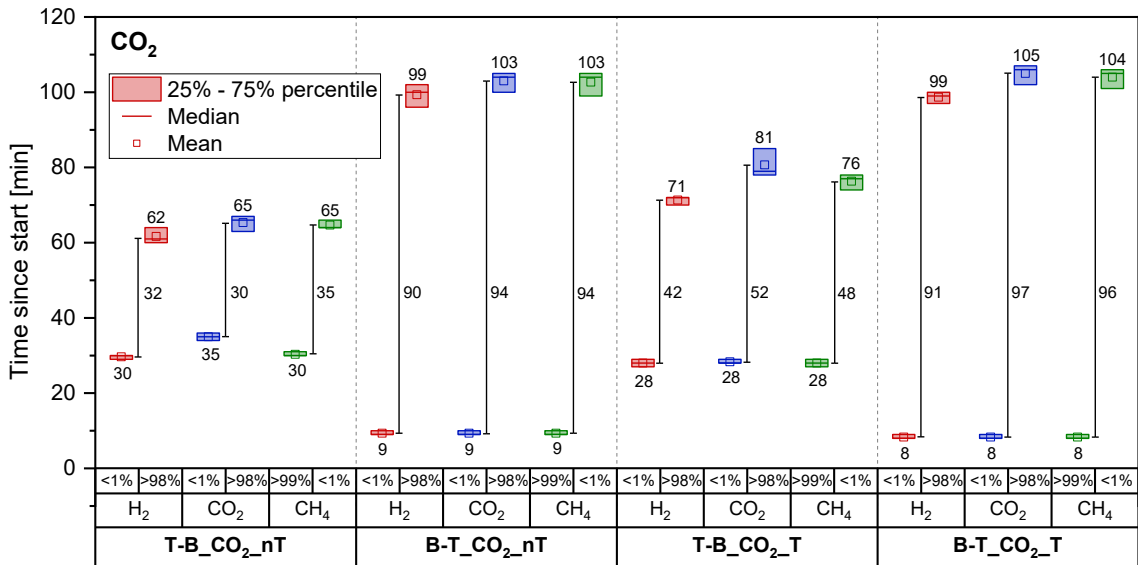
  

	T-B_Biogas_nT	B-T_Biogas_nT	T-B_Biogas_T	B-T_Biogas_T
T-B_Biogas_nT		0.001 **	0.129	0.001 **
B-T_Biogas_nT			0.018 *	0.574
T-B_Biogas_T				0.003 **

p>0.05      insignificant  
 \* p<0.05      significant  
 \*\* p<0.01      highly significant

#### 4.4.1 Effect of gas flow direction on the gas flow behavior

The curve progressions of all experiments are displayed in Figure 4-4 and Figure 4-5. The results of the test of significance presented in Table 4-4 demonstrate that the top-to-bottom gas flow configuration behaves closer to plug flow. Particularly the experiments performed with pure CO<sub>2</sub> as CO<sub>2</sub> source show a considerable difference in the GRTs. The experiments conducted with biogas as CO<sub>2</sub> source in the top-to-bottom configuration show the same characteristics of a gas flow approaching plug flow (Figure 4-5). The comparison of the slope length of the top-to-bottom and bottom-to-top gas flow showed a highly significant difference for H<sub>2</sub> and CH<sub>4</sub>, even if the effect is less intense compared to the pure CO<sub>2</sub> experiments. The slope length comparison of CO<sub>2</sub> is not showing a significant or highly significant difference. This can be attributed to the lower share of CO<sub>2</sub> in the biogas of only 15%, making the curve progression less distinguishable.



**Figure 4-4:** Slope length as the time in minutes that is required to reach a concentration from < 1% to > 98% for H<sub>2</sub> and CO<sub>2</sub>, and from > 99% to < 1% for CH<sub>4</sub> of their respective maximum concentration for experiments performed with pure CO<sub>2</sub> as CO<sub>2</sub> source.

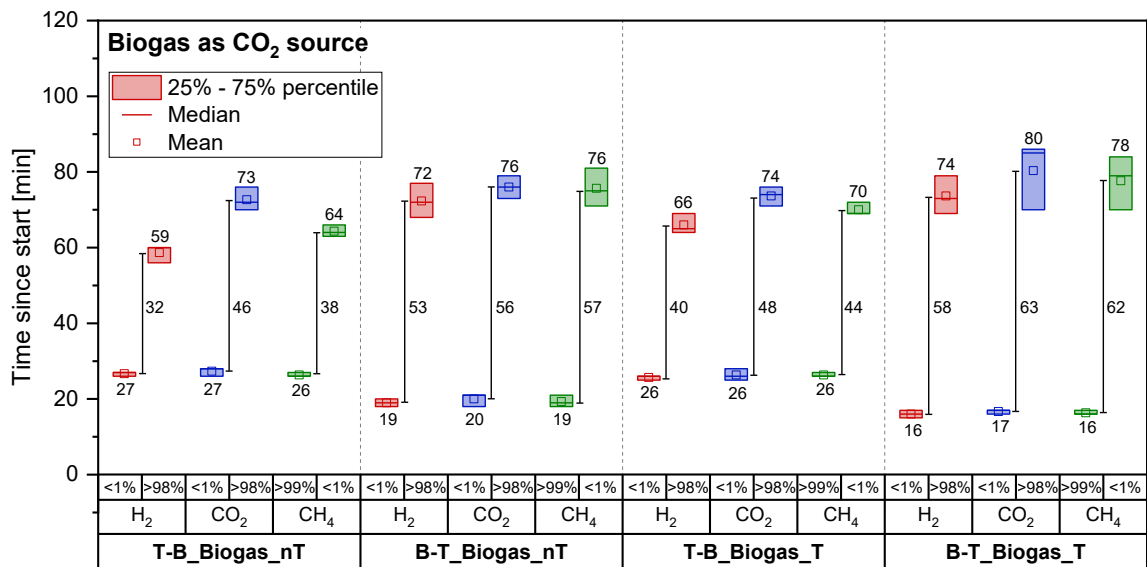


**Figure 4-5:** Slope length as the time in minutes that is required to reach a concentration from < 1% to > 98% for H<sub>2</sub> and CO<sub>2</sub>, and from > 99% to < 1% for CH<sub>4</sub> of their respective maximum concentration for experiments performed with biogas as CO<sub>2</sub> source.

Another interesting observation is that the curve progressions of the single gases in the same experiment show very similar results in slope start, slope end, and slope length. The experiments performed in the bottom-to-top gas flow configuration with pure CO<sub>2</sub> show a quick breakthrough of H<sub>2</sub> and CO<sub>2</sub> after 8 minutes for the experiments with trickling and after 9 minutes without trickling. The breakthrough in the biogas experiments with and without trickling is decelerated and starts after 16 and 19 minutes,

respectively. These observations indicate that the feed gases were already mixed before entering the reactor and flowed through the reactor as one gas mixture. This is an important factor in microbiological conversion as the H<sub>2</sub>/CO<sub>2</sub> ratio keeps locally constant. Moreover, the early breakthrough of the feed gas indicates that a channeling or bypassing effect was a potential reason for the impacted gas flow in the bottom-to-top direction.

An evident explanation for a channeling effect in the bottom-to-top configuration is the density difference between the initial CH<sub>4</sub> gas and the feed gases. As H<sub>2</sub> and CO<sub>2</sub>/biogas are already mixed in the pipes before entering the reactor, the gas properties are mutually dependent. The CH<sub>4</sub> in the reactor with a density of 0.612 kg/m<sup>3</sup> (at 55 °C and a pressure of 1.027 atm) is replaced by the mixed feed gas with an according to the stoichiometric ratio weighted gas density of 0.397 kg/m<sup>3</sup> for the experiments with pure CO<sub>2</sub> and 0.456 kg/m<sup>3</sup> for the experiments with biogas (Table 4-2). In the bottom-to-top gas flow experiments, the “lighter” feed gas likely tends to flow up even faster.

As observed in the experimental results shown in Figure 4-4 and Figure 4-5, the channeling effect in the bottom-to-top gas flow configuration, indicated by an early H<sub>2</sub> and CO<sub>2</sub> breakthrough, is smaller when biogas is applied as CO<sub>2</sub> source. This supports the hypothesis that the gas density difference is responsible for the poor plug flow behavior in the bottom-to-top configuration. The CH<sub>4</sub> content in the H<sub>2</sub>/biogas mixture of 26% (Table 4-2) reduces the gas density differences between the present (CH<sub>4</sub>) and added gas (0.612 kg/m<sup>3</sup> vs. 0.397 kg/m<sup>3</sup> (CO<sub>2</sub>) or 0.456 kg/m<sup>3</sup> (biogas), respectively). Thus, the reduced gas density difference resulted in a lower channeling effect.

Other explanations for the channeling or bypassing effect in the bottom-to-top gas flow experiments, such as a drift of the gas flow due to cross-section constrictions or protruding objects at the bottom part of the reactor, were not evident. The packing bed was filled homogeneously over a length of 3.5 m. The only indicative differences between the top and the bottom of the reactor were the water reservoir below the gas connection at the bottom and the porous stainless steel plate that holds the biocarrier (Figure 4-1). The headspace at the top with 0.047 m<sup>3</sup> is 38% larger compared to the bottom part with 0.034 m<sup>3</sup>. However, no cross-section constriction was identified that could have caused the channeling or bypassing flow pattern in the bottom-to-top configuration.

A gas flow rate of 1.17 m<sup>3</sup>/h results in a relatively low inlet gas velocity of 1.1 mm/s that lies in the range of recent publications of 0.6 mm/s [59] to 1.4 m/s [11]. Even at these low gas velocities, the results indicate that the feed gas behaves as one gas mixture and that there is no gas separation of the lighter H<sub>2</sub> and the heavier CO<sub>2</sub> over time.

Considering the CH<sub>4</sub> concentration in the product gas and the volumetric production rate of recent publications, there are no indications that the gas density difference limits



the methanation process in the bottom-to-top gas flow. Strübing et al. [11] achieved a volumetric CH<sub>4</sub> production rate of up to 15.4 m<sup>3</sup><sub>CH<sub>4</sub></sub>/(m<sup>3</sup><sub>RV</sub>·d) in the bottom-to-top gas flow mode and Strübing et al. [70] the same production rate in the top-to-bottom mode (both at > 95% CH<sub>4</sub>). Porté et al. [71] did not find significant differences in the methanation performance of two identical constructed reactors, one operated in a top-to-bottom and one in bottom-to-top gas flow direction. However, it is expected that the gas density difference will not influence the methanation process as long as the microorganisms are able to convert the feed gas entirely.

The capacity of microbiological conversion is highly influenced by the residence time of the gases in the reactor. The GRT increases with the microbiological conversion of the feed gas to CH<sub>4</sub> due to the volumetric reduction in the methanation process [72]. Assuming a complete feed gas conversion, the gas volume is reduced to one-fifth, which would extend the GRT in this study from 50 minutes to 250 minutes. Therefore, recent publications, reaching CH<sub>4</sub> concentrations of > 98%, might not have yet reached critical GRT to observe a breakthrough of the feed gas. Only if the gas flow rate is higher than the microbiological conversion capacity, the unconverted feed gases will breakthrough in the bottom-to-top gas flow configuration. Based on the results of this study, a reactor operation in the top-to-bottom gas flow configuration, approaching plug flow, would result in a feed gas conversion mainly in the first reactor section. The gas conversion would increase the GRT and therefore allow a higher gas load to further increase the CH<sub>4</sub> production rate.

The results of the gas flow experiments conducted in this study were performed without biological conversion. Important to consider is that the performance of the microbiology (whether in the liquid or on the packing) is not identical throughout the reactor, which might influence the gas conversion and the flow behavior. Porté et al. [71] found higher volatile fatty acid (VFA) concentrations in the reactor operated in top-to-bottom flow. The authors assumed that the comparable low density of H<sub>2</sub> promotes a higher H<sub>2</sub> partial pressure in the liquid for the top-to-bottom gas flow configuration, leading to enhanced homoacetogenesis in the trickling liquid. The gas flow experiments in this study demonstrated that H<sub>2</sub> and the CO<sub>2</sub> source behaved as one gas mixture and did not separate while flowing through the reactor. Therefore, enhanced homoacetogenesis due to a shift of the H<sub>2</sub>/CO<sub>2</sub> ratio, affecting the H<sub>2</sub> partial pressure, is not expected to take place in the reactor of this study.

However, to identify the influence of the microbiological conversion on the gas flow, advanced gas flow experiments measuring the gas concentrations over the reactor length or applying isotope tracing are recommended for future investigations.

#### 4.4.2 Physical effect of trickling on the gas flow behavior

The slope length of the curve progressions performed with trickling of the process liquid is slightly longer compared to the experiments without trickling (Figure 4-4 and Figure 4-5). This indicates that trickling negatively impacts the plug flow. However, according to the test of significance in Table 4-4, a highly significant difference exists only in the slope length of the experiments conducted with pure CO<sub>2</sub> in the top-to-bottom gas flow configuration. As the gas flow performed much closer to plug flow, it is expected that the trickling effect was more visible in the top-to-bottom experiments with pure CO<sub>2</sub>.

The effect of trickling on the gas flow will likely increase with higher trickling rates. The hydraulic loading of the trickling liquid on the packed bed in m<sup>3</sup>/(m<sup>2</sup>·h) known from the conventional wastewater treatment sector [73] is expected to be an appropriate parameter to compare the effect of trickling in TBRs. With a trickling rate of 180 L/h and a packing bed area of 0.28 m<sup>2</sup>, the hydraulic loading on the packed bed with 0.64 m<sup>3</sup>/(m<sup>2</sup>·h) is mostly lower than in recent studies: 0.08 m<sup>3</sup>/(m<sup>2</sup>·h) to 0.28 m<sup>3</sup>/(m<sup>2</sup>·h) in Strübing et al. [11] 1.27 m<sup>3</sup>/(m<sup>2</sup>·h) in Tsapekos et al. [65], 2.99 m<sup>3</sup>/(m<sup>2</sup>·h) in Rachbauer et al. [57] and 7.65 m<sup>3</sup>/(m<sup>2</sup>·h) in Thema et al. [59].

That the gas flow can be significantly influenced by the trickling was also simulated by Markthaler et al. [68]. A high GRT and a central liquid inlet with a relatively high hydraulic loading on the packed bed of 2.01 m<sup>3</sup>/(m<sup>2</sup>·h) to 8.21 m<sup>3</sup>/(m<sup>2</sup>·h) resulted in eddies and circulations of the streamline, which impact the plug flow. Ashraf et al. [74] identified a reduced H<sub>2</sub> conversion and CH<sub>4</sub> production capacity with increasing hydraulic loading of 0.26 m<sup>3</sup>/(m<sup>2</sup>·h) to 5.24 m<sup>3</sup>/(m<sup>2</sup>·h). They assume this to be a result of the high liquid hold-up and a thicker liquid film on the biofilm that reduces the transfer of gas to the methanogens in the biofilm. Also, Ullrich et al. [7] and Ashraf et al. [75] observed a lower CH<sub>4</sub> production rate when trickling was applied or when the trickling rate was increased.

According to Jensen et al. [76], a minimal trickling frequency supports biofilm growth, an essential factor in biofilm-based systems. This is particularly important under thermophilic conditions when biofilm development is known to be quite tricky [77, 78]. For instance, Strübing et al. [11] did not observe any macroscopic biofilm growth in their thermophilic TBR even after 313 days of operation. However, Ashraf et al. [74] identified that no trickling for a long time (~ 84 h) after flushing or flooding the packing bed impacts the methanation performance, but intermittent wetting strategies supply the microorganisms in the biofilm with nutrients. Therefore, keeping the hydraulic loading on the packed bed to a minimum is expected to be beneficial for both, gas flow conditions and biofilm formation.

Besides to the investigation of the axial gas flow, tracer tests can be applied to identify the liquid flow when trickling is applied [55]. A homogeneously distributed liquid flow is an important prerequisite to ensure complete wetting and growth of biofilm on the packing bed. Experiments focusing on the liquid flow might identify further optimization potentials.

#### 4.4.3 Effect of dead volumes on the gas residence

The mean GRTs  $\bar{t}$  in the experiments laid between 37 to 45 minutes, while the theoretical GRT  $\tau$  based on the entire reactor volume and the gas load was 50 minutes (Figure 4-6). This can most likely be explained by unused and dead volumes in the reactor [56]. Dead, unused, or stagnant volumes reduce the GRT in the reactor. The active flown volume can also be reduced during reactor operation, e.g., by clogging of the packing bed with biofilm. Identifying the active flown-through volume and the location of dead and unused zones can highlight optimization potentials in the reactor design.

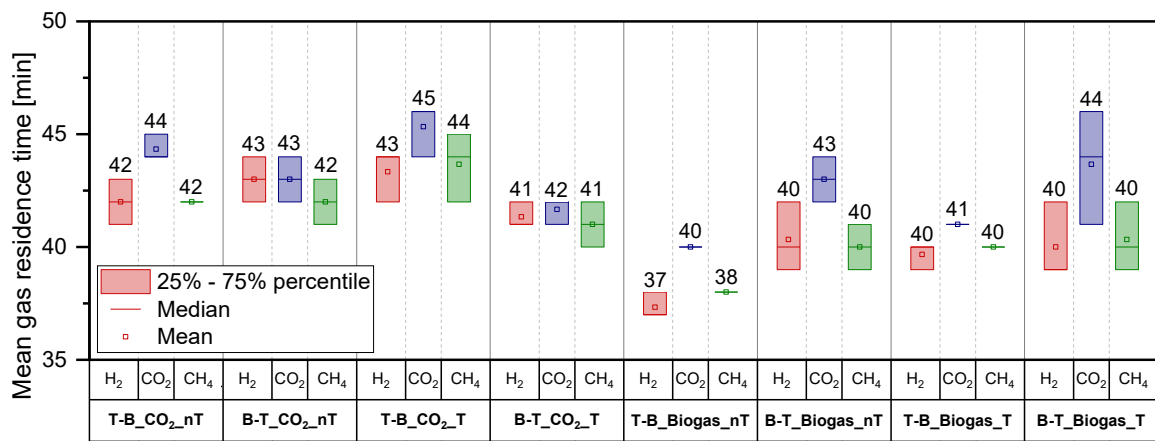


**Figure 4-6:** Mean GRTs of H<sub>2</sub>, CO<sub>2</sub>, and CH<sub>4</sub>.

With an average mean GRT of 43 minutes in the experiments with pure CO<sub>2</sub>, the gases passed through only 0.86 m<sup>3</sup> of the reactor volume, and 12% of the available gas volume was not used. In the biogas experiments with an average mean GRT of 40 minutes, 0.8 m<sup>3</sup> of the reactor volume was passed through, and 19% of the available gas volume was not used. The differences of 1 to maximum 3 minutes between the mean residence time of the single gases can be attributed to the measurement deviations of the gas analyzer (1.9%) and the gas concentration recording interval once per minute. As the maximum turning point of the gas concentration integral curve is the point where the fastest changes in gas concentrations take place, small deviations in the GRT due to a too short recording interval are very likely.

Potential dead volumes might be the volume above the gas pipe at the top and the volume below the gas pipe at the bottom of the reactor that cover 0.081 m<sup>3</sup> or 8% of the

gas volume (Figure 4-1). However, the position of the gas pipe at the bottom was designed to ensure a safety distance to the reservoir, avoiding the entrance of process liquid into the gas pipe. The gas pipe at the top has not been installed in the reactor head to avoid conflicts with the spraying nozzle for a homogenous trickling. Other dead volumes are expected in potential void spaces of the packing bed near the reactor wall.

The evidence that the feed gas (H<sub>2</sub> and CO<sub>2</sub>/biogas) behaves as one mixed gas is also visible in the calculations of the mean GRTs. The mean GRTs of all gases lie very close to each other. Only the mean GRTs of CO<sub>2</sub> are slightly longer, with 1-2 minutes in the experiments with pure CO<sub>2</sub> and 1-4 minutes in the experiments with biogas. A potential reason for this delay might be the CO<sub>2</sub> fraction that dissolved in the process liquid. With a CO<sub>2</sub> solubility in water of 16.72 mmolCO<sub>2</sub>/L according to the temperature dependent Henry constant (at 55 °C, 1.027 atm, and with 20% CO<sub>2</sub> for the pure CO<sub>2</sub> experiments and 15% for the biogas experiments) [79], 5.96 L of CO<sub>2</sub> would dissolve in the 66 L process liquid in the experiments with pure CO<sub>2</sub> and 4.47 L of CO<sub>2</sub> in the experiments performed with biogas (owing to the lower CO<sub>2</sub> partial pressure in the gas phase). With an inlet CO<sub>2</sub> gas flow rate of 4 L/min in the experiments with pure CO<sub>2</sub> and 3 L/min in the experiments with biogas, a delay of 1.5 minutes can be explained if CO<sub>2</sub> was dissolved in the process liquid right after the gas injection.

The experiments performed with pure CO<sub>2</sub> as CO<sub>2</sub> source show slightly longer mean GRTs compared to the biogas experiments. As in the experiments with pure CO<sub>2</sub> a final CO<sub>2</sub> concentration in the product gas of only 16% (Figure 4-2) instead of the expected 20% was reached, the CO<sub>2</sub> mass flow controller was probably not optimally calibrated. A small deviation can be explained by the fraction of CO<sub>2</sub> that dissolves in the process liquid, which would be 1.2% after two hours. This corresponds to a behavior of a reactive tracer substance in the reactor analysis and will understandably not impact the residence time behavior [56]. A lower total gas flow rate in the experiments performed with pure CO<sub>2</sub> would explain the prolonged mean GRTs in the reactor. However, the comparison of the experiments is relative to each other, wherefore systematic errors in the data evaluation and uncertainties of the gas analyzer are not affecting the conclusions drawn from the biogas and the CO<sub>2</sub> experiments results, respectively.

Overall, the gas flow experiments in this study were identified as simple and convenient method to identify operational and constructional reactor conditions that enhance plug flow. Conducting gas flow experiments before reactor inoculation allows the determination of the active flow through gas volume and shows to which extent H<sub>2</sub> and the CO<sub>2</sub> source were mixed before entering the reactor. However, to identify the microbiological influence on the gas flow advanced experiments during reactor operation are recommended. Comparing the gas flow, before and after the inoculation is expected

to deepen the knowledge on fluid dynamics in TBRs and provide explanations for reactors achieving low CH<sub>4</sub> production rates.

## 4.5 Conclusion

Gas flow experiments in a pilot-scale TBR with 1 m<sup>3</sup> gas volume prove that the feed gases of H<sub>2</sub> and a CO<sub>2</sub> source flow through the reactor as one gas mixture with mutual gas properties. The gas flow experiments highlighted optimization potentials in the reactor design and identified operational conditions to improve the methanation performance. An improved gas flow approaching plug flow was observed when the feed gases were introduced from top-to-bottom and when no trickling was applied. A breakthrough of the feed gases caused by gas density differences is only expected when the microbiological conversion activity is limited.

## 4.6 Acknowledgements

The authors are thankful for the funding of this study by the Bavarian Ministry of Economic Affairs, Energy and Technology (Grant: BE/19/03). In addition, the cooperation within the Network TUM.Hydrogen and PtX is acknowledged.

## 5. Biogas upgrading in a pilot-scale trickle bed reactor – Long-term biological methanation under real application conditions

With the aim of investigating upscaling effects and the biogas upgrading potential under the real field of application, the pilot-scale trickle bed reactor (TBR) at the wastewater treatment plant (WWTP) Garching was inoculated and operated on a long-term. The biogas upgrading potential was tested with research hypothesis #2.1.

**Hypothesis #2.1:** *A TBR on a pilot-scale level can upgrade real biogas of a WWTP to gas grid injection qualities ( $CH_4 > 96\%$ ) with  $CH_4$  production rates at full load comparable to previously studied biological methanation reactors applying biogas as a  $CO_2$  source ( $> 2 \text{ m}^3/(\text{m}^3_{\text{Reaction volume}} \cdot \text{d})$ ).*

In **Paper II**, proof of concept was demonstrated with the TBR operation for nearly 450 days, including two extended standby periods. Biogas was used as  $CO_2$  source, which already contained a significant  $CH_4$  content of  $63\% \pm 1\%$  and thus shortened the gas residence time. During the reactor operation, decreasing pH levels due to volatile fatty acid (VFA) accumulation was a critical challenge that limited the application of higher gas loads. However, a  $CH_4$  production of over  $2 \text{ m}^3/(\text{m}^3_{\text{RV}} \cdot \text{d})$  with gas grid injection qualities ( $CH_4 > 96\%$ ) was already reached 17 days after reactor inoculation. Therefore, **hypothesis #2.1 can be accepted**. After testing different strategies to control the pH level, long-term biogas upgrading with a  $CH_4$  production of  $6.1 \text{ m}^3/(\text{m}^3_{\text{RV}} \cdot \text{d})$  and gas grid injection quality ( $CH_4 > 96\%$ ) was achieved, which corresponds to a gas load of  $42.7 \text{ m}^3/(\text{m}^3_{\text{RV}} \cdot \text{d})$ . The results of the reactor operation give evidence that even higher gas loads can be applied by improved pH control, favoring the growth of hydrogenotrophic methanogens and improving biofilm formation.

Furthermore, **research hypothesis #2.2** is addressed: *The application of TBRs for biogas upgrading is beneficial to reduce the  $H_2S$  concentration in the product gas ( $< 100 \text{ ppm}$ ) and maintain a sulfur source for methanogenic archaea.*

No additional sulfur source was added at the beginning of the reactor operation to test if  $H_2S$  could be supplied as the only sulfur source. During stable methanation, when gas conversion rates of over 99% were achieved, the biogas  $H_2S$  concentration of about 200 ppm was reduced by half. However, the accumulation of VFA indicated that the  $H_2S$  content in the biogas was probably too low to cover the methanogenic demand completely. Furthermore, Strübing et al. [11] reported a limited gas conversion when

sulfide concentrations were below 0.02 mM. Thus, with increasing gas loads, Na<sub>2</sub>S was added as an alternative sulfur source, which increased the sulfide concentrations in the process liquid but also resulted in a high formation of H<sub>2</sub>S gas. Thus, ***hypothesis #2.2 cannot be accepted*** from a long-term perspective.

---

This chapter has been published with some editorial changes as follows:

*Feickert Fenske, Carolina; Kirzeder, Franz; Strübing, Dietmar; Koch, Konrad (2023): Biogas upgrading in a pilot-scale trickle bed reactor – Long-term biological methanation under real application conditions. Bioresource Technology 376, p. 128868. DOI: <https://doi.org/10.1016/j.biortech.2023.128868>*

Author contributions: Konrad Koch performed the funding acquisition. Konrad Koch, Dietmar Strübing, and Carolina Feickert Fenske planned the pilot-scale TBR and its integration into the infrastructure of the WWTP. Konrad Koch and Carolina Feickert Fenske were responsible for the planning approval and monitored the pilot-scale reactor construction and installation. Furthermore, they developed the research objective. Franz Kirzeder and Carolina Feickert Fenske conducted the long-term operation and analyzed the samples. Carolina Feickert Fenske processed the measurement data, accomplished the visualization in Origin, and wrote the original manuscript. Konrad Koch and Dietmar Strübing reviewed and edited the manuscript. All authors approved the final version of the manuscript.

## 5.1 Abstract

The biological methanation of H<sub>2</sub> and CO<sub>2</sub> in trickle bed reactors is one promising energy conversion technology for energy storage, but experiences at pilot-scale under real application conditions are still rare. Therefore, a trickle bed reactor with a reaction volume of 0.8 m<sup>3</sup> was constructed and installed in a wastewater treatment plant to upgrade raw biogas from the local digester. The biogas H<sub>2</sub>S concentration of about 200 ppm was reduced by half, but an artificial sulfur source was required to completely satisfy the sulfur demand of the methanogens. Increasing the NH<sub>4</sub><sup>+</sup> concentration to > 400 mg/L was the most successful pH control strategy, enabling stable long-term biogas upgrading at a CH<sub>4</sub> production of 6.1 m<sup>3</sup>/(m<sup>3</sup><sub>RV</sub>·d) with gas grid injection quality (CH<sub>4</sub> > 96%). The results of this study with a reactor operation period of nearly 450 days, including two shutdowns, represents an important step toward the necessary full-scale integration.

## 5.2 Introduction

In order to advance geopolitical energy independence and meet climate objectives, the European Commission has the target of accelerating the EU energy transition to renewable sources. By 2030, at least 40% of the EU's energy mix are intended to be covered by renewable energy [1]. Due to the intermittent and fluctuating availability of renewable energy, conversion and storage technologies are required for a safe and sustainable energy supply. For mid- and long-term purposes, energy can be stored as synthetic natural gas converted by Power-to-Gas. In this concept, unused electricity generated from renewable sources produces H<sub>2</sub> through water electrolysis. To improve the storage and application properties by generating biomethane identical to natural gas, H<sub>2</sub> can be further converted, in combination with CO<sub>2</sub>, into CH<sub>4</sub> and water ( $4\text{H}_2 + \text{CO}_2 \rightarrow \text{CH}_4 + 2\text{H}_2\text{O}$ ).

A CH<sub>4</sub>-rich product gas reaching synthetic natural gas quality can be fed into the existing gas grid, thus providing a huge energy storage capacity. Regulations on the gas quality for gas grid injection are nationally specific. For instance, in Germany a CH<sub>4</sub> concentration of > 95% is required according to the DWA set of rules DWA-M 361 [4]. The conversion of H<sub>2</sub> and CO<sub>2</sub> can be achieved through catalytical methanation, or by methanogenic microorganisms (methanogens) through a bioprocess. Reactors used for biological methanation are typically operated in a mesophilic to thermophilic temperature range of about 35 to 75 °C and at ambient pressure [8]. One factor limiting CH<sub>4</sub> production in biological systems is the low solubility of H<sub>2</sub> [9]. Among various reactor designs, TBRs were proven to achieve high performance while enabling flexible operation on demand [70]. TBRs are filled with gas and packed with a high surface area material. Process liquid is pumped to the reactor top and trickled over the packing bed to



supply the biofilm formed on the carrier material with essential macro nutrients and trace elements. The high volumetric surface area of the packing material and a gas flow approaching plug flow improve the mass transfer between the feed gases and the immobilized or suspended methanogenic microorganisms.

During recent years, an increasing number of studies on TBRs for biological methanation have been published, but the research has mostly been limited to small-scale reactors of up to 70 L operated in a laboratory environment [11, 60, 65]. Reactor upscaling and implementation at real application conditions are the necessary next steps in order to identify the TBR potential for energy conversion and storage technology. Promising implementation sites include biogas or WWTPs because biogas can be used as a CO<sub>2</sub> source. Biological methanation converts CO<sub>2</sub> to generate additional CH<sub>4</sub> instead of removing CO<sub>2</sub>, as performed in established biogas upgrading facilities (e.g., water scrubbing and physical absorption). In addition to a CO<sub>2</sub> content of 30-50%, biogas also consists of 50-70% CH<sub>4</sub>, which flows as inert gas through the methanation reactor, thus reducing the feed gas residence time (GRT). Furthermore, raw biogas typically contains compounds in trace concentrations, e.g., H<sub>2</sub>S, NH<sub>4</sub><sup>+</sup>, and moisture. Methanogens have a high tolerance to impurities in the feed gas (i.e., H<sub>2</sub>S), thus rendering gas pretreatment unnecessary for biological methanation. Given that methanogens need sulfur for metabolism [46], several studies added an artificial sulfur source like Na<sub>2</sub>S to the process liquid in TBRs [11, 57, 59]. So far, little is known about potential sulfur sources and optimal sulfur concentrations. For purposes of gas grid injection, H<sub>2</sub>S needs to be reduced to the national-specific thresholds because its highly corrosive nature can cause damage to gas network infrastructure [42]. The present study seeks to investigate the potential of H<sub>2</sub>S as a sulfur source while reducing the final H<sub>2</sub>S concentration in the product gas.

Integrating the TBR technology into WWTP infrastructure offers several advantages. Biogas can already be upgraded at the point of origin, and local resources can be used as inoculum and nutrient sources. Several studies applied biogas as CO<sub>2</sub> source, but the TBR system integration under real application conditions has thus far only been investigated by Jønson et al. [44]. The latter installed an electrolysis unit and two TBRs having 1 m<sup>3</sup> of reaction volume (RV) on a biogas plant, thus upgrading raw biogas to synthetic natural gas quality. A successful technology application was achieved, but some information is not presented regarding infrastructure integration and reactor operation, e.g., the H<sub>2</sub>S effect on methanation.

More upscaling projects under industrial operational conditions are required to demonstrate the potential of biological methanation in TBRs as an energy conversion technology. In this study, a pilot-scale TBR with a reaction volume of 0.8 m<sup>3</sup> was constructed at the WWTP Garching in Germany to upgrade the locally produced biogas

to synthetic natural gas quality. A detailed description is provided of the TBR construction, integration, and operation under real application conditions. Long-term operation at CH<sub>4</sub> production rates and synthetic natural gas quality within the range of published results were targeted in order to prove successful reactor upscaling. Several reactor management strategies were therefore tested to stabilize the pH level, e.g., the addition of buffer solutions and the adaptation of the H<sub>2</sub>/CO<sub>2</sub> feed gas ratio. Using a low H<sub>2</sub>S concentration in the biogas of only < 200 ppm should enable identification of whether a reduction in the concentration is possible, while also completely satisfying the sulfur demand of the methanogens. Furthermore, the cause for VFA accumulation, pH control strategies, and the requirement for nutrients were discussed comprehensively.

### **5.3 Material and Methods**

The biogas upgrading was performed in a pilot-scale TBR installed by RMEnergy Umweltverfahrenstechnik GmbH (Langenbach, Germany) at the WWTP in Garching (Germany).

#### **5.3.1 Reactor setup and system integration into the wastewater treatment plant**

The reactor design, dimensions, and TBR technical equipment were previously described in Feickert Fenske et al. [80]. The TBR setup, including the most important control and measurement devices, is illustrated in Figure 5-1.

Biogas originating from the full-scale WWTP mesophilic digester was used as a CO<sub>2</sub> source, with a gas composition of  $63 \pm 1\%$  CH<sub>4</sub>,  $37 \pm 1\%$  CO<sub>2</sub>, and < 200 ppm H<sub>2</sub>S. The biogas is used at the WWTP to generate electricity and heat by a combined heat and power unit. Excess biogas is stored in a low-pressure biogas tank (25-250 mbar) and, at a specific filling level, biogas is compressed and introduced to a high-pressure biogas tank (0.5-9.5 bar). These local conditions were beneficial to TBR operation because a connection between the high-pressure biogas tank and the TBR enabled facilitated control of the biogas flow, thus avoiding additional compression of the biogas. H<sub>2</sub> was obtained from gas bottles (Air Liquide Deutschland GmbH, Düsseldorf, Germany;  $\geq 99.5$  mol %). Based on the gas flow experiment results previously performed [80], H<sub>2</sub> and biogas were introduced at the top of the reactor, flowing to the bottom in a co-current direction to the trickling liquid flow in order to approach plug flow conditions. The product gas was cooled by a heat exchanger and conveyed to a condensate trap to eliminate water vapor prior to the gas counter (TG20, Dr.-Ing. RITTER Apparatebau GmbH & Co. K.G., Bochum, Germany). After the biogas upgrading process, the product gas was introduced to the low-pressure biogas tank.

An overflow device was connected to the trickling medium reservoir to discharge excess process liquid generated by both metabolic water production and the supply of a nutrient medium. A minimum reservoir filling level of about 50 L was required to close the overflow pipe, ensuring that no gas escaped. The maximum filling level was limited to a volume of about 100 L to avoid the entrance of process liquid into the outlet gas pipe. The filling volume in the reservoir was measured by a transparent pipe, and the minimum and maximum filling levels were monitored by rod sensors. The reactor was operated slightly above atmospheric pressure (gauge pressure:  $73 \pm 32$  mbar) in order to overcome the pressure in the low-pressure biogas tank. The process liquid was circulated in an external loop using a centrifugal pump (VMD1090, Verder Deutschland GmbH & Co. KG, Haan, Germany) to avoid the accumulation of particles potentially able to clog the system (e.g., the trickling nozzle). A membrane pump (NF300, KNF DAC GmbH, Hamburg, Germany) was applied to trickle the process liquid over the biocarrier material at a trickling rate of 180 L/h. Flow meters were installed in the trickling cycle and the mixing cycle to monitor the flow rates. Furthermore, gas flow rates, gas concentrations (in the educt and product gas), temperature, pressure, and pH were monitored and recorded continuously during reactor operation.

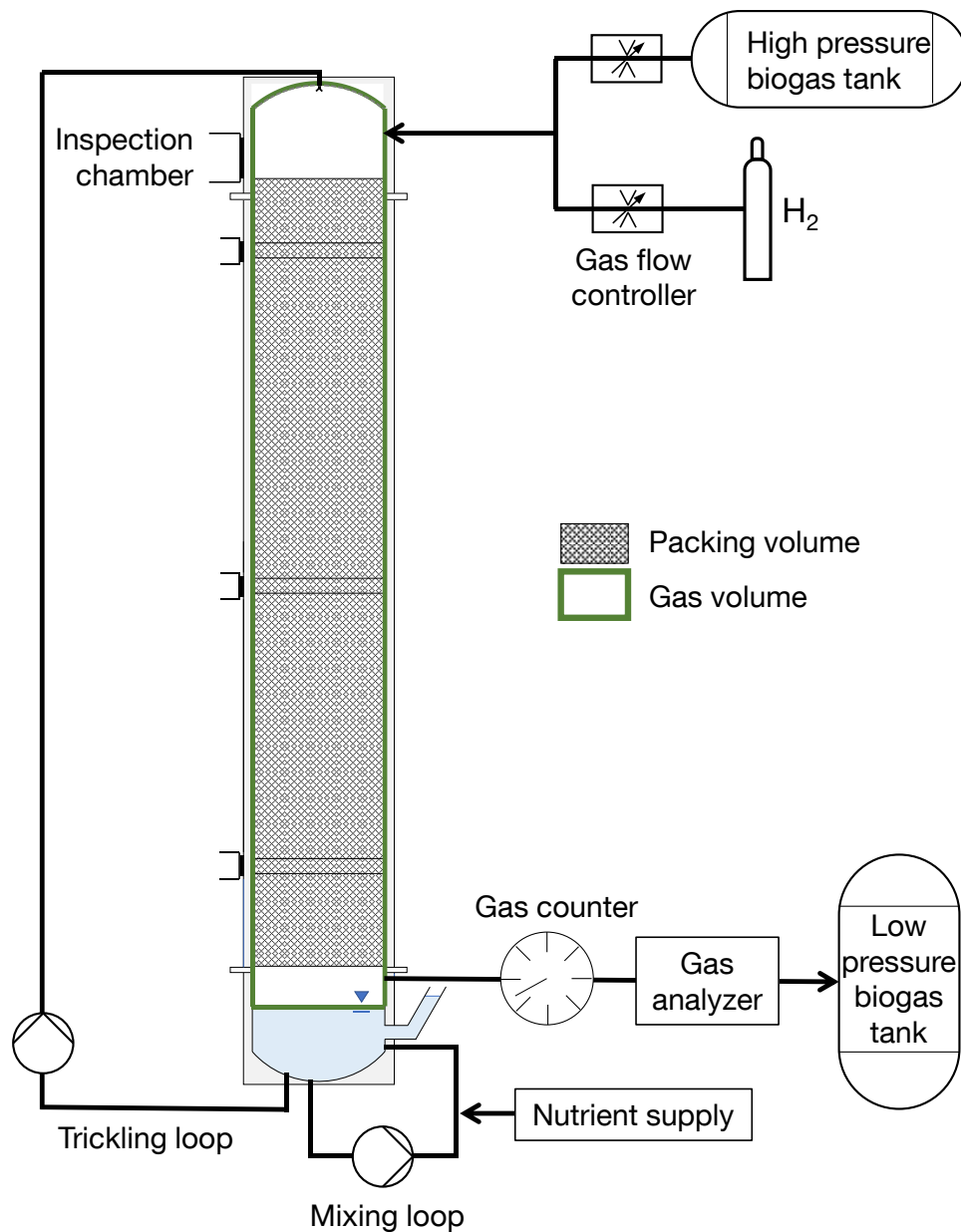


**Figure 5-1:** Setup of the TBR system, including the most important control and measurement devices.

### 5.3.2 Inoculation and operating conditions

About 63 L of sieved (< 125  $\mu\text{m}$ ) anaerobic sludge from the local mesophilic full-scale anaerobic digester was used for reactor inoculation. The reactor was first flushed with N<sub>2</sub> for both safety reasons and to provide anaerobic conditions. The reactor was operated at thermophilic temperatures ( $56 \pm 2$  °C at the reactor bottom and  $53 \pm 2$  °C at the reactor top). H<sub>2</sub> and biogas were introduced into the reactor at an H<sub>2</sub>/CO<sub>2</sub> feed gas ratio between 3.75 to 4.19. The feed gas rate was increased stepwise, with the CH<sub>4</sub> content in the product gas being the key parameter. Digester supernatant (reject water of digester effluent) in combination with a nutrient stock solution (supplementing the digester

supernatant with additional trace elements required by the methanogenic microorganisms) was used as a nutrient medium. Digester supernatant was added to the process liquid at a rate of 2 - 14.5 L/d. The same nutrient stock solution adopted from Taubner and Rittmann [81] and Strübing et al. [11] (18.40 mM  $\text{MgCl}_2 \cdot 6\text{H}_2\text{O}$ , 10.06 mM  $\text{FeCl}_2 \cdot 4\text{H}_2\text{O}$ , 0.17 mM  $\text{CoCl}_2 \cdot 6\text{H}_2\text{O}$ , 0.33 mM  $\text{NiCl}_2 \cdot 6\text{H}_2\text{O}$ , 1.01 mM  $(\text{NH}_4)_6\text{Mo}_7\text{O}_{24} \cdot 2\text{H}_2\text{O}$  and 5.0 g/L EDTA) was supplied at a rate of 40 - 100 mL/d. The digester supernatant and the nutrient stock solution were mixed in a separate tank, from where the mixed liquid was pumped to the reservoir by a dosing pump (VE1-C, Verder Liquids BV, Vleuten, Netherlands). The amount of nutrient stock solution added to the digester supernatant was calculated according to the metabolic water production ( $1.6 \text{ L}_{\text{H}_2\text{O}}$  per  $\text{m}^3 \text{ CH}_4$  produced) and the daily addition of digester supernatant, ensuring a constant nutrient concentration in the process liquid. Concentrations of trace elements,  $\text{NH}_4^+$ , and VFA of the digester supernatant and of the nutrient substitution are listed in Table 5-1.

**Table 5-1:** Trace element,  $\text{NH}_4^+$ , and VFA concentrations of the digester supernatant and the nutrient stock solution.

	Digester supernatant	Nutrient stock solution
Fe [ $\mu\text{g/L}$ ]	$363 \pm 83$	5,618
Co [ $\mu\text{g/L}$ ]	<10	99
Ni [ $\mu\text{g/L}$ ]	<10	592
Mo [ $\mu\text{g/L}$ ]	<10	31
$\text{NH}_4^+$ [mg/L]	$1,526 \pm 166$	-
VFA [mg/L]	$101 \pm 13$	-

### 5.3.3 Monitoring and experimental analysis

$\text{CH}_4$ ,  $\text{H}_2$ ,  $\text{CO}_2$ , and  $\text{H}_2\text{S}$  concentrations in the raw biogas and product gas were measured constantly once per minute over the experimental period, with some interruptions in the measurement of the gas analyzer during reactor maintenance and due to breaks in the product gas flow caused by fluctuating pressure in the reactor. The gas concentrations were normalized to 100%. The gas inflow of  $\text{H}_2$  and biogas, pH, temperatures, and pressure were monitored and recorded continuously once per minute. Due to communication issues with the pH sensor, the pH measurements first started on day 27. The  $\text{CH}_4$  production was calculated based on the  $\text{CH}_4$  gas flow rate at the outlet ( $Q_{\text{CH}_4,\text{out}}$ ) and the  $\text{CH}_4$  gas flow rate at the inlet ( $Q_{\text{CH}_4,\text{in}}$ ) at standard conditions ( $0^\circ\text{C}$ ; 1 atm), and the reaction volume ( $V_{\text{RV}}$ ), where the methanation reaction takes place

according to the definition of Thema et al. [4], ( $\text{CH}_4$  production =  $(Q_{\text{CH}_4,\text{out}} - Q_{\text{CH}_4,\text{in}}) / V_{\text{RV}}$ ).

Thema et al. [4] proposed to use the reactor volume ( $V_{\text{R}}$ ) instead of the reaction volume to specify the  $\text{CH}_4$  production rate describing plant productivity. However, most TBR studies have referred to the  $\text{CH}_4$  production rate per reaction volume  $V_{\text{RV}}$ . To contextualize the results of this study, the performance of the pilot-scale reactor was linked to the  $\text{CH}_4$  production rate per reaction volume  $V_{\text{RV}}$ . According to the definition by Thema et al. [4], reaction volume  $V_{\text{RV}}$  was calculated as the gas volume within the packing bed ( $0.827 \text{ m}^3_{\text{gasvolume}}/\text{m}^3_{\text{packing bed}}$ ). Table 5-2 provides an overview of the volumes to enable further comparison. If the intention is to compare reactor performance per reactor volume  $V_{\text{R}}$ , the results of this study can be divided by a factor of 1.540 ( $1.241/0.806=1.540$ ).

**Table 5-2:** Reactor, liquid, packing, gas and reaction volume of the experimental reactor.

	Volume [m <sup>3</sup> ]	Composition [%]
Reactor volume $V_{\text{R}}$	1.241	100
Liquid volume $V_{\text{L}}$	0.025-0.080	2-6
Packing volume $V_{\text{P}}$	0.193	16
Gas volume $V_{\text{G}}$	0.968-1.023	78-82
Reaction volume $V_{\text{RV}}$	0.806	65

The  $\text{CH}_4$  gas flow rate at the reactor outlet was calculated according to the stoichiometric conversion of the gas inflow and verified intermittently by gas counter measurements, when recently calibrated. Due to recurring cooling thermostat failures, the water vapor in the product gas was not always fully removed and condensed in the gas counter. Uncertainties in the measurements were reduced by regular calibration of the gas counter and verification with the theoretical product gas flow.

Given that several studies provided only the GRT as the ratio of the gas volume ( $V_{\text{G}}$ ) and the feed gas rate ( $Q_{\text{in}}$ ) ( $\text{GRT} = V_{\text{G}} / Q_{\text{in}}$ ), it was also calculated in this study. The process liquid was collected and analyzed at similar reservoir filling level conditions once to twice weekly. The sum of VFA and the  $\text{NH}_4^+$  concentrations were measured by photometric cuvette tests (Hach Lange GmbH, Düsseldorf, Germany). Total solids and volatile solids were measured following standard methods [82]. To better understand the composition of the VFAs, selected samples were analyzed in a gas chromatography flame ionization detector (GC-FID) for individual VFA determination (acetic acid, propionic acid, isobutyric acid, butyric acid, iso-valeric acid, valeric acid, hexanoic acid, and heptanoic acid).

The hourly average of the CH<sub>4</sub>, H<sub>2</sub>, CO<sub>2</sub>, and H<sub>2</sub>S concentrations, the CH<sub>4</sub> production rate, the inert CH<sub>4</sub> flow rate, and the pH level were calculated to visualize and interpret the reactor performance.

## 5.4 Results and discussion

The present study investigated the system integration and the biological methanation performance of a pilot-scale TBR at industrial conditions in a WWTP by applying raw biogas as a CO<sub>2</sub> source. Figure 5-2 shows the development of the inlet gas flow rate, the CH<sub>4</sub> produced, and the total CH<sub>4</sub> gas flow rate per V<sub>RV</sub> during start-up and long-term operation (days 0 – 447). Also depicted are the product gas concentrations (CH<sub>4</sub>, H<sub>2</sub>, and CO<sub>2</sub>), as well as pH level, VFA, and NH<sub>4</sub><sup>+</sup> concentrations in the process liquid, along with the daily addition of digester supernatant.

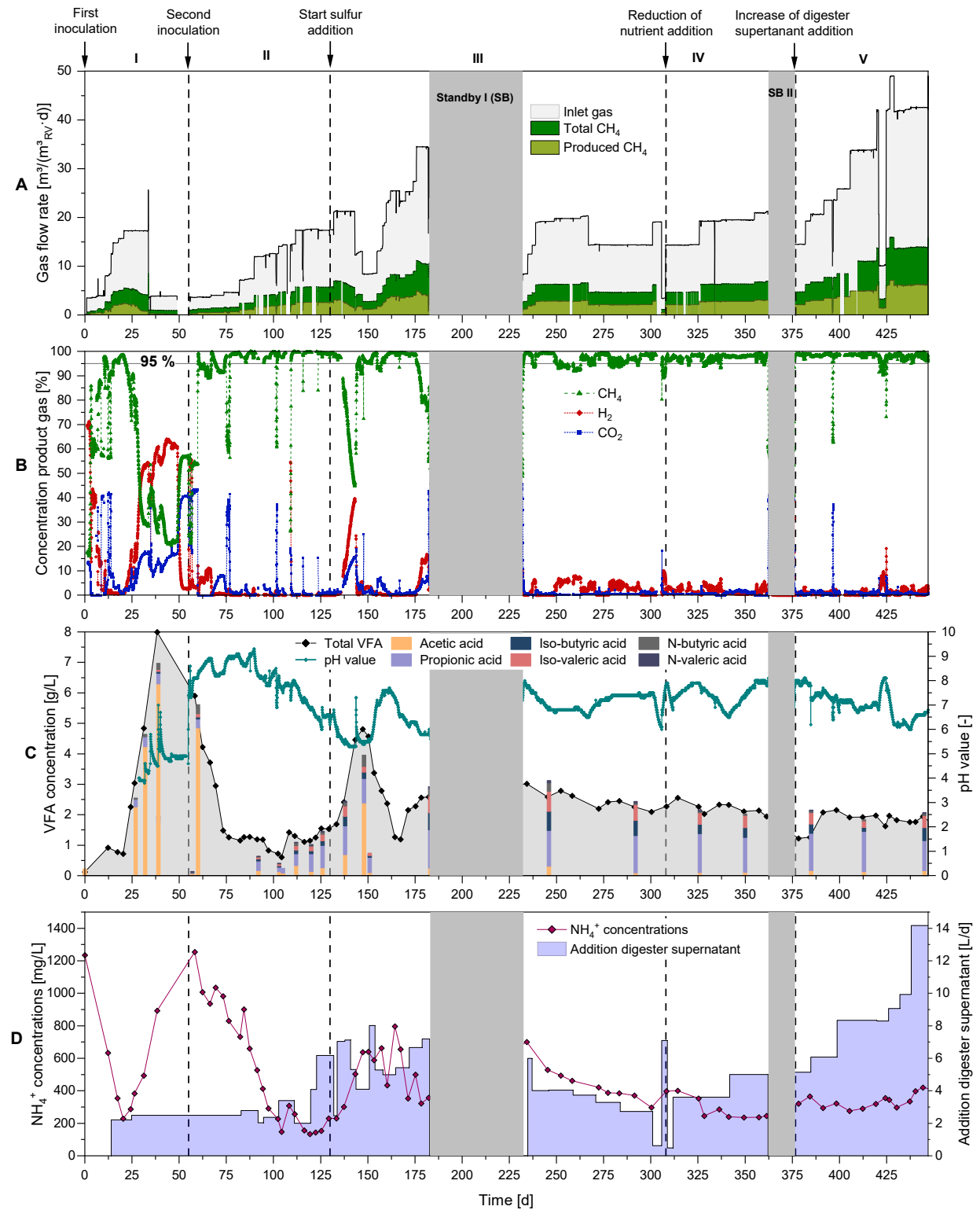


**Figure 5-2:** Development of the inlet, the produced  $\text{CH}_4$  and the total  $\text{CH}_4$  gas flow rates (A), product gas concentrations (B), pH level and VFA concentrations (C),  $\text{NH}_4^+$  concentration in the process liquid, and the daily addition of digester supernatant (D). The reactor start-up was performed in phase I, and a reinoculation was required in phase II. In phase III, the addition of an artificial sulfur source was started, and in phase IV, the



nutrient stock solution addition was reduced to half amount. Finally, the addition of digester supernatant was increased in phase V.

#### 5.4.1 Reactor start-up and technical challenges

The biological methanation in phase I started directly after the initial inoculation (day 0). The CH<sub>4</sub> concentration in the product gas was already over 80% on day 3. The feed gas inflow was continuously increased until day 32, when the CH<sub>4</sub> concentration in the product gas started to decrease. An extremely low process liquid pH level (pH level recording started on day 25) and high VFA concentrations of up to 8 g/L, particularly acetic acid, were measured during this period. Decreasing pH levels, combined with an accumulation of VFA, have been reported by several other studies during reactor start-up and when the gas load was increased too fast [11, 57, 58, 66]. The microbiological community analysis of Cheng et al. [83] and Asimakopoulos et al. [64] identified a high abundance of acetogenic bacteria in correlation with acetate accumulation, verifying the gas conversion through the homoacetogenesis pathway. Homoacetogens have a higher tolerance against elevated H<sub>2</sub> partial pressures than methanogens [84]. Therefore, the gas conversion through the homoacetogenesis pathway was probably favored at increasing gas loads.

However, as long as the VFA production is similar to their conversion rate to CH<sub>4</sub>, the pH level will not be greatly affected. Furthermore, the existing buffer capacity of the process liquid (mainly characterized by the NH<sub>4</sub><sup>+</sup>/NH<sub>3</sub> equilibrium) can stabilize the pH level [66]. The decreasing pH levels in phase I verified that the buffer capacity was already exhausted. The metabolic water produced during methanation has reduced the buffer capacity. The dilution effect in TBRs is more pronounced since the process liquid volume is typically much smaller than the reaction volume [11]. When a critical pH level for methanogenic activity below 6.0 was reached at day 32, the CH<sub>4</sub> concentration dropped drastically. To prove the hypothesis that mainly the low pH level inhibited the methanogens, NaOH (8 M) was added to the reactor on days 27, 32, and 39, thus elevating the pH level for just a couple of hours. The CH<sub>4</sub> concentration raised rapidly when the pH level increased, but the effect was weaker after each addition, even when increasing the dosage. Neither a continuous addition of a phosphate pH buffer solution from day 29 on, nor the addition of fresh nutrient medium sustainably stabilized the pH of the process liquid at this stage. One major advantage of TBRs is that the inoculation and start-up process can be performed quickly and with little effort due to a relatively low process liquid volume. Therefore, a second inoculation was done on day 55 with 60 L of sieved (< 355 µm) anaerobic sludge. A larger sieve pore size was used as no clogging was observed after the first inoculation (and to reduce the time and effort for sieving).

Several operational changes were applied during further reactor operation. After running dry, the NF300 membrane pump (KNF DAC GmbH, Hamburg, Germany) used for trickling was replaced by an EXTRONIC membrane pump (ProMinent GmbH, Heidelberg, Germany) on day 56. This reduced the trickling rate from 180 L/h to about 84 L/h, which was expected to improve the gas flow closer to plug flow as identified in preliminary gas flow experiments [80]. Unexpected high and fluctuating pressures in the low-pressure biogas tank of up to 248 mbar led to an uncontrolled overflow of process liquid through the passive overflow device. Therefore, the overflow pipe was sealed on day 117, and excess process liquid was removed manually every two to three days over a valve at the bottom of the reactor, thereby maintaining a volume in the reservoir between 25 and 80 L. The nutrient medium was added continuously, but, due to the changing filling levels in the reservoir, process liquid characteristics were expected to vary slightly, depending on the mixing ratio of nutrient medium and metabolic water. Sampling was performed when removing excess trickling media. Although the impact on the measured concentration is assumed to be negligible, continuous removal of the process liquid is recommended for future applications.

#### 5.4.2 pH control measures

After the second inoculation, CH<sub>4</sub> concentrations in the product gas increased rapidly with a few drops in the CH<sub>4</sub> concentrations when the feed gas ratio was not optimally. During operational phase II, the stepwise load increase was performed more slowly, giving the methanogens more time to adapt to the new conditions. Furthermore, a buffer solution (K<sub>2</sub>HPO<sub>4</sub>) was constantly added to the mineral medium from day 105 in order to buffer the process liquid, with a final concentration of 86 mM. In phase II, the gas load was increased until reaching a CH<sub>4</sub> production rate of 2.6 m<sup>3</sup>/(m<sup>3</sup><sub>RV</sub>·d) at day 122. However, by increasing the gas load, the pH level again decreased constantly. When a pH level < 5.6 was reached on day 136, the CH<sub>4</sub> concentration in the product gas again dropped drastically.

pH control was identified to be the key challenge during the entire TBR operation, particularly when the gas load was increased. Given ongoing reactor operation, a shift of the VFA distribution from acetic acid (being the most abundant) to longer chain acids was observed, e.g., propionic acid, iso-butyric acid and iso-valeric acid (Figure 5-2C). The accumulation of VFA may be a result of (1) decay of biomass [85], (2) degradation of organic material introduced through the digester supernatant, and (3) homoacetogenesis with subsequent chain elongation [86]. At a COD concentration in the digester supernatant of 1000 ± 100 mg/L, only a fraction of the VFA production can be explained through the degradation of organic material. Furthermore, the COD in the digester supernatant is known to be rather of recalcitrant nature [87].

Tsapekos et al. [84] identified an accumulation of propionic and iso-butyric acid when the  $H_2$  partial pressure was increased. Inanc et al. [88] suggested that this effect is not directly caused by an increased  $H_2$  partial pressure, but by a shift of the dominant microorganisms. In addition, studies by Strübing et al. [34] and Jønson et al. [44] reported propionic acid to be the most abundant. Since both studies applied comparably high gas loads, the elevated  $H_2$  partial pressure probably favored the growth of VFA producers over time. Further research, e.g. applying stable carbon isotope labeling, is recommended in order to identify the pathways for VFA production [89]. However, the total VFA concentration of  $2.12 \pm 0.7$  g/L with high shares of propionic acid did not limit the gas conversion as long the pH level was higher than 6. When considering that stoichiometrically 2.1  $L_{H_2}$  are consumed to form one gram of propionic acid, and that per liter of metabolic water 2.5  $m^3_{H_2}$  are converted, the loss in the removed liquid per gram propionic acid amounts to only 0.08% of the fed  $H_2$ .

However, future investigations should still focus on pH control measures and hydrogenotrophic methanogens enrichment in order to further increase the gas loads.

#### 5.4.2.1 Increasing the sulfur concentration

A limiting factor for the hydrogenotrophic methanogens during phases I and II was probably the low concentration of sulfur in the process liquid provided only by the  $H_2S$  content in the biogas. Strübing et al. [11], Thema et al. [59], and Cheng et al. [83] reported a positive effect by adding  $Na_2S$  to the process liquid. Strübing et al. [11] identified limiting gas conversion conditions when sulfide concentrations were below 0.02 mM. Figure 5-3 illustrates the  $H_2S$  concentration in the biogas and in the product gas for two specific periods. The comparison of the  $H_2S$  concentration in biogas and product gas is valid when  $H_2$  and  $CO_2$  are almost entirely converted at  $CH_4$  concentrations in the product gas of > 98%, resulting in nearly equal volumetric gas flow rates for biogas and the product gas according to the stoichiometric ratio, since one mole of  $CO_2$  in the raw biogas is replaced by one mole of  $CH_4$  in the product gas:  $4 H_2 + CO_2 + CH_{4,inert} \rightarrow CH_{4,produced} + 2H_2O (liq.) + CH_{4,inert}$ .

Figure 5-3 demonstrates that the  $H_2S$  concentration in the product gas of about 75 ppm during days 78 to 82 was reduced to half of the  $H_2S$  concentration in the raw biogas, with 150 ppm. However, it is expected that the relatively low  $H_2S$  concentration in the biogas (< 200 ppm) was too low to cover the sulfur demand by hydrogenotrophic methanogens completely. With an  $H_2S$  solubility in water of 53.22  $mmol_{H_2S}/(L \cdot atm)$  at 55 °C, the  $H_2S$  concentration in the liquid was 0.01 mM, which was even lower than the minimum sulfur concentration of 0.02 mM reported by Strübing et al. [11]. To test the insufficient sulfur hypothesis, an external sulfur source of  $Na_2S \cdot 9H_2O$  (0.1 M) was added by a VP2-R peristaltic pump (Verder Liquids BV, Vleuten, Netherlands) to the process

liquid from day 130 on at a flow rate of 370 - 700 mL/d, to a final concentration of 0.2 – 1.4 mM. After the addition, a fraction of Na<sub>2</sub>S was directly converted to H<sub>2</sub>S, as demonstrated from days 131 to 135 in Figure 5-3, resulting in H<sub>2</sub>S concentrations in the product gas exceeding the measurement limit of the sensor (250 ppm). The H<sub>2</sub> content in the product gas corroded the H<sub>2</sub>S sensor of the gas analyzer over time, rendering an exchange of the H<sub>2</sub>S sensor on day 334.

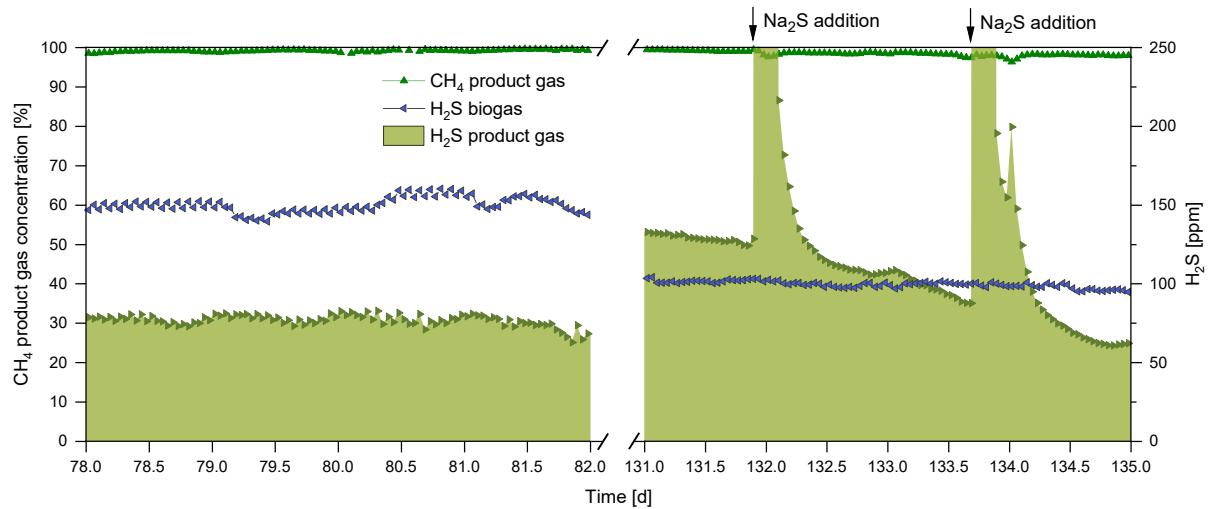


**Figure 5-3:** Development of H<sub>2</sub>S concentrations in the biogas and product gas when the CH<sub>4</sub> concentration in the product gas was > 98%.

After a drop in the CH<sub>4</sub> concentration on day 136 because too low pH levels were already reached prior to initiation of the Na<sub>2</sub>S addition, the gas load was decreased, leading to a recovery of the CH<sub>4</sub> content. The gas load was able to be steadily increased after adjustments in the Na<sub>2</sub>S supply to a more uniform and regular addition from day 153 on. Rising pH levels and decreasing VFA concentrations provided evidence that the addition of Na<sub>2</sub>S supported the performance of methanogens. The gas load was increased until day 176, then reaching CH<sub>4</sub> production rates of 4.8 m<sup>3</sup>/(m<sup>3</sup><sub>RV</sub>·d) at grid injection gas quality. Even when the pH level again started to decrease, the Na<sub>2</sub>S addition was maintained during phases III to V, i.e., expecting a long-term improvement by ensuring sufficient sulfur availability.

However, given an H<sub>2</sub>S limit in synthetic natural gas for the German gas grid injection of 5 ppm [4], the addition of Na<sub>2</sub>S even increased the gas treatment requirement for H<sub>2</sub>S removal. Identifying optimal sulfur concentrations, sulfur supply strategies, and alternative sulfur sources, e.g. biogas with higher H<sub>2</sub>S concentrations, should be part of future research in order to reduce the requirement for Na<sub>2</sub>S addition.

#### 5.4.2.2 Changing the H<sub>2</sub>/CO<sub>2</sub> feed gas ratio

Another factor able to influence the pH level is the fraction of CO<sub>2</sub> that dissolves in the aqueous phase, depending on the CO<sub>2</sub> partial pressure. Ashraf et al. [75] identified adapting the H<sub>2</sub>/CO<sub>2</sub> feed gas ratio to below 4 as being more effective than the addition of a buffer media in order to control the pH level to below 8.5. Decreasing the H<sub>2</sub>/CO<sub>2</sub> ratio of the feed gases to below 4 resulted in a higher CO<sub>2</sub> partial pressure, whereby more CO<sub>2</sub> dissociated in the liquid, leading to lower pH levels. The present research tested counteracting the decreasing pH trend by changing the H<sub>2</sub>/CO<sub>2</sub> feed ratio to higher than 4. An H<sub>2</sub>/CO<sub>2</sub> feed gas ratio of about 3.8 resulted in an almost complete gas conversion to CH<sub>4</sub>. On day 248, the H<sub>2</sub>/CO<sub>2</sub> feed gas ratio was changed to > 4, which stabilized the pH level to 6.8, as illustrated in Figure 5-4. All other operational conditions, such as the GRT, were kept constant, as a result other influences which could have stabilized the pH were able to be excluded. However, the deviation from the optimal H<sub>2</sub>/CO<sub>2</sub> ratio resulted in unconverted H<sub>2</sub> in the product gas, which negatively impacted the product gas quality to CH<sub>4</sub> concentrations below 95%. It is expected that changing the H<sub>2</sub>/CO<sub>2</sub> feed gas ratio is not a long-term solution for controlling the pH level. Therefore, the H<sub>2</sub>/CO<sub>2</sub> ratio was reset after two weeks (on day 262) to nearly optimal conditions, leading again to a decreasing pH level. The influence of the CO<sub>2</sub> partial pressure on the pH level was also clearly demonstrated from day 396 to 397, as shown in Figure 5-4, with respect to which only the H<sub>2</sub> supply was stopped for about nine hours. The pH level decreased abruptly from 7.3 to 6.4 when the H<sub>2</sub> inflow stopped, then recovered again to the initial level within several hours after the break in H<sub>2</sub> supply.

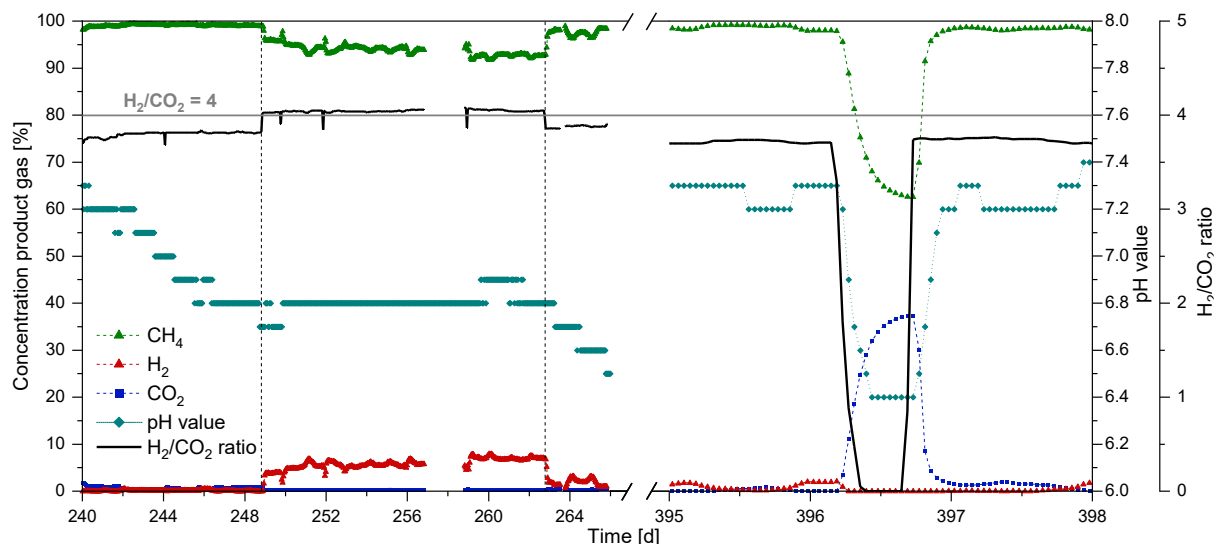


**Figure 5-4:** Development of the pH in the process liquid and the product gas concentrations (CH<sub>4</sub>, H<sub>2</sub> and CO<sub>2</sub>) depending on the H<sub>2</sub>/CO<sub>2</sub> ratio of the inflow gases from day 240 to 265 and from day 395 to 398.

### 5.4.2.3 Increasing the ammonium concentration in the trickling medium

A clear correlation between the pH and  $\text{NH}_4^+$  concentrations in the process liquid at high gas loads was observed during reactor operation while conducting the present research. Even given an  $\text{NH}_4^+$  concentration in the digester supernatant of  $1,530 \pm 170$  mg/L, the  $\text{NH}_4^+$  concentration in the process liquid decreased over time and reached a minimum concentration of only 134 mg/L on day 119. Ashraf et al. [74] and Thema et al. [59] also reported decreasing  $\text{NH}_4^+$  concentrations during reactor operation.

The highly reduced  $\text{NH}_4^+$  concentration was probably caused by a combination of effects, e.g., the dilution of the process liquid with metabolic produced water, the conversion to and loss as free  $\text{NH}_3$  under thermophilic conditions, and the consumption of  $\text{NH}_4^+$  by the microorganisms [90]. Figure 5-5 exemplary depicts the dilution with metabolic water and the addition of digester supernatant as an  $\text{NH}_4^+$  source. A reduction of  $\text{NH}_4^+$  to about half of the concentration during this period can be explained by the dilution with metabolic water (dilution of digester supernatant with metabolic water is evident from Figure 5-5). The effect of  $\text{NH}_4^+$  conversion to  $\text{NH}_3$  when digester supernatant was added continuously to the process liquid is expected to be minimal. Even if thermophilic temperatures promote the conversion to  $\text{NH}_3$  at a pH level below 7.4, only a small quantity of  $\text{NH}_3$  gas (< 9%) could have been stripped out. According to Dupnock and Deshusses [62],  $\text{NH}_4^+$  is required by hydrogenotrophic methanogens as a nutrient for sustaining biomass growth. Dupnock and Deshusses identified an optimal  $\text{NH}_4^+$  concentration of > 1,000 mg/L, even when elevated pH levels were detected. Jønson et al. [44] maintained a  $\text{NH}_4^+$  concentration in the process liquid of over 800 mg/L, which enabled a high level of methanation performance without being affected by a low pH level. Ashraf et al. [74] applied pasteurized cow manure as a nutrient source with relatively high  $\text{NH}_4^+$  concentrations (1,766 - 3,709 mg/L), observing a high methanation performance when a minimum  $\text{NH}_4^+$  concentration of 300 mg/L in the process liquid was ensured. Thema et al. [59] improved methanation performance by adding  $\text{NH}_4\text{OH}$  to an optimal  $\text{NH}_4^+$  concentration of about 60 mg/L. In addition to providing a nitrogen source to the microorganisms, they also applied  $\text{NH}_4\text{OH}$  for pH control, reporting that this was more effective than adding an alkaline or acid solution.

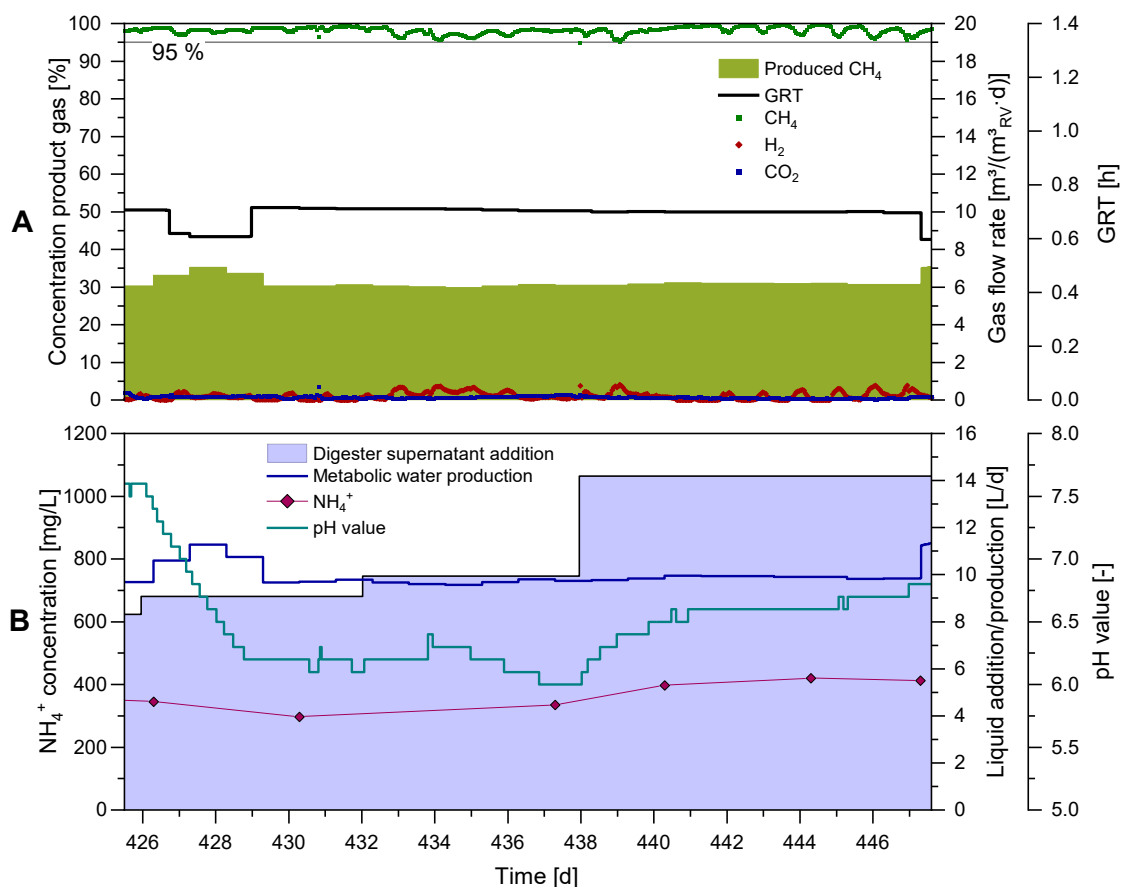


**Figure 5-5:** Development of the  $\text{CH}_4$  produced, the product gas concentrations and GRT (A), the pH level, the  $\text{NH}_4^+$  concentration in the process liquid, the daily addition of digester supernatant and metabolic produced water per day (B) during day 426 to day 447.

Therefore, the hypothesis that increasing  $\text{NH}_4^+$  concentrations in the process liquid can help to stabilize the pH level was tested during operational phase V. The daily addition of digester supernatant was steadily increased starting on day 376, with increasing gas loads. This effect is demonstrated by way of example in Figure 5-5 (days 426 to 447, when the gas load was relatively constant), thus maintaining synthetic natural gas quality. From day 438, the pH level of 6.0 started to recover and reached a level of 6.8 on day 447. Concordantly, the  $\text{NH}_4^+$  concentrations in the process liquid slightly increased from 335  $\text{mg/L}$  to 412  $\text{mg/L}$ , respectively. The increasing digester supernatant addition is expected to have improved the buffer capacity, since  $\text{NH}_4^+/\text{NH}_3$  is one of the key buffer systems under anaerobic conditions [91]. However, with a pH level in the digester supernatant of about 8, also other buffer systems could have supported the pH recovery.

The observation of this study verify the conclusion of Dupnock and Deshusses [62], Ashraf et al. [74], and Thema et al. [59] that a minimum  $\text{NH}_4^+$  concentration is required,

while the threshold of 60 mg/L defined by Thema et al. [59] was not sufficient for stable methanation performance in the present context.

### 5.4.3 Reduction of nutrient addition

From the beginning of the reactor operation, a nutrient stock solution containing trace elements was continuously added to the process liquid to compensate for the nutrient loss caused by dilution of the process liquid with metabolically produced water and, therefore, the necessary rejection of liquid. The preparation of the nutrient stock solution and its addition to the reactor was applied according to the research by Strübing et al. [70], in which stable reactor operation along with high methanation performance was achieved. The macro nutrient and trace element concentrations in the process liquid were periodically analyzed (Table 5-3). The trace element concentrations in the process liquid were already much lower than the concentrations reported by Strübing et al. [11] and Burkhardt et al. [58]. In contrast, the concentration of Fe was far above the 1.5 mg/L identified by Ashraf et al. [74] as being the minimum concentration required by hydrogenotrophic methanogens. Given that the trace element concentrations had been high enough to ensure stable methanation performance thus far, the addition of the trace element stock solution was reduced on day 309 to half of the amount added continuously to the process liquid. Since the addition of artificial nutrients is a significant cost factor, it should be reduced as much as possible while still satisfying the demand of the methanogens. As demonstrated in Table 5-3, the reduction of the nutrient stock solution addition resulted in lower concentrations of Fe, Ni, Co, and Mo in the process liquid, without affecting the biological methanation performance during phases IV and V (Figure 5-2).

**Table 5-3:** Trace element concentration in the process liquid before and after the nutrient addition reduction.

Time [d]	Fe [mg/L]	Ni [µg/L]	Co [µg/L]	Mo [µg/L]	
246	7.95	538	89	33	before nutrient addition reduction
292	7.26	404	91	66	
315	5.82	280	87	31	after nutrient addition reduction
326	5.82	224	61	44	
342	4.91	245	60	24	
431	3.44	289	60	38	
445	3.86	268	68	70	



Tsapekos et al. [65] achieved a stable performance at much lower trace element concentrations, which were supplied only by the addition of sieved digested municipal biowaste. However, the biogas upgrading efficiency to synthetic natural gas quality was limited to a GRT of not below 5 h, suggesting that nutrient concentrations were below the required concentration for higher feed gas rates. The requirement of adding additional trace elements at increasing H<sub>2</sub> loads using reject water from a biogas plant as trickling liquid was also identified by Kamravamanesh et al. [92]. The extent to which any further reduction of artificial nutrient stock solution addition would be feasible, or whether alternative nutrient sources more promising than the reject water from sewage digestion used herein, will be the subject of future research. Identifying the optimal concentrations of macro nutrients and trace elements in the process liquid and applying a membrane to remove the metabolically produced water is expected to enhance reactor management and reduce operational costs.

#### 5.4.4 Biofilm formation

Developing a robust biofilm represents an important factor in methanation performance. Sampling the biofilm carrier at the top, middle, and bottom portions of the packing bed revealed that a visible biofilm was only detected at the top of the packing bed, where the feed gases were supplied (see supplementary material). Microbiological growth and biofilm formation will more likely take place where substrate gases (H<sub>2</sub> and CO<sub>2</sub>) are available in the highest concentrations. The results indicate that most conversion was performed at the top, and the reduced availability of H<sub>2</sub> and CO<sub>2</sub> limited a biofilm formation at the bottom of the packing bed, thus providing evidence for a gas flow approaching plug flow and causing a clear concentration gradient along the reactor height. This outcome is in line with observations by Burkhardt et al. [58], who measured a CH<sub>4</sub> concentration of 83% as early as half of the reactor height.

However, once a biofilm rich in hydrogenotrophic methanogens has formed over the entire length of the packing bed, higher gas loads should be possible, while reducing the conversion of the inflow gas by homoacetogens. Other factors reported to have affected biofilm formation include the trickling rate (intensity and frequency), the packing bed inoculation strategy, and the packing material properties (e.g., specific surface area) [66, 74]. The present research performed a direct inoculation by trickling the inoculum over the still virgin packing bed. Alternatively, biofilm carriers can be precultivated by flooding the reactor with inoculum prior to the reactor start-up, as performed by Jønson et al. [44]. The hydraulic loading of 0.3 m<sup>3</sup>/(m<sup>2</sup>·h) on days 56 to 447 was already relatively low, and this loading reduced the impact on the gas flow and the risk of biomass and nutrient wash out. The packing bed was filled with packing material HXF12KLL (Christian Stöhr GmbH & Co. Elektro- und Kunststoffwaren KG, Marktrodach,

Germany) with a reported surface area of  $859 \text{ m}^2/\text{m}^3$ , well within the range reported by recent studies. Jensen et al. [45] performed a characterization of the packing material and measured lower mass transfer rates compared to clay-based materials. High methanation performance was reported by studies using packing materials with larger surface areas [44]. Ghofrani-Isfahani et al. [93] improved the methanation performance by increasing the surface area with denser polyurethane foam. However, Jensen et al. [45] identified that the surface area is not the only packing bed characteristic that should be considered and that the material type probably has a greater influence on the gas-liquid mass transfer. Applying packing materials with characteristics that result in higher mass transfer rates will probably enable elevated gas loads in the pilot-scale reactor of this study.

#### 5.4.5 Methanation performance and future perspectives

After optimizing the reactor operation to methanogen requirements at an  $\text{H}_2/\text{CO}_2$  feed gas ratio of 3.9, a stable reactor performance at high gas loads was demonstrated during phase V. Figure 5-5 shows the methanation performance with an inlet GRT of 0.7 h from day 429 to day 446, achieving a  $\text{CH}_4$  production rate of  $6.1 \text{ m}^3/(\text{m}^3_{\text{RV}}\cdot\text{d})$  at a mean  $\text{CH}_4$  concentration of 98%. Considering the inert  $\text{CH}_4$  content in the biogas, this resulted in a total  $\text{CH}_4$  flow rate in the product gas of  $17.1 \text{ m}^3/(\text{m}^3_{\text{RV}}\cdot\text{d})$ . Small fluctuations in the gas quality, with an excess of  $\text{H}_2$ , can be attributed to variations in the biogas composition. The fluctuation can thus be reduced by coupling the  $\text{H}_2$  feed gas rate to the  $\text{CO}_2$  concentration in the biogas and adjusting the stoichiometry according to the product gas concentrations.

With an inflow GRT of 0.7 h and an almost complete conversion, thus reaching synthetic natural gas quality, the pilot-scale reactor is already demonstrating a higher level of performance than in other studies using TBRs for biogas upgrading. Rachbauer et al. [57] were the first to investigate raw biogas as  $\text{CO}_2$  source in a lab-scale TBR, achieving synthetic natural gas quality ( $\text{CH}_4$  concentrations  $> 96\%$ ) at a  $\text{CH}_4$  production rate of about  $1.56 \text{ m}^3/(\text{m}^3_{\text{RV}}\cdot\text{d})$  at a GRT of 2.3 h. Tsapekos et al. [65] demonstrated the upgrading potential of raw biogas in a TBR with a reaction volume of 68 L, resulting in a GRT of 2 h at synthetic natural gas quality ( $\text{CH}_4$  production rate not stated). Most recently, Jønson et al. [44] published their results of two TBRs with  $1 \text{ m}^3$  reaction volume, demonstrating a high  $\text{CH}_4$  production of up to  $10.6 \text{ m}^3/(\text{m}^3_{\text{RV}}\cdot\text{d})$  at 97%  $\text{CH}_4$  with a GRT of 0.3 h. This greater performance can probably be attributed to the high surface area of the packing material of over  $3,500 \text{ m}^2/\text{m}^3$ . Furthermore, no process disturbance due to a low pH level was reported, probably because a  $\text{NH}_4^+$  concentration in the process liquid of over 800 mg/L was maintained.

In addition to the upgrading potential, the flexibility of the reactor system was demonstrated by the fast restart performance after long standby periods. After standby I of 49 days (from day 183 to day 232) and standby II of 14 days (from day 362 to day 376), CH<sub>4</sub> concentrations in the product gas recovered to > 96% within 24 hours at a reduced gas load. However, strategies for a fast reactor restart, regaining initial performance as developed by Strübing et al. [34] and Jønson et al. [94], must also be further investigated in larger reactors and at lower GRTs in order to prove the flexibility of TBRs for a dynamic operation at commercial scale.

The accomplishment of this study confirmed that WWTPs are a suitable location for the TBR integration. The local anaerobic digester provided biogas as an easily accessible CO<sub>2</sub> source. By using the existing gas infrastructure, relatively low investment costs for the installation of the TBR connections was required. Anaerobic sludge was used as inoculum and digester supernatant to provide the base for the trickling medium including a NH<sub>4</sub><sup>+</sup> source. The reactor reinoculation with local resources is simple and fast, thus enabling quick recovery of methanation performance when needed. Furthermore, the production site of the WWTP has the advantage that the excess process liquid need not to be transported and can be directly treated onsite or, owing to its elevated trace element concentrations, even be used to boost digester performance. A few technical challenges identified during reactor installation and operation (e.g., the fluctuating gas pressure, which prevented continuous removal of the process liquid) are expected to be solved by technical adaptations.

In addition to demonstrating successful biogas upgrading to synthetic natural gas quality, this study also identified optimization potentials in reactor management, e.g. a reduced nutrient addition requirement, and highlighted important research topics, including sulfur management and the production and temporary accumulation of long chain VFA. The results give evidence that even lower GRTs than 0.7 h can be applied by an improved pH control, favoring the growth of hydrogenotrophic methanogens and improving biofilm formation.

## 5.5 Conclusion

This study demonstrated the potential of biogas upgrading in a TBR on a pilot-scale level. The integration of the reactor at a WWTP elucidated benefits and challenges of operating the reactor in a real application environment. Appropriate NH<sub>4</sub><sup>+</sup> and sulfur supply strategies improved the methanation performance, reaching a stable CH<sub>4</sub> production of 6.1 m<sup>3</sup>/(m<sup>3</sup><sub>RV</sub>·d) at synthetic natural gas quality. The results give evidence that improved reactor management will result in even higher CH<sub>4</sub> production rates and

lower costs for the artificial nutrient addition, promoting energy conversion and biogas upgrading through TBRs.

## **5.6 Acknowledgements**

The authors are thankful for the funding of this study by the Bavarian Ministry of Economic Affairs, Energy and Technology (Grant: BE/19/03). In addition, the cooperation within the Network TUM.Hydrogen and PtX is acknowledged.

## 6. Biological methanation in trickle bed reactors - A critical review

Research on the biological methanation in trickle bed reactors (TBRs) increased highly in recent years, resulting in a high number of publications. As there is no comprehensive up-to-date literature review, *research objective #3* was conducted based on the results of the pilot-scale study and on peer-reviewed journal articles. The outcome *research objective #3* is presented in the following chapter as **Paper III**.

*Research objective #3: Providing an overview of TBR design and operation for biological methanation and concluding future research needs.*

A major part of the critical review provides information on the TBR concept, design, and process parameters, which includes basic knowledge and recent developments. Furthermore, reactor operation, including the inoculation, long-term and dynamic operation, is described. Comparison values, such as the hydraulic loading or the nutrient concentrations in the process liquid, were calculated to give reference points for reasonable operational modes and adjustments. Several process optimization potentials were identified by comparing the study's results, and future research needs were summarized to improve the techno-economic performance of TBRs as energy conversion and storage technology.

---

This chapter has been published with some editorial changes as follows:

*Feickert Fenske, Carolina; Strübing, Dietmar; Koch, Konrad (2023): Biological methanation in trickle bed reactors - A critical review. Bioresource Technology 385, p. 129383. DOI: <https://doi.org/10.1016/j.biortech.2023.129383>*

Author contributions: Carolina Feickert Fenske and Konrad Koch developed the research objective. Carolina Feickert Fenske performed the literature research and wrote the manuscript. Konrad Koch and Dietmar Strübing reviewed the manuscript. All authors approved the final version of the manuscript.

## 6.1 Abstract

Biological methanation of  $H_2$  and  $CO_2$  in trickle bed reactors is a promising energy conversion and storage approach that can support the energy transition toward a renewable-based system. Research in trickle bed reactor design and operation has significantly increased in recent years, but most studies were performed at laboratory scale and conditions. This review provides a comprehensive overview of the trickle bed reactor concept and current developments to support the decision-making process for future projects. In particular, the key design and operational parameters, such as trickling or nutrient provision, are presented, introducing the most recent advances. Furthermore, reactor operation, including the inoculation, long-term and dynamic operation, is described. To better assess the reactor upscaling, several parameters that enable reactor comparison are discussed. On the basis of this review, suitable operational strategies and further research needs were identified that will improve the overall trickle bed reactor performance.

## 6.2 Introduction

The energy transition from a fossil fuel- into a renewable energy-based system is irremissible in combating global warming. With the ambitious aim of the European Union to become climate neutral by 2050 [1], the share of renewable sources in the energy mix must be strongly increased. A significant amount of renewable energy is generated by wind and solar power. A major challenge of wind and solar power is their fluctuating and intermittent availability, which can affect electrical grid stability. To ensure a secure and sustainable energy supply, the application of energy storage technologies is required when energy generation from renewable sources is too low to cover the energy demand. On the other hand, unused renewable energy produced during energy overproduction can be converted into storable energy, the so-called Power-to-X approach. Energy can be stored in hydropower plants, flywheel, and battery power plants [95], but their storage potential is limited [96]. Gas grids are a widely used technology, which comprises a huge and long-term storage capacity. The European gas grid, for example, has a storage capacity of about 1,100 TWh [5], where natural gas can be flexibly stored from minutes to months. With the Power-to-Gas approach, electricity from renewables is converted into storable gas, such as green  $H_2$  and  $CH_4$ . The production of green  $H_2$  is performed by water electrolysis, which is operated with renewable electricity. Due to the chemical properties of  $H_2$ , the injection into the gas grid is limited in most countries to below 12% [97]. Therefore,  $H_2$  can be used to generate  $CH_4$  through the exothermic conversion of  $H_2$  in combination with  $CO_2$  (Eq. (6.1)).  $CH_4$  has a higher calorific value and better storage properties than  $H_2$ . The gas generated by the methanation process can be used directly as a fuel or introduced into the gas grid as synthetic natural gas, ensuring national specific

thresholds for gas grid injection. To reach the required effluent gas quality, high gas conversion rates  $> 95\%$  are required according to Eq. (6.1).



$\text{H}_2$  and  $\text{CO}_2$  methanation can be performed through the catalytic or biological process. The catalytic methanation uses metal catalysts, typically Ni, for the gas conversion that takes place at temperatures between  $250\text{ }^\circ\text{C}$  and  $700\text{ }^\circ\text{C}$  and pressures of up to 100 bar [6, 7]. Catalytic reactors require smaller volumes to produce the same  $\text{CH}_4$  output but have much higher restrictions on the feed gas purity because trace compounds, e.g., of sulfur and chlorine, can deactivate the metal catalyst [97]. Biological reactors use microorganisms of the domain archaea (methanogens) and operate at much milder conditions, typically with temperatures between  $35\text{ }^\circ\text{C}$  and  $65\text{ }^\circ\text{C}$  and ambient pressure. Methanogens are strictly anaerobic but show a high tolerance against feed gas impurities in trace concentrations, such as  $\text{H}_2\text{S}$ . The main drivers, which limit volumetric  $\text{CH}_4$  productivity, are the slow kinetic of methanogens [10] and the poor mass transfer between the feed gases and the methanogens in the liquid phase. In particular, the low solubility of  $\text{H}_2$  in water limits the methanation process, which at  $37\text{ }^\circ\text{C}$  is over 700 times lower and at  $55\text{ }^\circ\text{C}$  over 500 times lower than the one for  $\text{CO}_2$ . The mass transfer between  $\text{H}_2$  and methanogens can be enhanced by increasing the  $\text{H}_2$  partial pressure (e.g., increasing the operational pressure, enabling a gas flow close to plug flow) or by improving the phase boundary interface through the reactor design [11]. An improved phase boundary interface for mass transfer was identified in TBRs, which are filled with biocarriers of a porous material with a high surface area. The biocarriers are surrounded by a gas phase. In contrast to liquid-filled reactors, such as the continuous stirred tank reactor (CSTR), this enables independent control of the superficial gas velocity [11]. However, the TBR technology readiness was mostly limited to laboratory scale and conditions. Technology implementation under real environmental conditions and at pilot-scale was only rarely performed, e.g., by Jønson et al. [44] and Feickert Fenske et al. [38]. A review on biological methanation in TBRs was performed by Sposob et al. [61], but since then, many studies have been published, which broadened the knowledge of this technology. Therefore, this review presents a comprehensive overview of the TBR technology, including important information and recent developments on constructional and operational parameters, reactor inoculation and operation. This will support the decision-making process for future applications and promote the technology upscaling.

## 6.3 The trickle bed reactor concept

### 6.3.1 Reactor set-up

TBRs are gas-filled cylindrical columns packed with biocarrier material (packing bed), which are typically constructed horizontally. The methanogenic microorganisms are suspended in the process liquid, which is trickled over the packing bed. Through the trickling process microorganisms can be immobilized in a biofilm on the packing bed surface. Furthermore, trickling provides essential nutrients to the methanogenic microorganisms in the biofilm. It is expected that most biological gas conversion is performed in the gas phase around the packing bed (reaction volume). Figure 6-1 displays a typical TBR set-up with the volume definitions according to Thema et al. [4].

Information on the filling style of the packing material was scarce. Only Thema et al. [59], Jønson et al. [94], and Feickert Fenske et al. [80] reported to have filled the packing material randomly into the reactor, and Ghofrani-Isfahani et al. [93] packed the reactor with polyurethane foam in loose and dense layer structures.

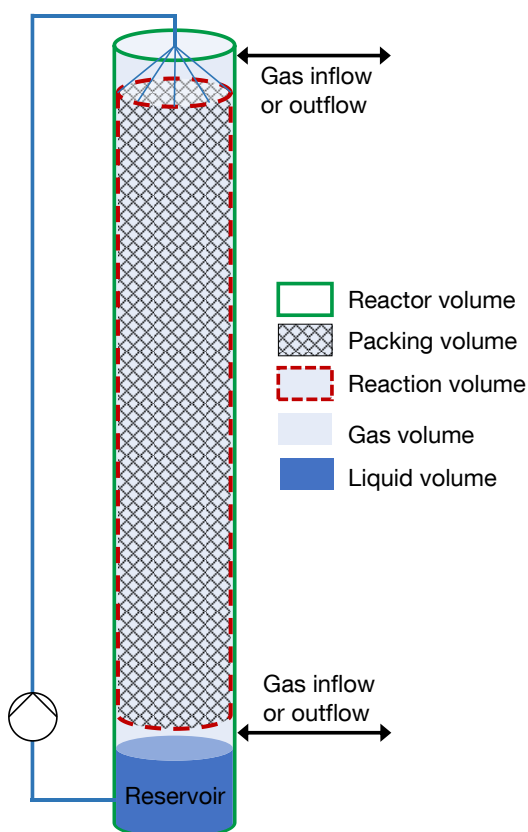


**Figure 6-1:** Simplified set-up of a typical trickle bed reactor adapted from Thema et al. [1].

The packing material properties strongly influence biofilm formation, the gas-liquid mass transfer rate, and thus methanation performance. A packing bed with a high volumetric surface area is often preferred in order to provide a large area where microorganisms can immobilize and get in contact with the gas phase, increasing the  $H_2$  mass transfer rate. Ghofrani-Isfahani et al. [93] observed an enhanced biofilm formation and an improved methanation performance by applying denser polyurethane foam, which provided a higher volumetric surface area. However, high  $CH_4$  production rates with gas grid injection qualities was achieved within surface areas ranging from  $305 \text{ m}^2/\text{m}^3$  [58] to  $> 3,500 \text{ m}^2/\text{m}^3$  [44]. While most studies focused on large volumetric surface areas, other packing material properties, e.g., material type, porosity, and liquid hold-up, should be considered to improve the gas-



liquid mass transfer rate [45]. Jensen et al. [45] performed abiotic O<sub>2</sub> gas-liquid mass transfer experiments where clay-based materials showed higher mass transfer values ( $K_{La}$ ), higher liquid hold-ups, and lower external porosities compared to plastic or cellulose-based materials. The results indicate that the material type is more important than the surface area. Table 6-1 provides an overview of different packing materials that were used in TBRs for biological methanation. Most studies only provided the material type and surface area to characterize the packing.

**Table 6-1:** Packing material name, type, manufacturer, and surface area that was used in TBRs for biological methanation.

Surface area [m <sup>2</sup> /m <sup>3</sup> ]	Name	Type	Manufacturer	Studies
305	Bioflow 40	Polyethylene/polypropylene	Paul Rauschert GmbH & Co. KG, Germany	[12, 58, 60]
313	Hiflow rings 15-7	Polypropylene	RVT Process Equipment GmbH, Germany	[57, 83]
560-580	Hydrophobic foam	Polyurethane	-	[75, 98, 99]
600	Foam	Polyurethane	-	[62, 63, 69, 72]
602	Hel-X HX17KLL	Polyethylene	Christian Stöhr GmbH & Co. KG, Germany	[100]
640	DuraTop	Ceramic	VVF GmbH & Co. KG, Germany	[59]
800	BioFLO 9	Polypropylene / polyethylene	Smoky Mountain Biomedica, USA	[64, 66]
859	Hel-X HXF12KLL	Polyethylene	Christian Stöhr GmbH & Co. KG, Germany	[11, 34, 38, 70]
861	HX09	Polyethylene	Christian Stöhr GmbH & Co. KG, Germany	[7, 101]
1020	Crushed clay	Clay	Leca, Denmark	[45]
1200	PE-10	Polyethylene	Pingxiang Xinfeng Chemical Packing Co. Ltd., China	[102]
2000	Linpor®	Polyethylene	Strabag Water Technologies, Austria	[102]
3500	PE08 (7x10 mm)	Polyethylene	Tongxiang Small Boss Special Plastic Products Ltd., China	[74, 103]
>3500	MBBR PE08 (5x10 mm)	Polyethylene	Tongxiang Small Boss Special Plastic Products Ltd., China	[44]
-	Raschig rings (5x6 mm)	Glass	Merck KGaA, Germany	[71]

TBRs can be constructed with an internal or external reservoir where the process liquid is stored. Most TBRs collect the process liquid at the reactor bottom where it is recirculated to the reactor top to be trickled over the packing bed [11, 12, 38, 45, 58–60,

62, 83, 93]. Other studies separated the reservoir from the reactor [66, 92, 98]. Strübing et al. [11] and Feickert Fenske et al. [38] additionally installed a mixing loop in the reservoir to avoid solid settlement and thus clogging in the pipes or trickling nozzle, for example.

In TBRs, a gas flow through the reactor approaching plug flow is aimed to ensure high methanation efficiency. When plug flow conditions are maintained, all fluid elements have the same residence time and velocity profile across the radius without mixing in the axial direction. The gas residence time (GRT) is then mainly influenced by the gas conversion rate. A plug flow creates a concentration gradient along the reactor length with a high gas partial pressure at the gas entrance, which supports the local gas-liquid mass transfer. TBRs are constructed with high height-to-diameter ratios to support plug flow conditions [39]. Most studies provided the packing height-to-diameter ratio, ranging from 1.3 [44] to 33.3 [62]. Only Savvas et al. [39] applied a very high height-to-diameter ratio of 538, which resulted in a comparable high methanation performance. However, high performance ( $10.6 \text{ L}_{\text{CH}_4}/(\text{L}_{\text{RV}} \cdot \text{d})$  with gas grid injection qualities) was also achieved with the lowest reported packing height-to-diameter of 1.3 in a pilot-scale TBR [44].

### 6.3.2 Process parameters

For a stable methanation performance several process parameters need to be considered, described in-depth in the following sections.

#### 6.3.2.1 Temperature

Methanogens grow and are active at psychrotolerant to hyperthermophile temperatures [104], but most TBRs were operated at temperatures between 35 °C [69] to 65 °C [59]. Biological methanation is an exothermic process, but due to the high heat loss caused by the TBR design (large reactor surface area) and insufficient heat insulation, most studies required reactor heating during the operation [59]. Temperature has a great influence on the CH<sub>4</sub> production rate. With increasing temperatures, the solubility of gases decreases, which reduces the gas-liquid mass transfer. However, thermophilic-operated methanation reactors showed accelerated gas conversion rates compared to mesophilic reactors [40]. This observation is in line with the results reported by Asimakopoulos et al. [64], who identified a higher CH<sub>4</sub> production rate in the TBR operated at 60 °C compared to the identically constructed reactor operated at 37 °C. The CH<sub>4</sub> production rate was demonstrated to increase from psychrotolerant to hyperthermophiles methanogens [104]. Furthermore, the operational temperature affects the microbial community development and the dominant methanogens selection. At mesophilic to thermophilic temperatures, hydrogenotrophic methanogens dominated the

H<sub>2</sub> conversion [105]. Higher methanogenic activities and more efficient methanogenic strains at increasing temperatures outcompete the decreasing solubility. Temperature also influences biofilm formation, which was reported to be more difficult at thermophilic temperatures [78].

To maintain a constant temperature, the heat transfer is typically performed with hot water flowing in tubes around the reactor [11] or through a heating jacket [38]. Improvements in reactor design and reactor upscaling are expected to reduce heat losses, although waste heat is occasionally available. If very high CH<sub>4</sub> production rates are achieved, probably reactor cooling must be applied, because of heat-exothermic conditions [106, 107].

### 6.3.2.2 Pressure

Operational pressure also has a great influence on reactor performance. Gas solubility increases at elevated pressures. Most TBRs for biological methanation applied ambient pressure, but a few studies operated TBRs at higher pressures [7, 58, 59, 101, 103]. Porté et al. [71] investigated the pressure influence on the productivity of three TBRs by increasing the pressure during the reactor operation from 1.5 to 9 bar, which resulted in improved gas conversion and product gas quality at higher pressure. Simultaneously, the elevated pressure caused a pH drop, which can be attributed to increased CO<sub>2</sub> solubility in the liquid phase. Enhanced CH<sub>4</sub> production rates with increasing pressure from 1 to 5 bar were also observed by Burkhardt et al. [58]. However, after a maximum performance at 5 bar, no further improvements with pressures up to 25 bar were observed, while the pH level continuously decreased. Ebrahimian et al. [103] reported that already a pressure increase of 0.7 bar from ambient pressure enabled halving the GRT from 0.67 h to 0.35 h, while maintaining CH<sub>4</sub> concentrations in the product gas of over 90%. The metagenomic analysis identified that the pressure increase did not significantly affect microbial composition. Concluding that a certain pressure increase can be beneficial for methanation efficiency, higher safety requirements for reactor construction and management need to be considered [7]. In Europe, for example, the Pressure Equipment Directive must be complied if an overpressure above 0.5 bar is reached in components with over one liter of volume. This results in higher costs for TBR reactor construction and operation. Furthermore, costs for compressing CO<sub>2</sub> need to be considered, while H<sub>2</sub> is typically already pressurized when leaving the electrolyzer. Still, the energy used to compress H<sub>2</sub> is lost when H<sub>2</sub> is applied at atmospheric pressure in the methanation reactor.

### 6.3.2.3 Co and CO<sub>2</sub> sources

Large CO<sub>2</sub> amounts are produced in the energy, manufacturing, and chemical industry. The suitability of a CO<sub>2</sub> source for biological methanation depends on the gas

source composition (CO<sub>2</sub> fraction) and the requirement for gas pretreatment to eliminate compounds that inhibit methanogens, e.g., O<sub>2</sub>. Gas pretreatment and CO<sub>2</sub> separation measures require energy and reduce the economic efficiency of the energy conversion technology. The separation of CO<sub>2</sub> from ambient air is technically feasible, but very costly due to the low partial pressure with a concentration of about 0.04% [10]. Biogas, which consists of 30-50% CO<sub>2</sub> and 50-70% CH<sub>4</sub>, is considered a very suitable CO<sub>2</sub> source for biological methanation. The CH<sub>4</sub> fraction in biogas does not need to be removed as it flows inertly through the reactor, but a reduced GRT and lower H<sub>2</sub> and CO<sub>2</sub> partial pressures need to be considered. Raw biogas typically contains trace compounds of H<sub>2</sub>S, NH<sub>4</sub><sup>+</sup>, and moisture. As biological H<sub>2</sub> and CO<sub>2</sub> conversion by methanogenic archaea is a sub-process in biogas digesters, the tolerance of methanogens toward impurities in the biogas is high. Consequently, biogas pretreatment is typically not required for biological methanation. Most TBRs were operated with high-purity synthetic feed gases [11, 12, 59, 71, 74, 75, 99], while few studies proved the system's efficiency and robustness with raw biogas [44, 45, 57, 65, 102]. The H<sub>2</sub>S concentration in biogas ranges from 0 to 10,000 ppm [108]. No negative effect of high H<sub>2</sub>S concentrations in biogas has been reported so far [44]. Due to its highly corrosive nature that damages the gas network infrastructure, H<sub>2</sub>S needs to be reduced to the national-specific thresholds before gas grid injection or utilization in the desired infrastructure, such as gas engines. Most likely, a product gas posttreatment is required to achieve the national specific limits, but an H<sub>2</sub>S concentration reduction during biological methanation was reported to be possible. Given that methanogens need sulfur for metabolism, Feickert Fenske et al. [38] compared the H<sub>2</sub>S concentration of the biogas and the product gas when high methanation performance was achieved. The H<sub>2</sub>S concentration was reduced by half, but at increasing gas loads the comparable low H<sub>2</sub>S concentration in the fed biogas of 200 ppm was expected to be too low to completely cover the sulfur demand of the methanogens. Therefore, further investigations on biogas with higher H<sub>2</sub>S concentrations are expected to identify the potential to remove H<sub>2</sub>S and cover the methanogenic sulfur demand. This could be beneficial for reducing the gas posttreatment and the addition of an artificial sulfur source. Dupnock and Deshusses [63] reduced the H<sub>2</sub>S concentration (210-2550 ppm) by feeding nitrate as electron acceptor. As nitrate competes with CO<sub>2</sub> for the H<sub>2</sub> electrons, the methanation performance decreased with increasing nitrate loads, resulting in an inhibition when 98% H<sub>2</sub>S removal was accomplished.

Syngas is another reasonable CO<sub>2</sub> and CO source for biological methanation, which is produced during industrial processes and the gasification of biomass. Syngas mainly consists of CO, H<sub>2</sub>, and CO<sub>2</sub>. Artificially mixed syngas was successfully upgraded with high product gas qualities in TBRs for biological methanation [64, 66, 83, 100], but the

suitability of raw syngas containing different contaminants, e.g. SO<sub>2</sub>, HCN, tars, NO<sub>x</sub>, still needs to be proved [8].

#### 6.3.2.4 Gas supply

Feed gases can be injected into the reactor either flowing from top-to-bottom [38, 44, 62, 64, 66, 69, 70, 74, 75, 98–100, 103], from bottom-to-top [11, 12, 34, 45, 57–60, 65, 83, 92, 93, 102], or directly into the process liquid [7, 101]. Porté et al. [71] compared the different gas flow directions in identical reactor systems with mixed cultures. Besides slightly higher volatile fatty acid (VFA) concentrations in the downward-operated reactor, no difference in the methanation performance was observed. Preliminary gas flow experiments without the consideration of biological conversion performed by Feickert Fenske et al. [80] revealed that the gas flow from top-to-bottom better approached plug flow conditions. Introducing the feed gases in reverse direction poses the risk of a breakthrough due to gas density differences if they are not converted to CH<sub>4</sub> fast enough. Furthermore, a bottom-to-top gas flow configuration increases the chance that dissolved CO<sub>2</sub> in the process liquid, which is higher at the reactor bottom, is stripped out at the reactor top outlet when trickling is performed. Some studies achieved a comparable methanation performance in both gas flow directions [11, 70, 71], indicating that neither the gas conversion capacity of methanogens nor the mass transfer was limited at the specific applied gas load. Thus, the maximum gas load capacity has probably not been reached.

The gas load is usually gradually increased after the TBR inoculation. The maximum gas load capacity highly depends on the gas conversion rate by methanogens, which is limited by the H<sub>2</sub> gas-liquid mass transfer and nutrient provision. A gradual gas load increase gives methanogens the time to adapt to the new conditions [38]. The GRT decreases with increasing gas loads and increases in the reactor due to the volume reduction to one fifth of its original caused by the gas conversion (Eq. 1). Plug flow conditions promote gas conversion at the gas entrance and increase the local gas partial pressure and hence, the gas-liquid mass transfer. Burkhardt et al. [58] measured the gas concentrations over the reactor height and identified a nonlinear gas conversion with a CH<sub>4</sub> concentration of 83% already after half of the reactor height.

Feed gases should be added to the TBR in an optimal ratio to achieve full gas conversion. According to the stoichiometric presented in Eq. 1, four moles of H<sub>2</sub> and one mole of CO<sub>2</sub> are required to form one mole of CH<sub>4</sub>. Therefore, most studies started with an H<sub>2</sub>/CO<sub>2</sub> ratio of 4 and adapted the ratio during the TBR operation, reporting full gas conversion when slightly lower H<sub>2</sub>/CO<sub>2</sub> ratios were applied (3.76 [60] and 3.78 [34]). The additional CO<sub>2</sub> is assumed to be required for biomass build-up [57, 60] and when feed gases are converted to acetic acid ( $4\text{H}_2 + 2\text{CO}_2 \rightarrow \text{CH}_3\text{COOH} + 2\text{H}_2\text{O}$ ). Furthermore, a

fraction of CO<sub>2</sub> dissolves in the process liquid, which is lost when process liquid is discharged or sampled. Depending on the process temperature, pressure, gas load, and liquid removal, the loss in CO<sub>2</sub> is typically below 1% in a low percentage range [80].

### 6.3.2.5 Metabolic water production

A major challenge for biological methanation reactors is the production of metabolic water. With 1 m<sup>3</sup> of produced CH<sub>4</sub>, about 1.6 L of water is generated [109]. In contrast to liquid-filled reactors, the reaction volume in TBRs is uncoupled from the liquid volume. The process liquid volume ( $V_L$ ) in TBRs is typically much smaller compared to the reaction volume ( $V_{RV}$ ) (Figure 6-2) with  $V_{RV}/V_L$  ratios ranging from 0.8 [64] to 49.6 [38]. The metabolic water dilution effect in TBRs increases with higher  $V_{RV}/V_L$  ratios [11]. Due to the immobilization of methanogens on the biocarrier material, methanogens are less affected by the dilution and removal of the process liquid in TBRs while nutrients and the buffer capacity are continuously reduced if not substituted. Furthermore, the dilution of the process liquid with metabolic water reduces the VFA concentration, which has probably a positive effect on the methanation performance.

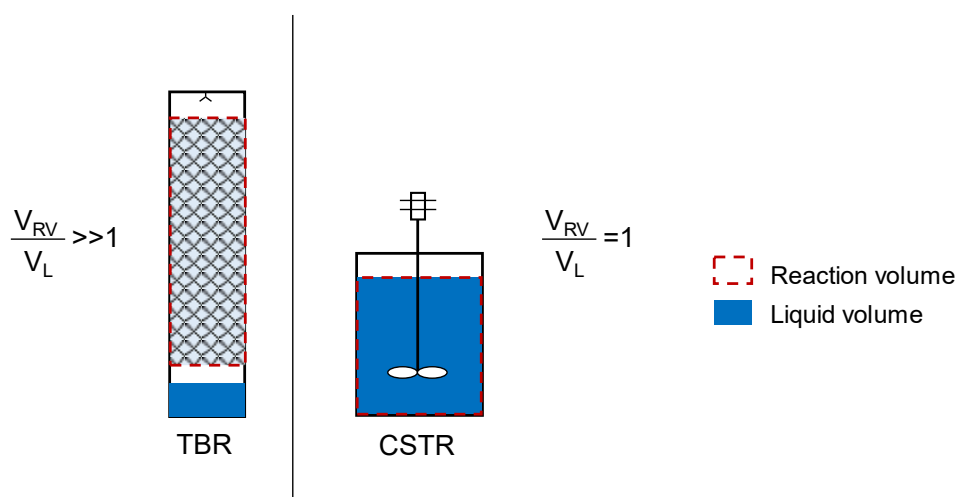


**Figure 6-2:** Comparison of reaction-to-liquid-volume ratio in an TBR and a CSTR (adopted from Strübing [35]).

### 6.3.2.6 pH level and VFA production

Methanogens perform the gas conversion into CH<sub>4</sub> within a pH range of 6.5 to 8.5 [110]. Deviations from the optimal pH level inhibit biological methanation. Several studies reported a CH<sub>4</sub> production breakdown when too low pH levels were observed [11, 65, 69], while no drop in the methanation performance was reported in studies that reached pH levels slightly above 8.5 [71, 75, 92]. However, controlling the pH level in the process liquid was reported to be a major challenge in the operation of TBRs. The pH level is affected when (i) the partial pressure of a gas changes, (ii) the process liquid buffer

capacity is limited, e.g., by the dilution with metabolically produced water, and (iii) specific compounds accumulate, such as VFA or  $\text{NH}_4^+$ .

Elevated pH levels were reported in combination with high  $\text{NH}_4^+$  concentrations in the process liquid or the inoculum [71, 75, 92] while decreasing pH levels were measured in mixed culture systems when VFAs accumulated [11, 38, 57, 58, 65, 66, 83, 93]. That comparable high VFA concentrations did not affect the pH level in some studies can be attributed to the process liquid buffer capacity [45]. Only if the buffer capacity is exhausted, a change in the pH level is expected. In some studies acetic acid was the most abundant VFA [65, 75, 98, 102] and propionic acid in other studies [34, 38, 44, 100]. The increase in the VFA concentration may be a result of biomass decay or organic material degradation, which was introduced with the inoculum or other liquid media into the reactor [92]. Furthermore, acetic acid can be produced by acetogenic bacteria that compete with methanogenic archaea for  $\text{H}_2$  [84]. Acetic acid can subsequently be converted to  $\text{CH}_4$  or also to longer chain fatty acids by chain elongation exclusively reported from mesophilic operated biological reactors [111]. The chain elongation always adds an acetate molecule to the chain meaning that VFAs generated by chain elongation only have always an even number of carbon atoms. In contrast, present formate (C1) or propionate (C3) might serve as the seed molecule for uneven long-chain fatty acids. The microbial analysis indicated the presence of homoacetogenic bacteria in several TBRs [64, 65, 71, 83, 103]. Homoacetogenic bacteria were identified to have a higher tolerance to elevated  $\text{H}_2$  partial pressures compared to hydrogenotrophic methanogens [84]. Thus, homoacetogenesis will be more likely when the gas load is increased, or higher operational pressures are applied. Ebrahimian et al. [103] measured slightly higher acetic acid concentrations in the reactor where a higher pressure was applied. Ghofrani-Isfahani et al. [93] and Feickert Fenske et al. [38] reported VFA accumulation when the gas load was increased.

To which extent  $\text{CH}_4$  is formed through the homoacetogenesis pathway depends on several factors. Tsapekos et al. [84] demonstrated that an adapted inoculum could compensate for elevated pressures without acetate build-up. Even if no impact on the methanation performance is expected as long as acetic acid is converted to  $\text{CH}_4$  without being accumulated [66], favoring the growth and activity of hydrogenotrophic methanogens comprise some advantages. This challenge can be avoided by applying pure hydrogenotrophic cultures instead of mixed cultures. The hydrogenotrophic pathway reduces the risk of VFA accumulation and requires less energy compared to  $\text{CH}_4$  production within two conversion steps [84]. Furthermore, VFAs are lost when process liquid is removed from the reactor, even if the amount of  $\text{H}_2$  lost per gram VFA is rather low. When considering that stoichiometrically 1.6 of  $\text{L}_{\text{H}_2}$  are consumed to form one gram

of acetic acid, and that per liter of metabolic water 2.5 m<sup>3</sup> of H<sub>2</sub> are converted, the loss in the removed liquid per gram acetic acid amounts to only 0.06% of the fed H<sub>2</sub>.

### 6.3.2.7 pH control

In the study of Dupnock and Deshusses [62], an increasing pH level was controlled to below 7.8 by adding HCl. A common measure for pH control is the addition of a buffer solution [11, 44, 66, 69]. Asimakopoulos et al. [66] stabilized the pH level in the process liquid by adding phosphate buffers but recommended not applying this in full-scale plants probably because of cost reasons (~100 euros/kg). Ashraf et al. [75] reduced the pH level only temporarily by adding a phosphate buffer solution. They identified that shifting the gas partial pressure by adapting the H<sub>2</sub>/CO<sub>2</sub> ratio was more effective. With an H<sub>2</sub>/CO<sub>2</sub> ratio of only 2, the CO<sub>2</sub> partial pressure was increased. Hence, more CO<sub>2</sub> dissolved in the liquid, and the pH level decreased to below 8. The other way around, Feickert Fenske et al. [38] stabilized a decreasing pH level with an H<sub>2</sub>/CO<sub>2</sub> ratio higher than 4. In both studies, the shift from the optimal H<sub>2</sub>/CO<sub>2</sub> ratio resulted in high amounts of unconverted feed gases in the product gas. Therefore, other pH control strategies are expected to be more suitable for long-term operation.

One of the main buffer systems under anaerobic conditions is the NH<sub>4</sub><sup>+</sup>/NH<sub>3</sub> equilibrium. Thema et al. [59] counteracted the decreasing pH level by adding NH<sub>4</sub>OH to the process liquid. The increase in NH<sub>4</sub><sup>+</sup> concentration as a buffer was reported to be more effective than adding an alkaline or acid solution. A correlation between the pH level and the NH<sub>4</sub><sup>+</sup> concentration in the process liquid was also observed by Feickert Fenske et al. [38]. A pH level elevation was achieved by adding NH<sub>4</sub>-rich digester supernatant, which resulted in an NH<sub>4</sub><sup>+</sup> concentration increase from 335 mg/L to 412 mg/L. In contrast, in studies that already had comparable high NH<sub>4</sub><sup>+</sup> concentrations (>800 mg/L) [92] or added nitrogen-rich media [71, 75, 99] relatively high pH levels were rather seen as challenge. A temporarily high VFA concentration (6,921 mg/L acetate) in the study of Jensen et al. [45] had no impact on the pH level, while an NH<sub>4</sub><sup>+</sup>-rich medium was added (3,800 mg<sub>NH4+</sub>/L). The different studies demonstrate the importance of monitoring the NH<sub>4</sub><sup>+</sup> concentration in the process liquid and compensating for losses by adding NH<sub>4</sub><sup>+</sup>-rich media. However, controlling the pH level by NH<sub>4</sub><sup>+</sup> addition leads to the formation of NH<sub>3</sub>, which injection into the natural gas grid is usually restricted by country-specific thresholds (e.g., < 10 mg/m<sup>3</sup> in Germany) [112].

### 6.3.2.8 Redox potential

Controlling and adjusting the redox potential in the process liquid to a level, which is optimal for the growth and metabolism of methanogens, will enable high CH<sub>4</sub> production rates. The reduction of CO<sub>2</sub> becomes favorable at a redox potential below -240 mV [113].



Hirano et al. [114] identified a higher CH<sub>4</sub> production and growth of *M. thermautotrophicus* when the redox potential was reduced to -800 mV. In TBRs for biological methanation, the redox potential was scarcely reported. Dupnock and Deshusses [62] reduced the initial redox potential of -100 mV to -240 mV by adding Na<sub>2</sub>S as a reducing agent, which highly improved the CH<sub>4</sub> production rate. However, the improved performance due to the Na<sub>2</sub>S supply could also have resulted by the sulfur provision, which is required by methanogens as a nutrient. Thema et al. [59] achieved high methanation performance and measured a redox potential below -550 mV during the reactor operation. The redox potential level in the process liquid is expected to be a suitable monitoring parameter that can probably identify process disturbances prior to complete performance inhibition [115]. The redox potential is readily used in the classic biogas process [116], indicating accumulation of acids, which can otherwise only be quantified by time-consuming offline measurements. If the reservoir is separated from the reactor, uncertainties in the measurements should be considered. Therefore, further investigation on optimal redox potential levels of different methanogens is recommended.

### 6.3.2.9 Trickling

Trickling in TBRs is performed to enable biofilm formation and to supply the methanogens in the biofilm with the required nutrients. Different devices and constructions were used to trickle the process liquid over the packing bed, e.g., spraying nozzles [11, 44], a drip funnel [57], and a distributor plate [98]. The key challenge is to provide a homogeneous liquid distribution over the packing bed, avoiding liquid channeling or areas where no liquid passes through.

Part of the trickling strategy is the trickling intensity and frequency. Both highly influence the liquid film thickness overlying the methanogenic biofilm, which is the main H<sub>2</sub> gas-liquid mass transfer barrier [45]. The liquid film thickness also depends on the water binding capacity (liquid hold-up) of the biocarrier material. Clay materials, for example, show much higher liquid hold-ups compared to plastic-based materials [45]. Thus, when deciding on the trickling strategy, the packing bed characteristics should be taken into account. Figure 6-3 provides an overview of the trickling intensity, which varies highly between the studies with surface loadings from 0.1 to 254.1 m<sup>3</sup>/(m<sup>2</sup>·d). The hydraulic loading as per m<sup>3</sup>/(m<sup>2</sup>·h) or m<sup>3</sup>/(m<sup>2</sup>·d) known from the conventional wastewater treatment sector (e.g., from TBRs for nitrification) is expected to be a suitable comparison parameter for trickling intensity [80]. To better compare the hydraulic loading rates among the studies, the rate per day was used in Figure 6-3. Most studies applied continuous trickling (dark blue bars in Figure 6-3), but some studies trickled the process liquid discontinuously, e.g., 20 minutes per hour [7], 3 minutes per day [75, 98, 99], and once per day [65]. High methanation performance was achieved with different trickling

intensities and frequencies [11, 59, 75, 94]. Thus, it is expected that optimal trickling can vary between reactor configurations, while some trends on proper trickling were identified.

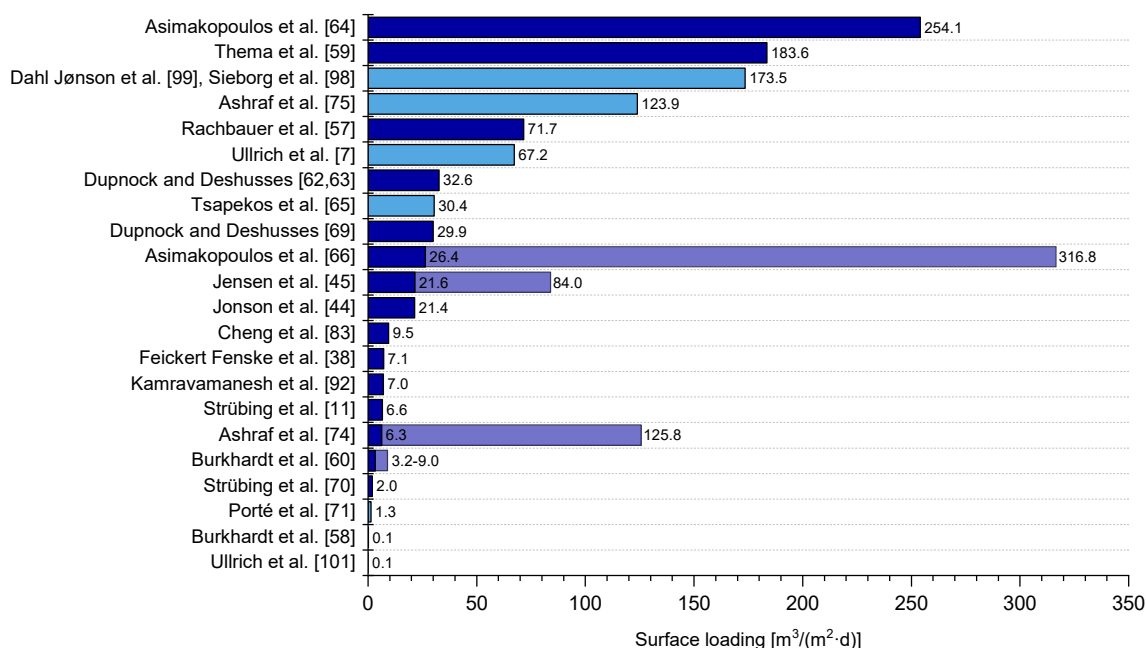


**Figure 6-3:** Trickling intensity of different studies (continuous trickling in dark blue and discontinuous trickling in light blue).

Several studies observed a lower  $\text{CH}_4$  production when trickling was applied or when the trickling rate was increased [7, 45, 62, 74]. For instance, Ashraf et al. [74] observed a reduced  $\text{H}_2$  conversion and  $\text{CH}_4$  production when the hydraulic load was increased from 6.2 to 125.8  $\text{m}^3/(\text{m}^2 \cdot \text{d})$ . Reducing the trickling rate instead was demonstrated to improve the methanation performance [60]. The liquid film thickness is expected to have a considerable influence on the methanation performance. Dupnock and Deshusses [62] promoted direct gas-biofilm mass transfer by stopping trickling, which improved the gas conversion rate by 20%. The mathematical model of Dupnock and Deshusses [72] supported the results, demonstrating that reducing the liquid layer on the biofilm enhanced the  $\text{H}_2$  mass transfer. In addition to the liquid hold-up, trickling was identified to influence the gas flow through the reactor [68, 80]. Preliminary gas flow experiments showed that trickling deteriorates the gas flow behavior through the reactor [80]. The impact on the gas flow was small with a comparable low hydraulic loading of 15.3  $\text{m}^3/(\text{m}^2 \cdot \text{d})$  but is expected to increase at higher hydraulic loads. Another effect that comes along with trickling are shear forces. With increasing hydraulic loads, shear forces can lead to biomass detachment or nutrient and microorganism wash-out. Ghofrani-Isfahani et al. [93] identified non-homogenous biofilm formation at the packed bed bottom, concluding that the high hydraulic loading (not specified) probably resulted in

biomass wash-out. They improved the methanation performance, measuring decreasing acetate concentrations by reducing the continuous trickling to once per day.

However, no trickling, too infrequent trickling, or too low trickling was also reported to negatively affect the methanation performance. Ashraf et al. [74] measured a decreasing gas conversion after stopping the nutrient supply (flushing or flooding the reactor) for about 48 hours. Asimakopoulos et al. [66] observed a fragmentary biofilm formation after 20 days of TBR operation, identifying a channeling liquid flow with dry packing bed parts. In order to ensure homogeneous liquid distribution over the packing bed, they increased the hydraulic loading, which resulted in a linear gas uptake increase and a complete biofilm formation.

Only few studies applied discontinuous trickling. Ashraf et al. [75] achieved a high methanation performance with a trickling frequency of only 3 minutes per day. Applying periodic trickling to improve the gas-liquid mass transfer was investigated by Ullrich and Lemmer [101]. They observed that increasing the trickling intermissions from 2 to 1440 minutes at a constant hydraulic load improved the conversion rates and product gas quality significantly. On the other hand, Tsapekos et al. [65] assumed that trickling once per day was probably not enough to provide lower packing bed areas with sufficient nutrients.

An alternative nutrient supply strategy is the temporary flooding of the entire reactor [74, 99, 103]. Ashraf et al. [74] measured a decreasing gas conversion in the first 24 hours after reactor flooding, which afterward resulted in a stable performance for 60 h without the need for trickling. Reactor flooding is expected to improve the nutrient supply and accelerate biofilm formation. On the other hand, a thicker water film is formed after flooding and applying flooding requires constructional and safety measures, e.g., avoid of liquid entrance in gas pipes. This is particularly the case with increasing reactor sizes [44]. A novel trickling modification was presented by Thema et al. [59] in which liquid distributors were installed above each of the three packing bed segments. This avoids the risk that nutrients are available only in the upper packing bed parts.

#### **6.3.2.10 Nutrient management**

Methanogens depend on the bioavailability of macronutrients (e.g., N, S), and trace elements (e.g., Fe, Ni, and Co). The latter are essential transition metals for electron transport [74]. Only a few studies investigating the biological methanation in TBRs provided information on the process liquid nutrient concentrations (Figure 6-4). Compared to the biogas digester operation, where the addition of nutrient stock solutions is an established procedure [117], knowledge on nutrient requirements for the biological methanation is scarce.

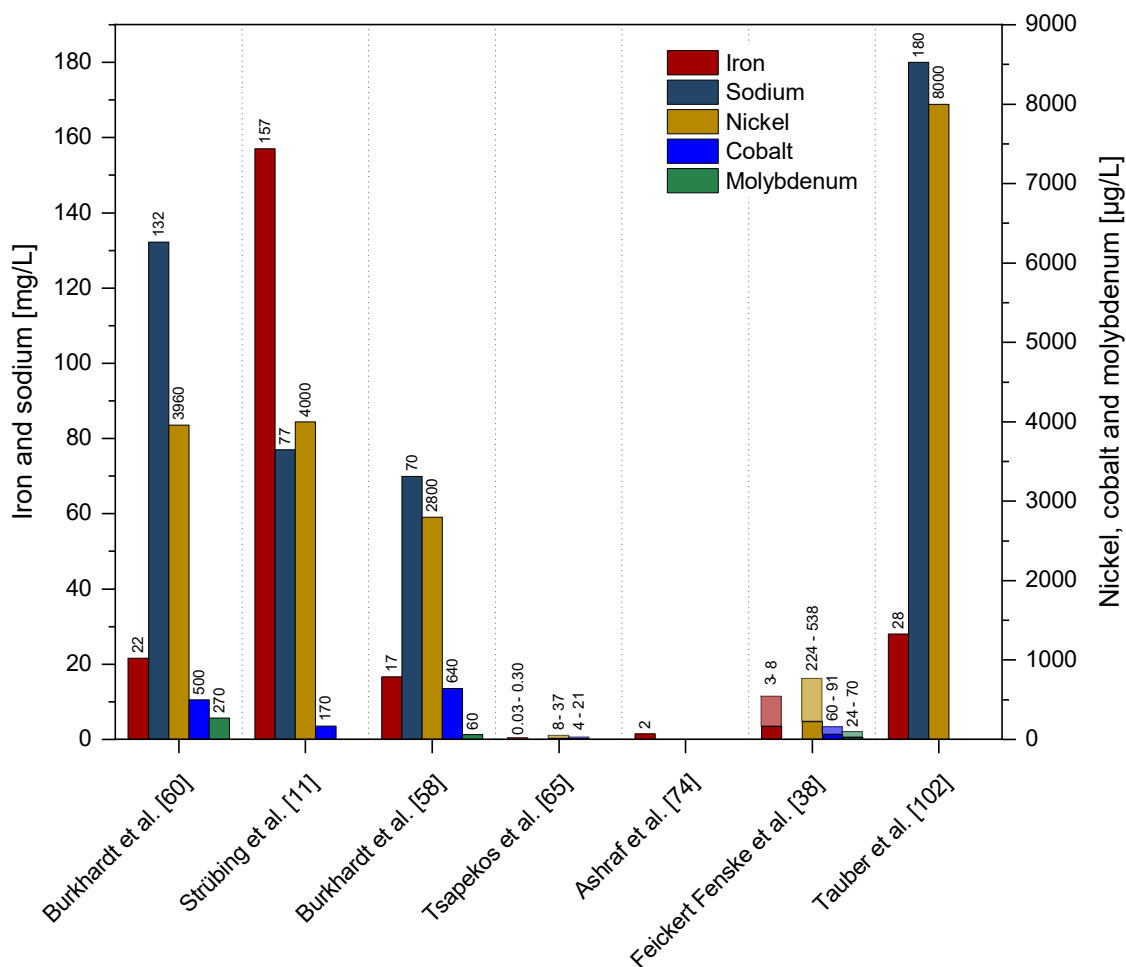


**Figure 6-4:** Macronutrient and trace element concentrations in the process liquid of different studies.

With the aim to maintain a stable nutrient concentration to cover the demand for methanogens, metabolic water production represents a major challenge in TBRs. To substitute nutrients, trace elements and buffering compounds that were removed with the process liquid withdrawal, artificial nutrient stock solutions [11, 34, 57, 58, 62–64, 66, 69, 72] or byproduct additive, e.g., treated cattle manure [74, 75, 98, 99], pure digestate [45, 60, 71], treated digestate [65, 93], the liquid fraction of digestate (also defined as digestate reject water or digester supernatant) [92], or a mixture of a trace element solution and digestate reject water [70] were added to the process liquid. Cheng et al. [83] tested three different nutrient sources (nutrients and concentrations not stated). A stable but relatively low  $\text{CH}_4$  production of  $1.26 \text{ m}^3/(\text{m}^3_{\text{RV}} \cdot \text{d})$  was achieved independently if an artificial nutrient source or a digestate-based medium was applied or not. It must be considered that the nutrient concentrations in the process liquid can strongly deviate from the added nutrient source, depending on the metabolic water production (which is in turn depending on the methanation performance), the added volume and concentration of media and precipitation effects. Furthermore, the nutrient supply only becomes essential

during longer operation as the inoculum can provide nutrients for short term operation and low gas conversion rates.

To substitute at least a fraction of the required nutrients, available byproducts can be a cost-effective alternative for mixed culture systems, particularly when onsite products at the methanation plant location can be used. Ashraf et al. [74] analyzed the composition of cow manure and found that it was a good source of  $\text{NH}_4^+$ , Fe, Co, Ni, and Mn (concentrations not stated). Tsapekos et al. [65] applied sieved digested municipal biowaste as the only nutrient source, achieving stable methanation performance at a GRT of 5 h, which corresponds to a comparable low gas load of  $12.0 \text{ m}^3/(\text{m}^3_{\text{RV}}\cdot\text{d})$ . Trace element concentrations decreased during reactor operation and were therefore probably too low to enable higher gas loads. Kamravamanesh et al. [92] identified that adding digestate reject water as the only nutrient source was insufficient at increasing  $\text{H}_2$  loads. To determine the suitability of a medium to substitute nutrients while avoiding inhibitory effects due to toxic compounds, e.g., by Pb, As, or too high nutrient concentrations, prior analysis of the medium is recommended.

The knowledge about the minimum, maximum, and optimum concentrations of macronutrients and trace elements is still scarce. Feickert Fenske et al. [38] demonstrated that a reduction in the trace element addition by half was possible without affecting the methanation performance at a comparable high gas load of  $43 \text{ m}^3/(\text{m}^3_{\text{RV}}\cdot\text{d})$  (GRT of 0.7 h) (Figure 6-4). On the other hand, Asimakopoulos et al. [66] identified limited biofilm growth at increasing gas inflow rates, which was improved by adding 2.5 times more trace metals stock solution (concentration in process liquid not stated), resulting in higher gas conversion rates. In a recently published study, Tauber et al. [102] tested the uptake of different elements, identifying a load depended uptake for some elements, e.g., for Na, K, Ca, and Mg, while other elements such as Ni and Fe were required independently from the gas load. Furthermore, the necessary concentrations of Fe and P depended on the oxidation state of the provided element. The required nutrient concentrations may depend on several factors, e.g., the abundance of methanogens, the trickling strategy [65], and the nutrient bioavailability. However, some information on essential nutrients and limiting concentrations were obtained and is presented in the following two sections on macronutrients and trace elements.

### **Macronutrients**

Typical macronutrients required by methanogens are N (because of the reducing environment under anaerobic conditions the dominant species is  $\text{NH}_4^+$ ), S, and Na [92]. In addition to its buffer capacity,  $\text{NH}_4^+$  is required as a nutrient by hydrogenotrophic methanogens to sustain biomass growth [62]. Declining  $\text{NH}_4^+$  concentrations during the reactor operation were observed in several studies [59, 74, 92]. With increasing

temperatures and pH levels, the dissociation equilibrium shifts into the formation of gaseous unionized  $\text{NH}_3$ . While optimal  $\text{NH}_4^+$  concentrations vary from 60 mg/L [59] to 1000 mg/L [62], no inhibition was reported in TBRs because of too high  $\text{NH}_4^+$  concentrations. Ashraf et al. [74] and Jønson et al. [44] observed a high methanation performance when a minimum  $\text{NH}_4^+$  concentration of 300 mg/L and 800 mg/L, respectively, in the process liquid was ensured. A minimum  $\text{NH}_4^+$  concentration of 60 mg/L was required in the study of Thema et al. [59], while Feickert Fenske et al. [38] increased the  $\text{NH}_4^+$  concentration to  $> 400$  mg/L to achieve a stable methanation performance. The latter probably required a higher minimum concentration because higher gas loads were applied. Tauber et al. [102] observed an accumulation of acetic acid when the  $\text{NH}_4^+$  level fall below 1,000 mg/L concluding that acetoclastic methanogens became more dominant. The  $\text{NH}_4^+$  concentration was increased by adding  $\text{NH}_4\text{Cl}$ . However, to which extent  $\text{NH}_4^+$  is required as a buffer or as nutrient needs further investigation.

Several studies added  $\text{Na}_2\text{S}$  as sulfur source to the process liquid [11, 34, 57, 59, 62, 64, 66, 69, 70, 83]. Strübing et al. [11], Thema et al. [59] and Cheng et al. [83] described a direct relationship between the addition of  $\text{Na}_2\text{S}$  and improved methanation. Thema et al. [59] measured a strongly decreasing concentration of sulfide ions ( $\text{S}^{2-}$ ) during reactor operation and improved the methanation performance by adding  $\text{Na}_2\text{S}$ . Strübing et al. [11] assumed limiting grow conditions for the archaea when the sulfide concentration in the process liquid was below 0.02 mM. However,  $\text{Na}_2\text{S}$  precipitates mineral elements, e.g., Fe, Ni, or Co, and is in an equilibrium with  $\text{H}_2\text{S}$  [38]. Therefore, alternative sulfur sources will probably improve the bioavailability of nutrients. Feickert Fenske et al. [38] investigated the potential to cover the sulfur need of the methanogens with  $\text{H}_2\text{S}$  from the biogas. In addition to the cost reduction for artificial  $\text{Na}_2\text{S}$  supplementation, applying  $\text{H}_2\text{S}$  as only sulfur source can reduce the final  $\text{H}_2\text{S}$  concentration in the product gas. When high gas conversion rates were achieved only half of the biogas  $\text{H}_2\text{S}$  concentration was measured in the product gas [38]. However, the comparable low biogas  $\text{H}_2\text{S}$  concentration of only 200 ppm resulted in a process liquid  $\text{H}_2\text{S}$  concentration of just 0.01 mM. This was probably too low to cover the sulfur demand by methanogens completely; wherefore  $\text{Na}_2\text{S}$  was added to enable a high methanation performance.

### Trace elements

Methanogens require some metals in trace amounts. Typical trace elements of nutrient stock solutions are Fe, Ni, Co, and Mo [11, 34, 57, 59, 66, 69, 92]. These trace elements were identified to be essential for the growth and metabolism of methanogens [118–120]. Fe is typically the most abundant trace element, followed by Ni, Co, and Mo (Figure 6-4). Ashraf et al. [74] estimated a minimum Fe concentration of 1.5 mg/L, and

Dupnock and Deshusses [62] indicated an optimal concentration of 2.0 mg/L. Comparable high Fe concentrations > 100 mg/L were maintained by Kamravamanesh et al. [92], which decreased when higher gas loads were applied. Zn, W, and B are other trace elements that were sometimes reported to be important for methanogens and were found in the nutrient stock solution of some studies [57, 66]. However, the information on which trace elements are essential or can stimulate the methanation process varies in the literature, and more research is required to identify optimal concentrations. Kamravamanesh et al. [92] measured higher CH<sub>4</sub> concentrations after adding Fe, Ni, Co, Mo, and Se, but no effect was detected when Zn, Cu, W, and Mn were added. It must be considered that the addition of specific trace elements replace the metal bond of other trace elements, which are then available once again for methanogens. Thus, the addition of cheap trace elements with a high bond energy (e.g., Fe) can be used in TBRs to increase the bioavailability of other trace elements.

A measure to improve the bioavailability of specific nutrients to methanogens is the application of complexing agents that form highly soluble complexes with metal ions [118]. Less trace elements need to be added and the risk of trace element precipitation is reduced. Several studies added the complexing agent EDTA to the nutrient stock solution [11, 34, 38, 57]. Another strategy to reduce the nutrient addition requirement is to remove or separate the metabolic water from the process liquid while retaining nutrients, microorganisms, and other compounds in the reactor. So far, only Choi et al. [109] have investigated this approach by applying membrane distillation in different reactor configurations. The study demonstrated that water removal was feasible, but there is still much room for improvement. Alternative approaches, in particular applicable for TBR such as the separate collection of the nutrient-rich trickling liquid and metabolic water during intermittent trickling, still needs to be researched.

### 6.3.2.11 Microbiology

The microbial composition and abundance highly determine the conversion efficiency in biological methanation reactors. The microbiological conversion of H<sub>2</sub> and CO<sub>2</sub> to CH<sub>4</sub> can be performed through the hydrogenotrophic pathway or within a two-step process where acetate is produced as an intermediate (homoacetogenesis) and is subsequently converted to CH<sub>4</sub> by aceticlastic methanogens [42]. The microorganisms are introduced into the reactor either as a pure or mixed culture inoculum. Digestate from wastewater treatment plant (WWTP) or biogas plants is often applied as inoculum. The community profile of reactors inoculated with mixed cultures changes during the reactor operation [64, 65, 93, 102, 103]. In the study of Ebrahimian et al. [103] only a few species from the original inoculum were still abundant in the process liquid samples after about one month of reactor operation. Furthermore, operational parameters, such as temperature

and the H<sub>2</sub> partial pressure, shape the microbial community composition. Cheng et al. [83] identified a different microbial community composition after changing the nutrient source, which returned to its initial composition after some time. Most studies operated the TBR with a mixed culture. Mixed culture operated reactors are more robust against contaminants in the gas, and operational changes. Dupnock and Deshusses [62] and Thema et al. [59] were the only studies inoculating the reactor with a pure methanogenic strain, while the latter required a comparable long start-up phase. Ensuring sterile conditions for pure cultures is challenging, particularly when applying biogas and other liquid media that can introduce undesired microorganisms into the reactor. In the study of Dupnock and Deshusses [62] the pure culture was contaminated during the reactor operation, resulting in the development of a mixed consortium.

The gas conversion by hydrogenotrophic methanogens is favored when aiming for an efficient process. The direct hydrogenotrophic pathway requires less energy than homoacetogenesis with subsequent acetate conversion by aceticlastic methanogens [84]. Furthermore, the risk of process disturbances due to acetate accumulation is reduced. Hydrogenotrophic methanogens compete with homoacetogens for H<sub>2</sub>. The study of Tsapekos et al. [84] revealed that the permissive H<sub>2</sub> partial pressure was higher for homoacetogenesis. Thus, homoacetogenesis is probably favored when higher gas loads are applied and H<sub>2</sub> and CO<sub>2</sub> are not converted to CH<sub>4</sub> fast enough. In TBRs, the H<sub>2</sub> partial pressure is usually highest at the gas entrance when plug flow conditions are enabled. That increasing gas loads change the microbial composition was observed by Ebrahimian et al. [103], Kamravamanesh et al. [92] and Tauber et al. [102]. In contrast to the previous findings, the abundance of methanogenic archaea increased in the study of Kamravamanesh et al. [92] and Tauber et al. [102] when higher gas loads were applied. Probably, the H<sub>2</sub> partial pressure was too low or the feed gases were converted fast enough to shift toward homoacetogenic growth. Tsapekos et al. [84] demonstrated that the application of an inoculum that was adapted to the gaseous feedstock could compensate for the increased H<sub>2</sub> partial pressure. Another parameter that was identified to shape the microbial composition is the operational temperature. Asimakopoulos et al. [64] identified a change in the microbial community after long-term exposure to syngas, with *Methanobrevibacter* dominating the mesophilic TBR and *Methanothermobacter* the thermophilic TBR. In contrast to the expectations, elevating the pressure in the study of Ebrahimian et al. [103] did not significantly affect the microbial composition.

While hydrogenotrophic methanogens often prevailed in the reactor [69, 92, 99], a great variety of bacterial and archaeal species were detected in general [71, 75, 93, 103]. Ashraf et al. [75] identified 18 different phyla within the bacterial community in the biofilm. In the archaeal community, the hydrogenotrophic methanogens *Methanobacterium* [58, 75, 83, 92, 99, 102, 103], *Methanothermobacter* [11, 58, 59, 64,



71, 92, 99], and *Methanobrevibacter* [62, 64, 99, 102] were most prominent. Ashraf et al. [75] reported that *Methanobacterium* and *Methanoculleus* dominated the archaeal community with over 94%. Acetotrophic methanogens were only rarely identified [100], while the presence of syntrophic oxidizing bacteria revealed the conversion of acetate back to H<sub>2</sub> and CO<sub>2</sub> [71, 93]. Also, the microbial composition between the biofilm and the process liquid was reported to vary clearly, with typically a higher abundance of archaea in the biofilm [64, 71]. As the microbial composition varies over time, sampling dates should be reported. Porté et al. [71] stated that the sampling was done on day 94. Only Ghofrani-Isfahani et al. [93] reported a higher abundance of hydrogenotrophic methanogens in the process liquid and syntrophic acetate oxidizing bacteria in the biofilm in the samples, which were taken after about 60, 110 and 120 days.

### 6.3.2.12 Biofilm formation

A biofilm is composed of immobilized microorganisms and extracellular polymeric substances [93]. Biofilm formation was reported in mixed and pure culture systems. The biofilm acts as a protective layer that reduces the risk of microorganisms being washed out when process liquid is removed. After the development of a suitable biofilm, trickling is only required to provide nutrients to the methanogens and can thus be reduced and/or operated intermittently. This diminishes the liquid layer over the biofilm and improves the contact between methanogens and feed gases. Biofilm density and thickness also seem to play a vital role in the methanation performance [72]. Tauber et al. [102] measured a biofilm thickness of 5-10 µm. A mathematical model developed by Dupnock and Deshusses [72] predicted that a thicker biofilm would enhance the methanation performance. However, biofilms overcoming a specific thickness can suffer from diffusion limitations, which inactivate methanogens.

Several studies reported a fast biofilm formation within the first weeks after reactor inoculation [64, 99]. Dahl Jønson et al. [99] identified biofilm formation on the polyurethane foam packing when they examined the material after 40 days of TBR operation at 52 °C. The DNA biofilm analysis showed an enrichment in hydrogenotrophic methanogens, which were the most dominant archaeal consortium. Asimakopoulos et al. [64] operated TBRs for over one month to develop a stable biofilm on the packing bed. However, Strübing et al. [11] did not observe any macroscopic biofilm formation even after 313 days of reactor operation while achieving a very high methanation performance (CH<sub>4</sub> production of 15.4 m<sup>3</sup>/(m<sup>3</sup><sub>RV</sub>·d) with a GRT of 0.3 h). As they operated the TBR at thermophilic temperatures, biofilm formation was probably hampered. Meanwhile, an increasing biomass concentration in the process liquid was measured. This indicates that gas conversion can also be performed at a high rate through planktonic microorganisms in the process liquid. To which extent the gas conversion is performed by methanogens

in the biofilm or planktonic methanogens in the liquid layer over the biofilm still needs clarification and is likely changing during operation.

Biofilm formation and microbial composition over the packing bed length were often reported to be inhomogeneous [45, 65, 69, 92, 102, 103]. A higher abundance of methanogens in the biofilm is expected at the gas entrance, where the gas-liquid-mass transfer is highest as long as plug flow conditions are ensured [65]. Dupnock and Deshusses [69] measured a higher fraction of active cells, and Jensen et al. [45] determined a higher biomass density at the gas entrance. In contrast, Kamravamanesh et al. [92] and Ebrahimian et al. [103] measured a higher abundance of hydrogenotrophic methanogens in the middle of the packing bed and close to the gas outlet. Probably, the gas flow was not approaching plug flow conditions, or other factors, such as trickling, influenced the growth and immobilization of methanogens. Tsapekos et al. [65] identified a thicker biofilm with a high abundance of biofilm-forming microorganisms at the top (gas outlet), suggesting that once-per-day trickling limited the nutrient provision in the packing bed section below. On the other hand, high trickling rates pose the risk of methanogens being washed out from the biofilm [93], while high trickling or reactor flooding were used to detach dead cells or excessive biofilm [57, 69]. Rachbauer et al. [57] occasionally flushed the packing bed with process liquid to remove excessive biofilm formed during the reactor start-up. Dupnock and Deshusses [69] identified a low share of active methanogens and a high share of inactive biomass after longer reactor operation, and proposed to detach the inactive biofilm by intensive trickling.

Biofilm formation can also challenge the reactor operation when growing excessively, which can result in packing bed clogging. Ashraf et al. [75] opened the reactor after a gas conversion decline and found severe clogging over the packing length, possibly due to biofilm overgrowth and accumulation of dead biomass and solids. To avoid blockages by large particles of the nutrient medium, Ashraf et al. [74] installed a mesh filter (125  $\mu\text{m}$ ).

Overall, no clear trend of biofilm formation and microbial distribution between the studies could be identified. While biofilm formation was identified with mixed and pure culture operated reactors, improved biofilm formation is expected for mixed cultures. More research on methanogens and biofilm formation is required to identify boundary conditions that support fast biofilm formation and enrich hydrogenotrophic methanogens in the biofilm. In particular, a more homogeneous biofilm over the reactor length with a high share of hydrogenotrophic methanogens is expected to enable higher gas loads and, thus, improve methanation performance [38]. Furthermore, biofilm analysis during the dynamic operation of TBRs can identify the biofilm potential to accelerate or improve the restart performance after different standby periods.

### 6.3.3 Reactor operation

The operation of TBRs starts with a reactor inoculation, followed by a start-up phase, where the gas load is typically increased little by little until a stable operation at high gas conversion rates is reached. The dynamic operation of TBRs was only rarely researched and includes the stop of gas inflow, the standby period, and a restart phase. It distinguishes between hot standbys, where the operating temperature is maintained, and cold standbys, where the temperature is reduced during the standby and set back prior or during the restart phase. The terminology can vary among the studies, but the TBR operation typically follows the concept depicted in Figure 6-5.

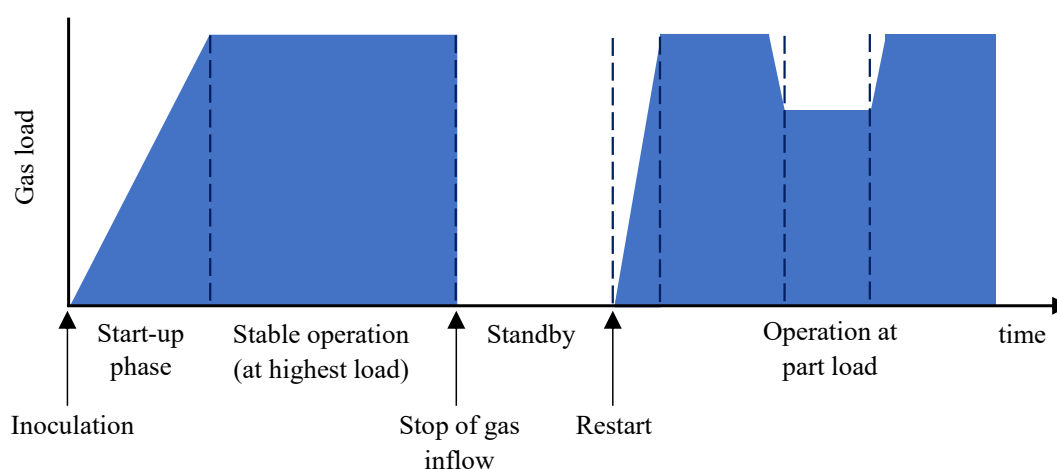


**Figure 6-5:** Simplified scheme of the reactor operation depending on the gas load.

#### 6.3.3.1 Inoculation

Mainly digestate was applied as inoculum in TBRs, originating from different sources, e.g., WWTP digesters [11, 12, 39, 60], manure and/or crop-based digesters [7, 45, 57, 69, 83], biogas upgrading reactors [71, 93], or a mixture of several digestates was used [65, 66, 100]. Only a few TBRs were inoculated with a pure culture [59, 62], but the methanation performance did not exceed the one of mixed cultures. That the inoculum influences the community development was demonstrated in the study of Aryal et al. [100]. They applied a manure-based inoculum and digestate from a WWTP, measuring a profoundly different microbial community development. However, similar methanation rates were achieved regardless of the inoculum.

The inoculum is often sieved as a first step applying screens with a pore size in a range between 25  $\mu\text{m}$  to 800  $\mu\text{m}$  [11, 45, 74, 75, 92, 100] to avoid clogging, e.g., of the trickling nozzle. Further inoculum processing is sometimes performed. Ashraf et al. [74] degassed the inoculum for one week in an incubator. Other studies applied “culture enrichment processes” with different procedures among the studies to shorten the start-

up phase [64–66, 69]. However, the culture enrichment did not improve the start-up performance, biofilm formation, or reduced the inoculation time, while higher costs are expected for the enrichment process [44].

Most studies performed the inoculation of the biocarrier material by trickling the inoculum over the virgin packing bed in the reactor [11, 12, 38, 57, 64, 66, 99, 100]. Alternatively, the reactor was flooded with inoculum for a period [44, 71, 74, 94]. Flooding the reactor ensures the contact of the inoculum with the entire packing bed, which is expected to enhance biofilm formation [71]. Furthermore, the risk of liquid channeling is reduced [74]. According to Jønson et al. [44] inoculating the reactor by flooding reduces the start-up time to reach CH<sub>4</sub> concentrations > 90%. However, flooding needs to be considered in reactor design to avoid damage to technical devices or unwanted liquid entrances. Particularly with increasing reactor sizes, flooding will result in higher costs, and will require safety measures [44].

The feed gas supply during the start-up typically starts with an H<sub>2</sub>/CO<sub>2</sub> ratio of 4 and is afterward adapted depending on the product gas composition. The start-up phase is often characterized by a gradual gas load increase and a development of the microbial population selected by the operational conditions. A reactor start-up with CH<sub>4</sub> concentrations of over 90% within the first seven days of operation was described by several studies [11, 38, 65, 71, 93]. Ghofrani-Isfahani et al. [93] reported that the inoculation with an enriched hydrogenotrophic culture resulted in CH<sub>4</sub> concentrations of 96% as early as after one day. To support the orientation for reactor start-ups in future projects, it is encouraged to provide information on the initially applied gas load, and the gradual gas load increase relative to the maximum achieved gas load.

### **6.3.3.2 Reactor performance**

Most TBRs presented in this review were constructed with reaction volumes smaller than 100 L and operated under laboratory-controlled conditions. The studies of Jønson et al. [44] and Feickert Fenske et al. [38] are the only peer-reviewed studies that used larger TBRs, investigating the biogas upgrading potential at the point of origin under real conditions. Jønson et al. [44] built two TBRs with a reaction volume of 1 m<sup>3</sup> at a biogas plant. This is the only study that applied an electrolysis unit to generate H<sub>2</sub>. Feickert Fenske et al. [38] investigated the performance of a TBR with 0.8 m<sup>3</sup> reaction volume, which was installed at a WWTP.

Reactor performance was mainly described by the CH<sub>4</sub> production per reaction volume and the corresponding CH<sub>4</sub> concentration in the product gas. The reaction volume defined by Thema et al. [4] is the gas volume within the packing bed. In smaller-scale reactors, the entire packing bed volume, including the volume of the biocarrier itself, was

often referenced as reaction volume. Thus, comparing reactor performance of different studies should be done with caution. Thema et al. [4] suggested providing plant productivity based on the entire reactor volume. Another parameter is the theoretical inflow GRT, as inert feed gases, e.g., the CH<sub>4</sub> fraction in biogas, can be considered in the reactor performance. While the reactor volume is sometimes used to calculate the GRT [4], applying the gas volume V<sub>G</sub> is more precise to depict the theoretical GRT when no feed gas inflow Q<sub>in</sub> is converted ( $GRT=V_G/Q_{in}$ ). Alternatively to the GRT, the gas load of the feed gases per reaction (or reactor) volume per day ( $m^3/(m^3_{RV}\cdot d)$ ) can be used to compare the efficiency between reactors. The CH<sub>4</sub> concentration in the product gas is one of the most critical performance parameters. The aim is to achieve CH<sub>4</sub> concentration in the product gas, which meets the national specific thresholds for gas grid injection, which reduces the effort for gas posttreatment. In this context, limits to CO<sub>2</sub>, H<sub>2</sub>, and H<sub>2</sub>S concentrations need to be considered, which vary highly between the national regulations for gas grid injection [4].

The highest CH<sub>4</sub> production with long-term pure CO<sub>2</sub> methanation to synthetic natural gas quality (CH<sub>4</sub> concentrations > 95%) was reported by Strübing et al. [11] with  $15.4 m^3/(m^3_{RV}\cdot d)$  and a GRT of 0.3 h (Figure 6-6). The same GRT was also accomplished by Jønson et al. [44] with a marginally lower CH<sub>4</sub> production of  $10.6 m^3/(m^3_{RV}\cdot d)$ , because raw biogas was applied. The serial operation of the two pilot-scale TBRs enabled a slightly higher CH<sub>4</sub> production compared to the parallel process of  $9.4 m^3/(m^3_{RV}\cdot d)$ . Higher CH<sub>4</sub> production rates were reported from CSTRs [37, 121]. However, either very small reaction volumes of below 2 L [121] were used or the company reported values were not published in a peer review study. Furthermore, in recent years, the number of publications on biological methanation in CSTRs has decreased while more studies focus on TBRs.

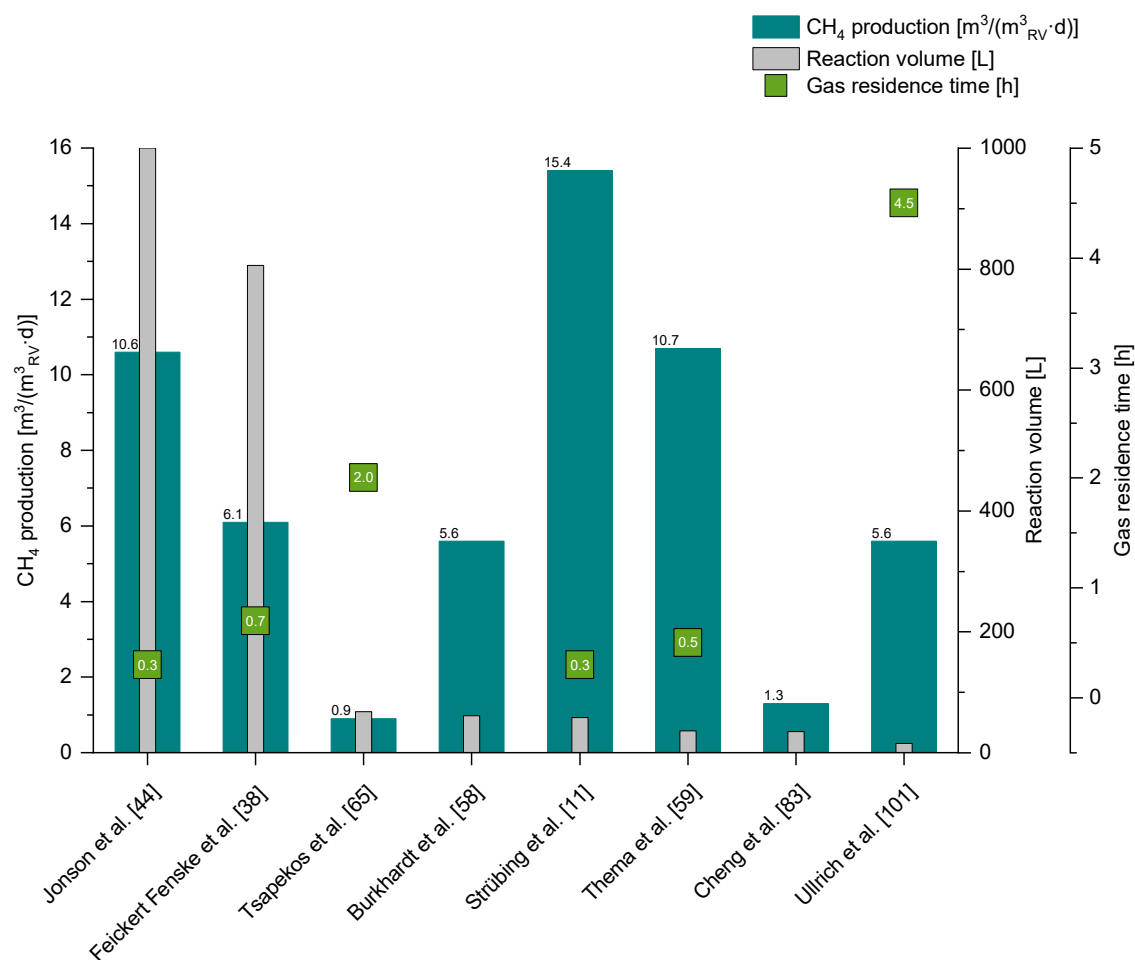


**Figure 6-6:** Methanation performance of TBRs with reaction volumes > 10 L. CH<sub>4</sub> production and gas inflow residence time meet synthetic natural gas quality (CH<sub>4</sub> concentrations > 95%).

### 6.3.3.3 Dynamic operation

The Power-to-Gas concept aims to convert and store unused energy, which is generated when energy production – mainly from renewable sources – exceeds energy demand. To implement TBRs as Power-to-Gas technology, the reactor will be operated when unused renewable electricity is available to generate H<sub>2</sub>. The intermediate storage of H<sub>2</sub> should be avoided due to economic reasons. Therefore, a flexible and dynamic reactor operation must be enabled. In several studies, standby periods were included [38, 58, 59, 94]. Burkhardt et al. [58] showed that a dynamic operation with hourly alternating standbys did not negatively affect the methanation performance. A good recovery reaching previous performance within 6 hours was demonstrated by Thema et al. [59] even after a 10-day cold standby. However, in-depth investigations on the dynamic TBR operation were only performed by Strübing et al. [34], Strübing et al. [70], and Jønson et al. [94]. A significant consideration in the dynamic operation of TBRs is the duration when no cheap energy is available, and the TBR is operated in standby mode. This period

varies highly depending on several parameters, e.g., the share of renewable sources in the energy mix and current weather conditions. The standby duration and operational conditions during the TBR standby highly influence the restart performance. Therefore, Strübing et al. [34], Strübing et al. [70], and Jønson et al. [94] developed strategies to improve the restart performance after different standby periods.

Strübing et al. [34] investigated the TBR restart performance after standby periods of 1 to 8 days, identifying that with longer standby durations, more time was required to reach the previous methanation performance at full gas load. Reducing the temperature from 55 to 25 °C during the standby was the most effective measure to accelerate the restart performance. The cold standbys at 25 °C with a stepwise gas load increase enabled a restart within 4.5 hours, reaching full gas load with effluent CH<sub>4</sub> concentrations above 96%. The restart performance after hot standbys showed a deteriorated performance with comparable high VFA concentrations. Higher VFA concentrations and variations were identified during the standbys in general, indicating biomass decay. It is expected that the hot standby resulted in higher decay rates of methanogens when the gas supply stopped. Lowering the temperature to a level below the metabolism range of the methanogens instead is expected to reduce the starvation rate when no substrate gas is available. Furthermore, microorganisms e.g., bacteria, that consume methanogens are also inactivated during the standby period, while they are expected to remain active during hot standbys.

A better restart performance after lowering the temperature during standbys of 72 hours was also demonstrated in the experiments of Jønson et al. [94]. However, for a standby of 6 and 24 hours, maintaining the operating temperature of 52 °C showed better restart performance than active cooling to 12 °C. It must be considered that a lower gas load was used compared to the previous studies [34, 70] and that the restart temperature was only 36.4 °C due to slow reheating. The gas load increase was performed stepwise. Compared to the study of Strübing et al. [70] a little more time was required to reach full gas conversion with synthetic natural gas quality after 24-hour standbys. Improving the heating and cooling is beneficial to reduce the recovery time for full gas conversion. Compared to liquid-filled reactors, accelerated heating or cooling of the gas phase in TBRs is expected and less energy required.

In addition to the temperature, the gas refeeding strategy plays an important role in the restart performance, too. Strübing et al. [70] researched different restart feed gas patterns after 30-minute to 24-hour standbys. While an almost immediate return to full gas load reaching synthetic natural gas quality was possible after 30 minutes of hot standbys, an improved restart within 60 minutes was achieved for 24 hours of cold standbys with a stepwise gas load increase. Immediate load change from 0 to 100% after

24 hours standbys showed the worst performance. That a gradual gas load increase resulted in a better restart performance was also demonstrated at the pilot-scale level by Jønson et al. [44]. The experiments performed by Jønson et al. [94] furthermore discovered an improved recovery to full load when a low load of 20% was applied for 24- and 72-hours instead of a standby without gas supply.

There are still many open research questions on the dynamic operation of TBRs, e.g., trickling and nutrient supply during standby periods. Other strategies to improve the conservation of methanogens during standby periods and reactivate them during the restart are required to accelerate and enhance the reactor restart. One approach is, for example, the addition of an acid solution to the process liquid during the standby period, reducing the pH to a level below methanogenic activity, and adding alkaline solution for reactor restart. However, how successful this can be applied and whether the methanogens will be negatively affected remains to be tested.

The following conclusions can be drawn based on the results of the studies that investigated strategies for the dynamic operation of TBRs:

- a) With increasing standby periods, more time is required to regain initial methanation performance.
- b) Particularly for longer standby periods, cold standbys can result in better restart performance compared to hot standbys. This period can vary between TBRs depending on the constructional (e.g., heat transfer) and operational conditions (e.g., gas load).
- c) Cold standbys should reduce the temperature below the activity of methanogens and bacteria.
- d) A stepwise gas load increase can improve the restart performance, particularly after longer standby periods.
- e) Important parameters to consider for standby and restart: temperature, time to retain temperature, gas refeeding strategy, trickling, and nutrient supply.

## 6.4 Research needs and future direction

A conclusion on the most important findings and research needs is provided in Table 6-2. Besides the technical feasibility of TBRs, an economic assessment is required to identify the potential of integration of TBRs on an industrial level that can compete with other energy conversion technologies. To the best of the authors' knowledge, no single study performed an economic analysis on biological methanation in TBRs, and only a few studies investigated the economic potential of biological methanation reactors in general [43, 122]. A techno-economic analysis case study on biological biogas upgrading



was performed by Nashmin Elyasi et al. [43]. The results demonstrate that the economic competitiveness of biological methanation highly depends on the boundary conditions, e.g., the cost of electricity and granted subsidies. In the past years, the costs of electrolysis and methanation equipment have substantially decreased [27]. Furthermore, scaling effects and process optimizations will reduce the costs further [43]. It is highly encouraged for future research articles on TBRs to provide information on the capital and operational costs helping to evaluate the economic potential of TBRs. Furthermore, reactor upscaling on an industrial level is a necessary step in identifying the techno-economic potential of TBRs. With increasing height-to-diameter ratios, static measures to protect the reactor against wind loads should be considered. On the other hand, lower reactor heights are required to meet the same height-to-diameter ratio ( $H/D=h/(V_R/(\pi \cdot h)^{0.5}) \cdot 2$ ). Furthermore, it is still not clear to which extent a higher height-to-diameter ratio is really essential, as a high methanation performance was also achieved with a comparable low height-to-diameter ratio, e.g., 1.3 in the study of Jønson et al. [44]. To better assess the economic feasibility of TBRs, reactor upscaling to an industrial level (volumes  $\gg 1 \text{ m}^3$ ), higher  $\text{CH}_4$  production rates, and further investigation of the dynamic operation are required.

Within this review, several optimization potentials and strategies were identified that can enhance the reactor performance. An improved reactor operation and higher gas conversion rates are expected by (1) applying biofilm carrier material with high specific surface area of over  $300 \text{ m}^2/\text{m}^3$  and high mass transfer values, e.g., clay-based materials, (2) a homogeneous biofilm formation over the entire packing bed, dominated by hydrogenotrophic methanogens, (3) suitable trickling strategies, e.g. hydraulic loading of below  $10 \text{ m}^3/(\text{m}^2 \cdot \text{h})$  or higher loadings with intermittent trickling, (4) targeted nutrient management, (5) stabilizing the pH level through maintaining  $\text{NH}_4^+$  concentration of about  $400\text{--}800 \text{ mg/L}$ , (6) reducing the dilution effect with metabolic water, e.g., by integrating a membrane system for water removal, and (7) a real-time monitoring system, including parameters such as the redox potential. Most points are interacting with each other (positively as negatively). However, further research is still needed, particularly regarding specific nutrient requirements and their optimal/limiting concentrations for the methanogens in methanation system, the dynamic operation of TBRs, the development and dynamic of the microbial population, and biofilm formation. Next to experimental analysis, mathematical models can identify optimization potentials and predict the methanation performance for upscaling projects, eliminating the costs for reactor construction. Modeling and simulation of hydrodynamics and TBR performance were already performed in a few studies [67, 68, 72]. Dupnock and Deshusses [72] developed a model for biogas upgrading, which successfully predicted the performance of a laboratory-scale TBR and enabled the conclusion on optimization measures. However,

mathematical modeling poses the risk that inadequate assumptions are made, and validation of models requires experimental data.

**Table 6-2:** Overview of important developments, findings, and research needs of TBRs.

Biocarrier material	- A packing bed with a high volumetric surface area improves the gas-liquid mass transfer and provides a large surface area for biofilm formation. However, other properties, such as material type, should also be considered.
Temperature	- Higher CH <sub>4</sub> production rates at thermophilic temperatures than at mesophilic conditions prove that the higher microbial activity outcompetes the decreasing gas solubility.
Pressure	- Elevated pressures improves the CH <sub>4</sub> production, but declining pH levels and higher costs and safety measures need to be considered.
CO <sub>2</sub> sources	- Biogas is a suitable CO <sub>2</sub> source, but the additional CH <sub>4</sub> reduces the GRT. - H <sub>2</sub> S in biogas can serve as a sulfur source for methanogens while the total corrosive H <sub>2</sub> S is reduced.
Gas supply	- A bottom-to-top gas flow direction poses the risk of a feed gas breakthrough, while a gas injection from top-to-bottom is recommended. - Due to biomass build-up, acetic acid formation and CO <sub>2</sub> dissolution typically slightly lower H <sub>2</sub> /CO <sub>2</sub> ratios than 4 should be applied.
Metabolic water production	- The metabolic water dilution effect in TBRs increases with higher V <sub>RV</sub> /V <sub>L</sub> ratios and is, thus, much higher than in liquor-filled reactors.
pH level and VFA production	- Elevated pH levels were reported with high NH <sub>4</sub> <sup>+</sup> concentrations and low pH levels when VFAs accumulated. - pH level is affected when process liquid buffer capacity is limited, which is intensified by metabolic water production. - VFAs are formed through homoacetogenesis, biomass decay, or organic material degradation.
pH control	- Maintaining a specific NH <sub>4</sub> <sup>+</sup> concentration is probably the most effective pH control strategy, while the formation of NH <sub>3</sub> in the product gas needs to be considered.
Redox potential	- The redox potential is rarely studied so far, but is actually a promising monitoring parameter for process disturbances.
Trickling	- Reducing the trickling rate and frequency can improve the methanation performance but should be high enough to enable biofilm formation in

---

	<p>the entire packing bed by ensuring the necessary nutrient supply to the methanogens in the biofilm.</p>
Nutrient management	<ul style="list-style-type: none"> <li>- Methanogens require macronutrients (e.g., N, S, and Na) and trace elements (e.g., Fe, Ni, and Co) for their growth and the CH<sub>4</sub> formation. However, investigations on specific nutrient requirements and optimal/limiting concentrations are scarce and dosing to-date is just empirical and potentially higher than really needed.</li> <li>- Byproducts of AD of organic material, e.g., reject water from digestate dewatering, can partially cover the continuous nutrient demand caused by metabolic water dilution.</li> </ul>
Microbiology	<ul style="list-style-type: none"> <li>- CH<sub>4</sub> can be formed through homoacetogenesis or the hydrogenotrophic pathway, while the latter is favored due to less energy requirement and lower risk of VFA accumulation.</li> <li>- Pure cultures can achieve higher CH<sub>4</sub> production rates, but are less resilient to impurities and process disturbances.</li> <li>- The microbial community often differs from the inoculum as it develops over time and is influenced by several parameters, e.g., gas load and temperatures.</li> </ul>
Biofilm formation	<ul style="list-style-type: none"> <li>- Biofilm composition, density, and thickness are expected to affect the methanation performance.</li> <li>- Higher biofilm formation was often identified at the gas entrance.</li> <li>- A homogeneous biofilm over the entire packing bed is expected to improve and stabilize the methanation performance especially after stand-by periods, while a high-rate gas conversion is also possible through planktonic microorganisms.</li> </ul>
Upscaling potential	<ul style="list-style-type: none"> <li>- For reactor upscaling, lower heights are required to meet the same height-to-diameter ratio supporting plug flow conditions.</li> <li>- To prove the suitability of TBRs as Power-to-X technology, reactor upscaling to an industrial level (volumes <math>\gg 1 \text{ m}^3</math>), higher CH<sub>4</sub> production rates, and further investigation on the dynamic operation are required.</li> </ul>

---

## 6.5 Conclusion

This study provides an overview on the reactor set-up and operational parameters that are important for a stable operation. By comparing the study's results, several process optimization potentials were identified, e.g., process liquid trickling and biofilm formation. Higher methanation performance is expected by improving the contact of the methanogens with the feed gases and by enriching hydrogenotrophic methanogens. The potential of TBRs has been demonstrated on a semi-industrial level with reaction volumes of up to  $1 \text{ m}^3$ , but research on the technical and economic feasibility of TBRs at the commercial scale is still required.

## **6.6 Acknowledgements**

The authors are thankful for the funding of this study by the Bavarian Ministry of Economic Affairs, Energy and Technology (Grant: BE/19/03). In addition, the cooperation within the Network TUM.Hydrogen and PtX is acknowledged.

## 7. Research outcomes and conclusions

Whether biological H<sub>2</sub> and CO<sub>2</sub> methanation in trickle bed reactors (TBRs) will be techno-economically feasible for industrial applications depends on many factors, such as the technology development, cost reduction potentials, and the political framework. The ability of TBRs to produce synthetic natural gas in high qualities with CH<sub>4</sub> concentrations of over 96% was already demonstrated on laboratory scale with reaction volumes of below 100 L and mostly at sterile conditions. The scope of this dissertation was investigating the technology potential on a pilot-scale level and optimizing the process performance to support the way toward industrial application. The first step included planning, constructing, and installing of a TBR at wastewater treatment plant (WWTP) Garching. With a reactor volume of 1.2 m<sup>3</sup> and a reaction volume of 0.8 m<sup>3</sup>, this is one of the largest reported TBRs for biological methanation by now.

One factor limiting volumetric CH<sub>4</sub> production in biological systems is the low H<sub>2</sub> gas-to-liquid mass transfer [9]. A gas flow through the reactors approaching plug flow enables a high initial H<sub>2</sub> partial pressure and reduces the risk that the feed gases leave the reactor before being converted. With the aim to identify operational and constructional conditions that enhance plug flow, preliminary gas flow experiments were performed with the pilot-scale TBR. The gas flow experiments in the form of a step input tracer test were conducted with virgin biofilm carrier material to avoid the influence of biological conversion. Before every experiment, the reactor was flushed with CH<sub>4</sub> to mimic restart conditions after standby periods. An important finding of the gas flow experiments was that the feed gases of H<sub>2</sub> and a CO<sub>2</sub> source (pure CO<sub>2</sub> and biogas) were already mixed before entering the reactor and behaved as one gas mixture. Furthermore, even with comparable low gas flow velocities of 1.2 mm/s, the lighter H<sub>2</sub> did not separate from the heavier CO<sub>2</sub>, which ensures a locally constant H<sub>2</sub>/CO<sub>2</sub> ratio.

An improved gas flow approaching plug flow was observed when the feed gases were applied in a top-to-bottom direction, while an early feed gas breakthrough in the reverse direction indicated channeling or bypassing effects. The most evident explanation for the breakthrough in the bottom-to-top gas flow direction are density differences between the CH<sub>4</sub> and the lighter feed gases that tend to flow up. As long as the microorganisms are able to convert the feed gases entirely, the gas flow direction will not impact the methanation process. However, a gas flow from top-to-bottom is recommended to reduce the risk that the feed gases leave the reactor before being converted and promote the gas conversion at the gas entrance, which increases the gas residence time (GRT), enabling the application of higher gas loads. Furthermore, trickling reduced plug flow conditions

to a lesser extent than the gas flow direction. As a relatively low hydraulic loading of  $15.3 \text{ m}^3/(\text{m}^2 \cdot \text{d})$  was applied, the effect will likely increase with higher trickling rates. Furthermore, reducing the trickling to a minimum, which is still required to supply the methanogens in the biofilm with nutrients, lowers the liquid film thickness over the biofilm [74]. Thus, an improved gas-liquid mass transfer is expected when trickling is reduced.

The gas flow experiments further elucidated the pilot-scale reactor's share of unused and stagnant zones. About 19% of the gas volume was calculated to have not been actively flown through. Potential dead volumes are above the gas pipe at the top and below the gas pipe at the bottom of the reactor, covering 8% of the gas volume. Computational fluid dynamics can predict possible dead volumes and simulate the hydrodynamic interactions, but modelling is dependent on the selected boundary conditions, which limits the accuracy. Applying gas flow experiments before reactor start-up is a simple and convenient method to identify operational conditions that support plug flow and individual reactor properties, e.g., stagnant zones that reduce the GRT or reactor installations that enable an initial mixing of the feed gases. Furthermore, by comparing the gas flow before and after the inoculation allows the identification of process disturbances, such as clogging of the packing bed. Overall, from a fluid dynamic perspective, it is recommended to operate TBRs in a top-to-bottom gas flow direction and with a minimum hydraulic loading, while the influences of the microbiological conversion on the gas flow still need to be investigated.

During the installation and operation of the TBR at the WWTP, the site-specific advantages were proved. Next to valuable local resources, such as digestate and digester supernatant, the WWTP infrastructure offered a facilitated installation of the pilot-scale reactor, reducing investment costs.

With the aim to investigate upscaling effects and the biogas upgrading potential, the following steps included the inoculation and long-term operation of the pilot-scale TBR. Inoculation was performed with anaerobic sludge from the local digester and with a step-wise gas load increase. During the reactor operation, decreasing pH levels due to volatile fatty acid (VFA) accumulation was a critical challenge, which was often reported in biological reactors to result in a methanation breakdown. The accumulation of acetic acid during the first operational phases indicated a partial  $\text{H}_2$  and  $\text{CO}_2$  conversion through the homoacetogenic pathway, while a higher accumulation of propionic acid in the latter phases is more reasonable because of organic matter degradation and biomass decay. A limiting condition for the hydrogenotrophic pathway was probably the low sulfur content in the biogas, which was applied as the only sulfur source for methanogens initially. The  $\text{H}_2\text{S}$  concentration of about 200 ppm was reduced by half when high gas conversion rates

of over 99% were achieved, but it was probably too low to cover the methanogenic demand completely. By adding  $\text{Na}_2\text{S}$  as an alternative sulfur source, sulfide concentrations above 0.02 mM were maintained, which was identified to be the minimum level [11]. In the long-term, higher gas loads could be applied after  $\text{Na}_2\text{S}$  addition, but also other parameters could have stabilized the methanation process. Furthermore,  $\text{Na}_2\text{S}$  addition resulted in a high conversion of  $\text{H}_2\text{S}$  gas, which increases the gas posttreatment requirement. As this was the first study investigating the potential to reduce corrosive  $\text{H}_2\text{S}$  by methanogens, future research should focus on this topic.

The hydrogenotrophic pathway actually requires less energy than homoacetogenesis with subsequent acetate conversion. Furthermore,  $\text{H}_2$  and  $\text{CO}_2$  conversion through hydrogenotrophic methanogens reduce the risk for VFA accumulation. However, as long as the pH level is stabilized, no impact on the methanation performance is expected. Strategies for pH control, such as adding alkaline and buffer solutions, and decreasing the  $\text{H}_2/\text{CO}_2$  ratio, were not sustainable for long-term purposes. Maintaining the  $\text{NH}_4^+$  concentration in the process liquid to 400 mg/L minimum was the most successful pH control strategy in this study, enabling stable long-term biogas upgrading.

A major factor that reduces the buffer capacity of the process liquid is the production of metabolic water. Furthermore, metabolic water dilutes the nutrients in the process liquid, which needs to be regularly supplemented. As the knowledge about essential nutrients and trace elements is still scarce, their addition varies highly between the studies in formulation and concentration. The nutrient and trace element concentration in the process liquid of the pilot-scale reactor was already comparatively low. However, reducing the nutrient stock solution addition to half of the amount did not affect the methanation performance, indicating a potential for cost reduction.

Increasing gas loads could be applied with the stabilization of the pH level. Finally, a stable methanation performance with a  $\text{CH}_4$  production of  $6.1 \text{ m}^3/(\text{m}^3_{\text{RV}}\cdot\text{d})$  at gas grid injection quality for over two weeks was achieved. With a corresponding gas load of  $42.7 \text{ m}^3/(\text{m}^3_{\text{RV}}\cdot\text{d})$ , the output lies in the range of recently published results, confirming the feasibility of biological methanation in TBRs on a pilot scale. Next to the recently published study of Jønson et al. [44], this is the first study investigating the methanation performance in TBRs on a pilot-scale level with reactor volumes of over  $1 \text{ m}^3$ . The reactor operation of nearly 450 days, including two shutdowns, is an essential step toward the necessary full-scale integration. Furthermore, the results indicate that higher gas loads can be handled by the pilot-scale reactor as long as the pH level is controlled, and the methanation through the hydrogenotrophic pathway is enforced.

## 8. Outlook and future research needs

The results of the pilot-scale trickle bed reactor (TBR) operation at real application conditions proved the potential of this technology to generate synthetic natural gas with gas grid injection quality ( $\text{CH}_4 > 96\%$ ). However, if the biological  $\text{H}_2$  and  $\text{CO}_2$  methanation in TBRs can compete with other methanation technologies or even with the  $\text{H}_2$  transportation, storage, and application costs depends on future developments and the political framework. A cost reduction for catalytic methanation of about 67% with 800 €/kW in 2017 to 130-400 €/kW in 2050 and biological methanation of about 75% with 1200 €/kW in 2017 to 300 €/kW in 2050 were predicted [27]. However, particularly for TBRs, cost calculations are highly uncertain as predictions are mainly based on laboratory-scale reactors. Nashmin Elyasi et al. [43] already demonstrated in a case study that biological  $\text{H}_2$  and  $\text{CO}_2$  methanation can be an economical alternative to water scrubbing as biogas upgrading technology. To better assess the economic feasibility of TBRs, reactor upscaling to an industrial level (volumes  $\gg 1 \text{ m}^3$ ), higher  $\text{CH}_4$  production rates, and further investigation of the dynamic operation are required.

The potential of the TBR technology application can be demonstrated exemplary with the aim to fully convert the generated biogas at the wastewater treatment plant (WWTP) Garching (~45,000 population equivalent) with an average daily production of about 900  $\text{m}^3/\text{d}$ . With a gas load of  $42.7 \text{ m}^3/(\text{m}^3_{\text{RV}} \cdot \text{d})$  at stable methanation performance, only about 1.6% of the total produced biogas was upgraded in the pilot-scale TBR. Enabling complete biogas upgrading would require the construction of a TBR with a reaction volume of  $51 \text{ m}^3$ . With a height-to-diameter ratio of 7.5, the TBR dimensions would result in a packing bed height of about 15.4 m and a diameter of 2.05 m. Compared to the local anaerobic digester size of  $1,050 \text{ m}^3$ , the TBR would be 21 times smaller. Alternatively, high height-to-diameter ratios can be achieved by constructing the TBR in a series of columns. Nonetheless, higher volumetric  $\text{CH}_4$  production rates would result in smaller reactor size requirements.

During the operation of the pilot-scale reactor at the WWTP Garching, several optimization potentials were identified, which could stabilize the methanation process and even increase the  $\text{CH}_4$  production rate. The most successful pH control strategy was adding digester supernatant to maintain an  $\text{NH}_4^+$  concentration of over 400 mg/L. With higher gas loads, and thus, metabolic water production, digester supernatant addition and withdrawal of the excess process liquid will increase. A direct connection of the digester supernatant tank with the TBR reservoir and an automatized digester supernatant addition depending on the pH level, for example, is expected to facilitate the management and



ensure a stable pH level. Furthermore, since a passive overflow of the excess process liquid was not feasible due to fluctuating pressures in the low-pressure tank, the process liquid was removed manually every two to three days. As a result, the volume in the reservoir, and thus the effect of digester supernatant and nutrient stock solution addition, highly varied before and after liquid removal. A continuous withdrawal of the process liquid, e.g., by a level-controlled pump, enables a steady process liquid volume as well as stable nutrient concentrations and buffer capacities in the reservoir.

An essential research need for the pilot-scale reactor is the microbial analysis of the biofilm and the process liquid. Particularly research in biofilm formation, composition, and importance for the methanation process should be extended. Strübing et al. [11] achieved high CH<sub>4</sub> production rates of 15.4 m<sup>3</sup>/(m<sup>3</sup><sub>RV</sub>·d) without a microscopic biofilm formation. Moreover, excessive biofilm growth leading to packing bed clogging should be avoided. However, biofilm density and thickness were identified to play a vital role in the methanation performance [72], and particularly a homogeneous biofilm formation over the entire packing bed, dominated by hydrogenotrophic methanogens, is expected to improve the interface between the feed gases and the methanogens. Furthermore, biofilm acts as a protective layer and reduces the risk of washing microorganisms out when the process liquid is removed. This also enables the decoupling of the trickling from metabolic water production. Immobilizing the methanogens in the biofilm can also have some advantages for the dynamic operation, e.g., reduced microbial decay during more extended standby periods.

Particularly the packing material highly influence biofilm formation and, thereby, the interfacial area for mass transfer [45]. Among a large specific surface area of the packing bed, other packing material properties, such as the material type, are important to consider. The polyethylene packing material HXF12KLL (Christian Stöhr GmbH & Co. Elektro- und Kunststoffwaren KG, Marktrodach, Germany) that was used in the pilot-scale reactor and partially in the TBR operated by Strübing et al. [11] had a comparable high specific surface area with 859 m<sup>2</sup>/m<sup>3</sup>. Still, it required a long operation to form a visible biofilm. Jensen et al. [45] identified that packing material type is more important than the surface area, with clay-based materials showing higher mass transfer values than plastic or cellulose-based materials. If a homogeneous biofilm formation over the entire packing bed or the application of alternative packing materials can improve the methanation performance of the pilot-scale TBR are interesting investigations for the future. Research on suitable packing bed materials for optimal biofilm formation and high mass transfer rates should be performed in batch experiments on a smaller scale first and tested afterward on a pilot-scale level.

Another parameter that influences biofilm formation and the mass transfer rate is trickling. Too high trickling rates can result in biomass washout, while too low trickling poses the risk of nutrient deficiencies and liquid channeling or bypassing effects. Several strategies for a homogeneous trickling distribution, such as reactor flooding [44, 74] or packing bed segment-wise trickling [59], were proposed and should be researched in more detail. The pilot-scale reactor applied comparable low hydraulic loading rates of  $7.1 \text{ m}^3/(\text{m}^2 \cdot \text{d})$ , while no adverse effects were identified. Intermittent trickling can be tested to investigate if higher gas loads can be applied by a reduced liquid hold-up and improved plug flow conditions.

An approach to increase the volumetric  $\text{CH}_4$  production rate while enabling more stable operational conditions is strengthening the  $\text{H}_2$  and  $\text{CO}_2$  methanation through the hydrogenotrophic pathway. The direct hydrogenotrophic pathway requires less energy than homoacetogenesis with subsequent acetate conversion by acetoclastic methanogens [84]. The risk of process disturbances due to acetate accumulation is reduced, and less acetate as an intermediate product is lost with the process liquid removal. Possible strategies to enhance the growth and activity of hydrogenotrophic methanogens are processing the inoculum, addition of pure hydrogenotrophic cultures, or increasing the microbial selectivity by elevating the temperature or pressure. However, to what extent  $\text{CH}_4$  was produced through homoacetogenesis in the pilot-scale reactor and studies identifying the presence of homoacetogenic bacteria [64, 65, 71, 83, 103] is unclear. Furthermore, after some time, propionic acid was the most abundant volatile fatty acid (VFA) in the pilot-scale reactor and also in other studies [34, 38, 44, 100], indicating biomass decay. In mixed culture operated reactors, VFA can be converted into  $\text{CH}_4$  by specific methanogens. Thus, applying a diverse culture has several advantages, mainly when using local resources at the WWTP or biogas plant. Microbial analysis of the biofilm and process liquid is expected to provide a better understanding of the metabolic pathways and should therefore be a focus in future projects.

Nutrient management is another critical research topic with cost reduction potential. That a reduction of the nutrient stock solution to half of the amount is possible without affecting the methanation performance was already demonstrated during the operation of the pilot-scale reactor. Nutrient management can be performed more target-oriented by identifying the essential nutrients and the optimal concentrations depending on the biocenosis in biological reactors. To substitute a fraction of the required nutrients, available byproducts from WWTPs, agriculture biogas plants, or biowaste plants can be a cost-effective alternative for mixed culture systems, particularly when onsite products at the methanation plant location can be used. This also accounts for  $\text{H}_2\text{S}$  in biogas that is expected to cover at least a fraction of the methanogenic sulfur demand while final  $\text{H}_2\text{S}$

concentrations are reduced. Testing biogas with much higher H<sub>2</sub>S concentrations than the 200 ppm in the pilot-scale study can give more clear and distinguishable results.

An approach to reduce the nutrient substitution requirement is to remove or separate the metabolic water from the process liquid while retaining nutrients, microorganisms, and other compounds in the reactor, which can be performed by applying a membrane module. The metabolic water production in laboratory-scale TBRs is relatively low, challenging the membrane filtration process and providing only limited conclusions for industrial application. Thus, integrating a membrane module into the infrastructure of the pilot reactor is expected to provide more practical results. If the extracted water meets the specific requirements for water electrolysis, it can be recycled back to the electrolyzer unit. With a water requirement of about 0.8 L per m<sup>3</sup> H<sub>2</sub> [29] and metabolic water production of 0.4 L per m<sup>3</sup> of H<sub>2</sub>, a substantial amount of metabolic water could be used for the electrolyzer water demand, even if slightly higher electrolyzer water requirements and losses of metabolically produced water are expected. Nevertheless, the costs and energy requirements for metabolic water purification must be compared with those for tap water, which needs less purification. In addition to H<sub>2</sub>, electrolysis produces O<sub>2</sub> and heat, which can be applied onsite or sold to other industries, improving the economic viability of the Power-to-Gas system. Per m<sup>3</sup> of H<sub>2</sub>, 0.5 m<sup>3</sup> of O<sub>2</sub> is generated, which can be applied in aeration tanks and added to combined heat and power plants to increase efficiency or sold to other sectors, e.g., for healthcare or industrial operations.

A major advantage of biological reactors compared to catalytic methanation is the ability of a flexible and dynamic operation on demand when unused renewable electricity is available to generate H<sub>2</sub>. A few studies already researched the restart performance after different standby periods, identifying strategies for an improved restart as quickly as possible [34, 70, 94]. Next to temperature reductions that typically require energy-intensive cooling and corresponding heating, inactivation of methanogens during standbys can probably be achieved by artificially lowering or increasing the pH level in the process liquid. This can be done by adding an acidic or alkaline solution directly to the process liquid or by injecting only biogas or CO<sub>2</sub> into the reactor. During the restart phase, the process liquid can be exchanged with fresh liquid to regain the initial pH level. While there is still room for improving the restart performance after different standby periods, the first step should be the dynamic operation with the established restart strategies on a pilot scale. Furthermore, the influence of the dynamic operation on biocenosis and on the methanogens' decay rate are important research topics.

H<sub>2</sub> storage tanks can be applied to reduce or even avoid the dynamic operation of TBRs. Furthermore, smaller TBR sizes are expected, which could compensate for the costs of an H<sub>2</sub> storage tank. Comparing the costs for an H<sub>2</sub> storage tank combined with a

possibly more stable and efficient reactor operation with the dynamic operation of TBRs is an interesting aspect for future investigations.

As the biological methanation in TBRs is still in development, proof of the reactor concept must be boarded in industrial-scale projects. A factor in the techno-economic feasibility of Power-to-CH<sub>4</sub> systems is the coupling of the electrolyzer unit with the methanation reactor. Due to the ability to operate at a broad power input and fast restart performance after standbys, PEM electrolysis is probably the most promising electrolysis technology [19]. Capital cost for PEM electrolysis is predicted to decrease in the range of alkaline electrolysis costs, which will further promote the PEM technology. Only Jønson et al. [44] have installed an electrolyzer in the TBR system and researched the methanation performance with the generated H<sub>2</sub>. Integrating an electrolysis unit is the next necessary step for the pilot-scale TBR at the WWTP Garching. Important application aspects, such as the installation on an explosion protection area, electrolyzer water quality requirement, and electrolyzer dynamic operation ability, will provide more information for the techno-economic assessment. Overall, more upscaling projects under real application conditions are required to assess the suitability of TBRs as energy conversion and storage technology.

## 9. Appendix

### 9.1 List of publications

#### **Research articles (peer-reviewed)**

1. Feickert Fenske, Carolina; Md, Yasin; Strübing, Dietmar; Koch, Konrad (2023): Preliminary gas flow experiments identify improved gas flow conditions in a pilot-scale trickle bed reactor for H<sub>2</sub> and CO<sub>2</sub> biological methanation. In *Bioresource Technology* 371, p. 128648. DOI: <https://doi.org/10.1016/j.biortech.2023.128648>

This publication is included in Chapter 4.

2. Feickert Fenske, Carolina; Kirzeder, Franz; Strübing, Dietmar; Koch, Konrad (2023): Biogas upgrading in a pilot-scale trickle bed reactor – Long-term biological methanation under real application conditions. *Bioresource Technology* 376, p. 128868. DOI: <https://doi.org/10.1016/j.biortech.2023.128868>

This publication is included in Chapter 5.

3. Feickert Fenske, Carolina; Strübing, Dietmar; Koch, Konrad (2023): Biological methanation in trickle bed reactors - A critical review. *Bioresource Technology* 385, p. 129383. DOI: <https://doi.org/10.1016/j.biortech.2023.129383>

This publication is included in Chapter 6.

#### **Further research contributions**

##### **Conference talks**

1. Feickert Fenske, Carolina; Koch, Konrad (2023): 'Biogas upgrading in a pilot-scale trickle bed reactor' at 6th CMP International Conference on Monitoring and Control of Anaerobic Digestion Processes in Leipzig, Germany, 22.03.2023

##### **Conference posters**

1. Feickert Fenske, Carolina; Koch, Konrad (2022): 'Biogas upgrading by biological methanation in a pilot-scale trickle bed reactor with 0.8 m<sup>3</sup> reaction volume' 17th CMP International Conference on Anaerobic Digestion in Ann Arbor, USA, 21.06.2022

## 9.2 List of supervised student theses

### Master theses

1. Fianelli, Francesco: 'Restart of a Thermophilic TBR and Optimization of Process Conditions', submitted 31.03.2021.
2. Güreli, Emine Nil: 'Biomethanation in a Trickle Bed Reactor: Comparison of CO<sub>2</sub> Sources with an Evaluation of Sulfur Source Effects', submitted 11.07.2022.
3. Heimann, Amelie: 'Wirtschaftlichkeitsanalyse einer Power-to-Gas Anlage in Deutschland', submitted 04.01.2023.
4. Kart, Ömer: 'Biomethanation in a Trickle Bed Reactor: Configuration and Optimization of a Measurement and Control System for a Biological Power-to-Gas System', submitted 01.09.2021.
5. Kirzeder, Franz: 'Biogas Upgrading in Trickle Bed Reactors with Biological Methanation – Investigation and Challenges of a Long-term Operation at Real Application Conditions', submitted 31.01.2023.
6. Kugler, Dominik: 'Effects of Trickling Intermision and Acidification on the Operation of Anaerobic Thermophilic Trickle Bed Reactors', submitted 30.11.2022.
7. Majiya, Baba Mohammed: 'Comparison of the Performance of Biocarriers in Anaerobic Trickle Bed Reactors', submitted 16.02.2021.
8. Md, Yasin: 'Improved Gas Flow Conditions in an Anaerobic Trickle Bed Reactor in a Co-Current Configuration', submitted 16.12.2021.
9. Prasad, Meenakshi: 'Selection of a Suitable Membrane for the Elimination of Metabolically Produced Water in Trickle Bed Reactors – A Techno-economical Assessment', submitted 23.09.2022.
10. Straub, Julian: 'Applying a nanofiltration membrane to reject metabolically produced water of a trickle bed reactor', submitted 04.04.2023.

### Study projects

1. Fianelli, Francesco: 'DemoMeth: Gas Utilization Proposal Reactors', submitted 31.08.2020.
2. Heimann, Amelie: 'Design Approaches to Integrate a Membrane System for Metabolic Water Removal in Biomethanation Reactors', submitted 04.01.2023.
3. Irshad, Umar: 'Nutrient Requirement and Microbial Biocenosis in Anaerobic Trickle Bed Reactors', submitted 25.05.2021.
4. Kirzeder, Franz: 'Übersicht der Aufbau- und Betriebsparameter von Rieselbettreaktoren für die biologische Methanisierung', submitted 27.07.2022.
5. Md, Yasin: 'Gas Flow Condition in the Trickling Bed Reactor', submitted 18.04.2021.

### Bachelor theses

1. Nägele, Gregori: 'Vergleich der Prozesse der konventionellen Biogasaufbereitung mit der biologischen Methanisierung', submitted 25.04.2020.
2. Pena Islas, Maria Fernanda: 'Comparison of biogas upgrading in ex-situ biological methanation reactors', submitted 07.11.2021.

### 9.3 Supplementary information for Chapter 4

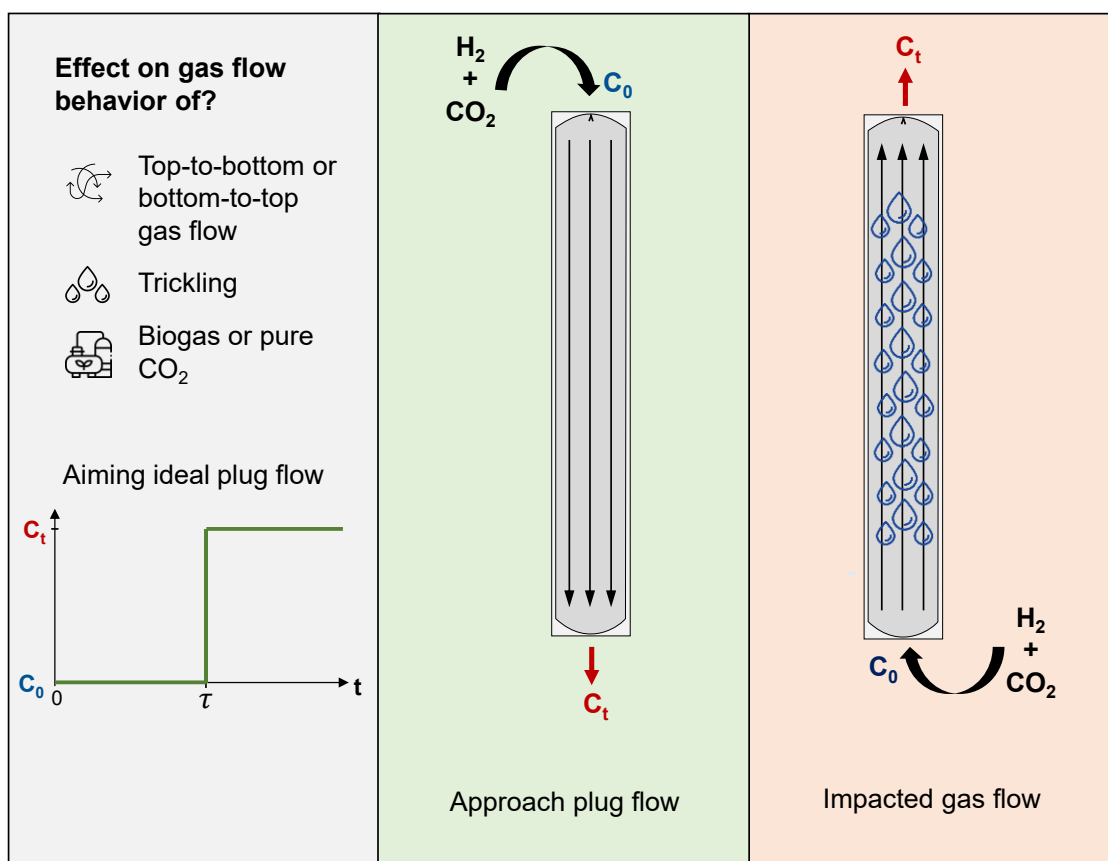


**Figure 9-1:** Graphical abstract Paper I (Preliminary gas flow experiments identify improved gas flow conditions in a pilot-scale trickle bed reactor for  $\text{H}_2$  and  $\text{CO}_2$  biological methanation).

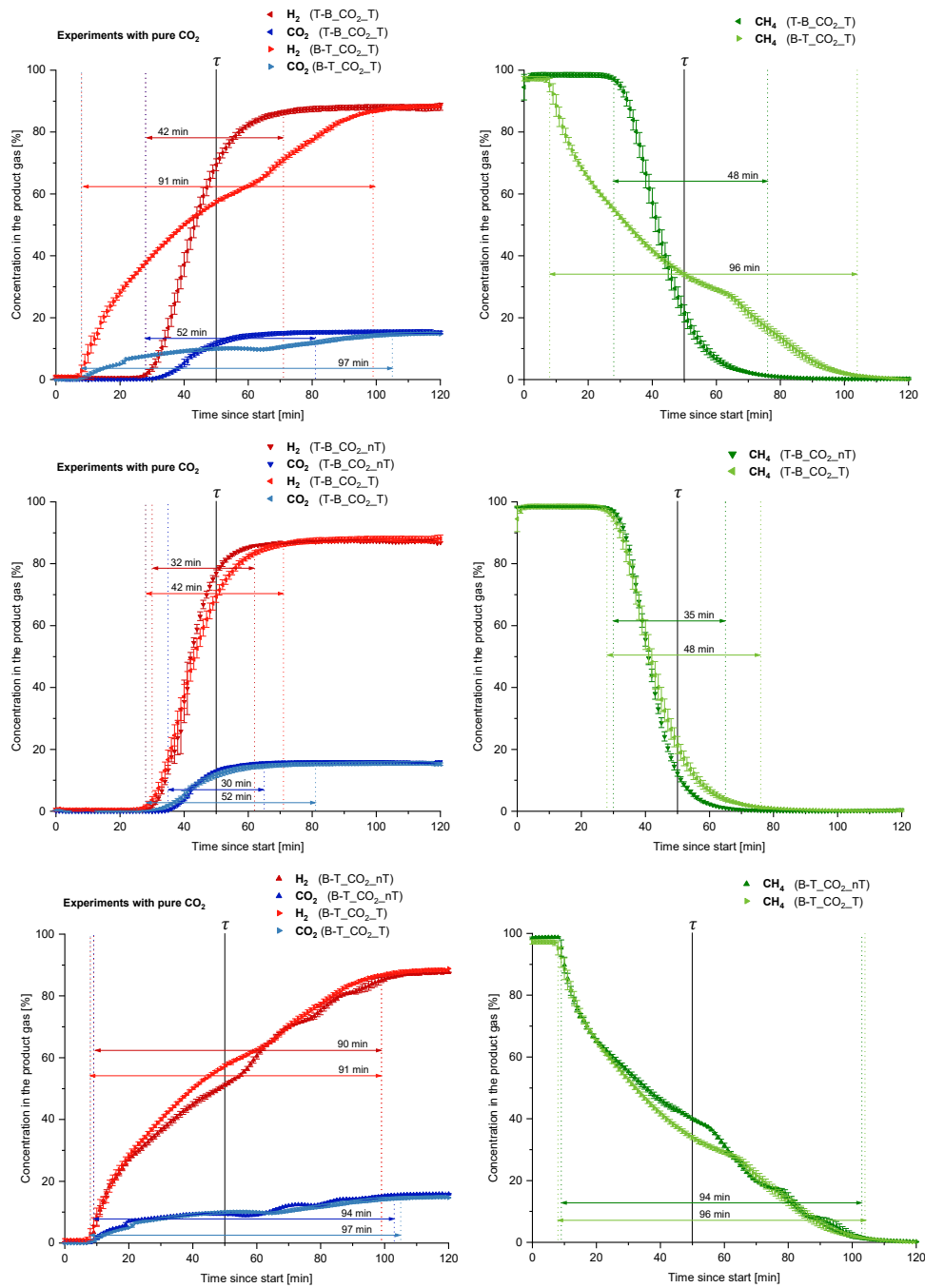


**Figure 9-2:** Curve progression of H<sub>2</sub>, CO<sub>2</sub> and CH<sub>4</sub> (mean  $\pm$  standard deviation) of the pure CO<sub>2</sub> experiments and trickling (A), in the top-to-bottom gas flow configuration (B) and in the bottom-to-top gas flow configuration (C).



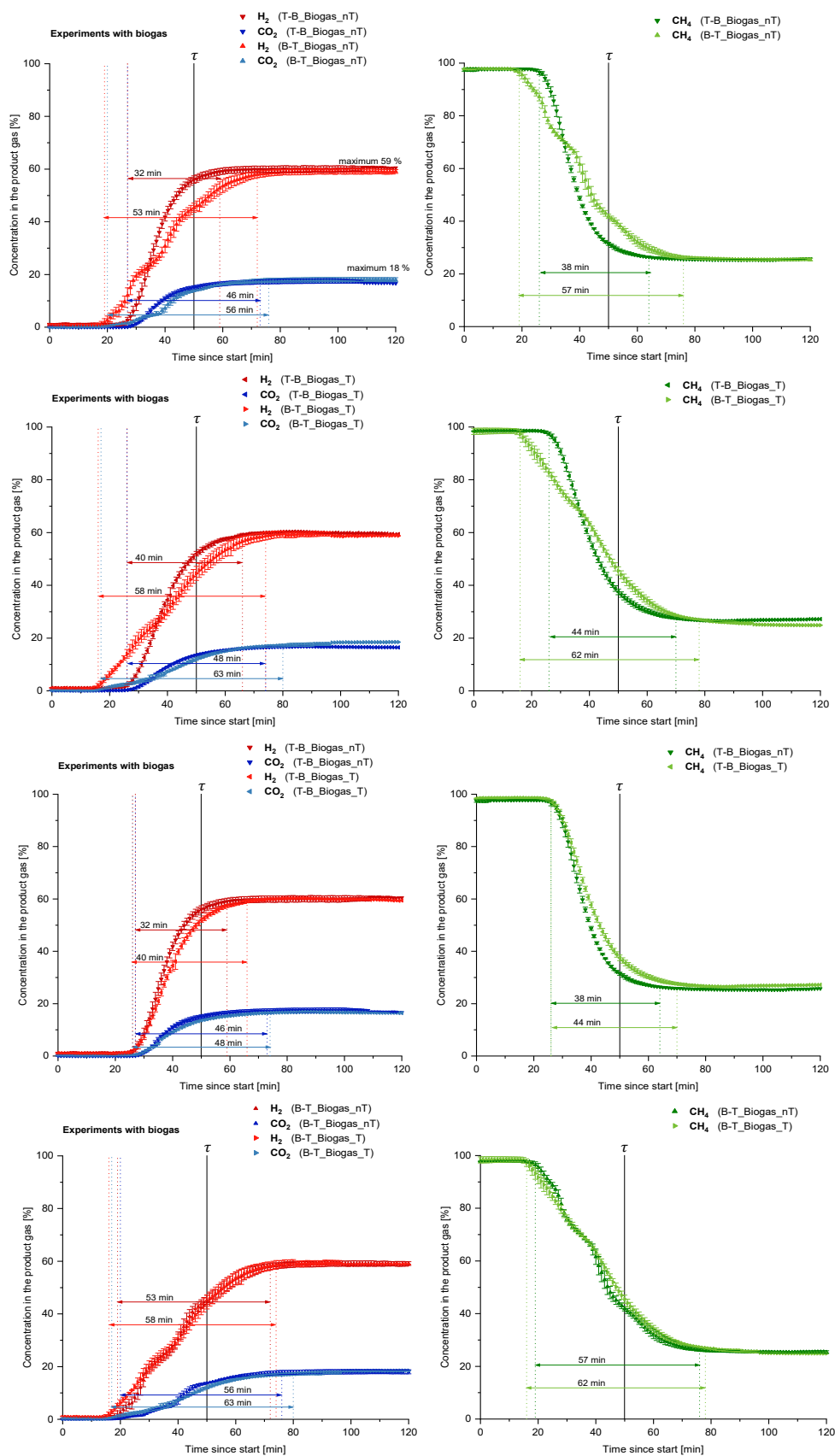


**Figure 9-3:** Curve progression of H<sub>2</sub>, CO<sub>2</sub> and CH<sub>4</sub> (mean ± standard deviation) of the biogas experiments without trickling (A), with trickling (B), in the top-to-bottom gas flow configuration (C) and in the bottom-to-top gas flow configuration (D).

**Table 9-1:** Test of significance by a one-way ANOVA with post-hoc Tukey HSD of the CO<sub>2</sub> slope lengths for pure CO<sub>2</sub> (above) and biogas as CO<sub>2</sub> source (below) at a significance level of 5% and 1%, respectively.

	T-B_CO <sub>2</sub> _nT	B-T_CO <sub>2</sub> _nT	T-B_CO <sub>2</sub> _T	B-T_CO <sub>2</sub> _T
T-B_CO <sub>2</sub> _nT		0.001 **	0.001 **	0.001 **
B-T_CO <sub>2</sub> _nT			0.001 **	0.663
T-B_CO <sub>2</sub> _T				0.001 **

	T-B_Biogas_nT	B-T_Biogas_nT	T-B_Biogas_T	B-T_Biogas_T
T-B_Biogas_nT		0.149	0.900	0.013 *
B-T_Biogas_nT			0.274	0.364
T-B_Biogas_T				0.025 *

p>0.05      insignificant  
 \* p<0.05      significant  
 \*\* p<0.01      highly significant

**Table 9-2:** Test of significance by a one-way ANOVA with post-hoc Tukey HSD of the CH<sub>4</sub> slope lengths for pure CO<sub>2</sub> (above) and biogas as CO<sub>2</sub> source (below) at a significance level of 5% and 1%, respectively.

	T-B_CO <sub>2</sub> _nT	B-T_CO <sub>2</sub> _nT	T-B_CO <sub>2</sub> _T	B-T_CO <sub>2</sub> _T
T-B_CO <sub>2</sub> _nT		0.001 **	0.001 **	0.001 **
B-T_CO <sub>2</sub> _nT			0.001 **	0.599
T-B_CO <sub>2</sub> _T				0.001 **

	T-B_Biogas_nT	B-T_Biogas_nT	T-B_Biogas_T	B-T_Biogas_T
T-B_Biogas_nT		0.009 **	0.534	0.002 *
B-T_Biogas_nT			0.056	0.618
T-B_Biogas_T				0.011 *

p>0.05      insignificant  
 \* p<0.05      significant  
 \*\* p<0.01      highly significant

## 9.4 Supplementary information for Chapter 5

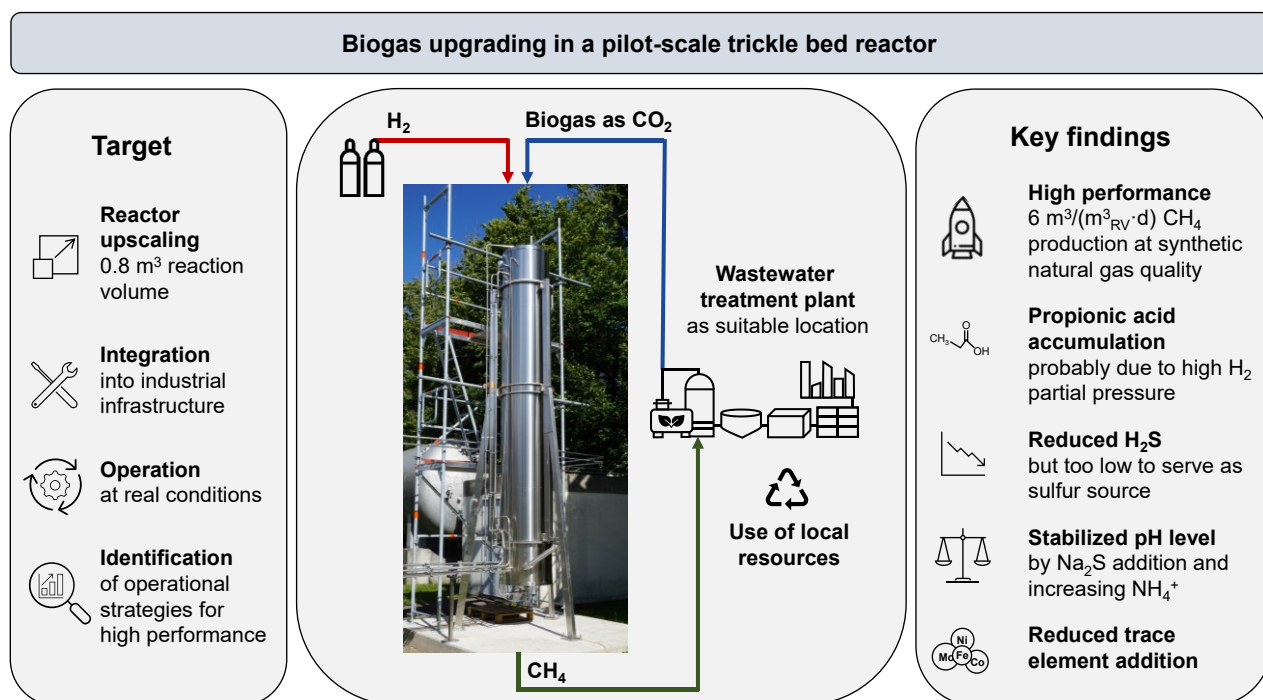


**Figure 9-4:** Graphical abstract Paper II (Biogas upgrading in a pilot-scale trickle bed reactor – Long-term biological methanation under real application conditions).



**Figure 9-5:** Sampling of the biofilm carrier from the bottom of the packing bed (left) and from the top (right) after 447 days.

## 9.5 Supplementary information for Chapter 6



**Figure 9-6:** Graphical abstract Paper III (Biological methanation in trickle bed reactors - A critical review).

## References

- [1] European Commission. Commission presents Renewable Energy Directive revision 2021. [https://commission.europa.eu/news/commission-presents-renewable-energy-directive-revision-2021-07-14\\_en](https://commission.europa.eu/news/commission-presents-renewable-energy-directive-revision-2021-07-14_en).
- [2] German Gas and Water Association (DVGW). Gasnetz als Speicher für grünes Gas. Speicherwunder Erdgasnetz. 2020. <https://www.dvgw.de/blog/gas/das-gasnetz-infrastruktur-fuer-erneuerbare-energien>.
- [3] Schaaf T, Grünig J, Schuster MR, Rothenfluh T, Orth A. Methanation of CO<sub>2</sub> - storage of renewable energy in a gas distribution system. *Energy, Sustainability and Society* 2014. <https://doi.org/10.1186/s13705-014-0029-1>.
- [4] Thema M, Weidlich T, Hörl M, Bellack A, Mörs F, Hackl F, Kohlmayer M, Gleich J, Stabenau C, Trabold T, Neubert M, Ortloff F, Brotsack R, Schmack D, Huber H, Hafenbradl D, Karl J, Sterner M. Biological CO<sub>2</sub>-methanation: An approach to standardization. *Energies* 2019;12(9):1670. <https://doi.org/10.3390/en12091670>.
- [5] European Commission. European Commission - Questions and answers Questions and Answers on the new EU rules on gas storage 2022. [https://ec.europa.eu/commission/presscorner/detail/en/qanda\\_22\\_1937](https://ec.europa.eu/commission/presscorner/detail/en/qanda_22_1937).
- [6] Rönsch S, Schneider J, Matthischke S, Schlüter M, Götz M, Lefebvre J, Prabhakaran P, Bajohr S. Review on methanation – From fundamentals to current projects. *Fuel* 2016;166:276–296. <https://doi.org/10.1016/j.fuel.2015.10.111>.
- [7] Ullrich T, Lindner J, Bär K, Mörs F, Graf F, Lemmer A. Influence of operating pressure on the biological hydrogen methanation in trickle-bed reactors. *Bioresource Technology* 2018;247:7–13. <https://doi.org/10.1016/j.biortech.2017.09.069>.
- [8] Paniagua S, Lebrero R, Muñoz R. Syngas biomethanation: Current state and future perspectives. *Bioresource Technology* 2022;358:127436. <https://doi.org/10.1016/j.biortech.2022.127436>.
- [9] Rittmann SK-MR. A critical assessment of microbiological biogas to biomethane upgrading systems. *Advances in Biochemical Engineering/Biotechnology* 2015;151:117–135. [https://doi.org/10.1007/978-3-319-21993-6\\_5](https://doi.org/10.1007/978-3-319-21993-6_5).
- [10] Ghaib K, Ben-Fares F-Z. Power-to-Methane: A state-of-the-art review. *Renewable and Sustainable Energy Reviews* 2018;81:433–446. <https://doi.org/10.1016/j.rser.2017.08.004>.
- [11] Strübing D, Huber B, Lebuhn M, Drewes JE, Koch K. High performance biological methanation in a thermophilic anaerobic trickle bed reactor. *Bioresource Technology* 2017;245:1176–1183. <https://doi.org/10.1016/j.biortech.2017.08.088>.
- [12] Burkhardt M, Busch G. Methanation of hydrogen and carbon dioxide. *Applied Energy* 2013;111:74–79. <https://doi.org/10.1016/j.apenergy.2013.04.080>.
- [13] REN21. Renewable energy data in perspective 2022. [https://www.ren21.net/wp-content/uploads/2019/05/GSR2022\\_Key\\_Messages.pdf](https://www.ren21.net/wp-content/uploads/2019/05/GSR2022_Key_Messages.pdf).
- [14] International Energy Agency (IEA). World Energy Outlook 2020 2020. <https://www.iea.org/reports/world-energy-outlook-2020>.

- [15] German Federal Network Agency. Monitoring Report 2018 – Key Findings 2018. [www.bundesnetzagentur.de/SharedDocs/Downloads/EN/Areas/ElectricityGas/Collection Company](http://www.bundesnetzagentur.de/SharedDocs/Downloads/EN/Areas/ElectricityGas/CollectionCompany).
- [16] International Energy Agency (IEA). Grid-Scale Storage 2022. <https://www.iea.org/reports/grid-scale-storage>.
- [17] International Energy Agency (IEA). Pumped storage hydropower storage capability by countries, 2020-2026 2022. <https://www.iea.org/data-and-statistics/charts/pumped-storage-hydropower-storage-capability-by-countries-2020-2026>.
- [18] Götz M, Lefebvre J, Mörs F, McDaniel Koch A, Graf F, Bajohr S, Reimert R, Kolb T. Renewable Power-to-Gas: A technological and economic review. *Renewable Energy* 2016;85:1371–1390. <https://doi.org/10.1016/j.renene.2015.07.066>.
- [19] Rego de Vasconcelos B, Lavoie J-M. Recent Advances in Power-to-X Technology for the Production of Fuels and Chemicals. *Frontiers in Chemistry* 2019;7:392. <https://doi.org/10.3389/fchem.2019.00392>.
- [20] Dieterich V, Buttler A, Hanel A, Spliethoff H, Fendt S. Power-to-liquid via synthesis of methanol, DME or Fischer–Tropsch-fuels: a review. *Energy & Environmental Science* 2020;13(10):3207–3252. <https://doi.org/10.1039/D0EE01187H>.
- [21] International Energy Agency (IEA). The Future of Hydrogen: Seizing today’s opportunities 2019. <https://www.iea.org/reports/the-future-of-hydrogen>.
- [22] Buttler A, Spliethoff H. Current status of water electrolysis for energy storage, grid balancing and sector coupling via power-to-gas and power-to-liquids: A review. *Renewable and Sustainable Energy Reviews* 2018;82:2440–2454. <https://doi.org/10.1016/j.rser.2017.09.003>.
- [23] Dahiru AR, Vuokila A, Huuhtanen M. Recent development in Power-to-X: Part I - A review on techno-economic analysis. *Journal of Energy Storage* 2022;56:105861. <https://doi.org/10.1016/j.est.2022.105861>.
- [24] Nechache A, Hody S. Alternative and innovative solid oxide electrolysis cell materials: A short review. *Renewable and Sustainable Energy Reviews* 2021;149:111322. <https://doi.org/10.1016/j.rser.2021.111322>.
- [25] Borge-Diez D, Rosales-Asensio E, Açikkalp E, Alonso-Martínez D. Analysis of Power to Gas Technologies for Energy Intensive Industries in European Union. *Energies* 2023;16(1):538. <https://doi.org/10.3390/en16010538>.
- [26] Olshausen Cvon. Sunfire - liquid hydrocarbonates from CO<sub>2</sub> and H<sub>2</sub>O and renewable energy. 2015.
- [27] Thema M, Bauer F, Sterner M. Power-to-Gas: Electrolysis and methanation status review. *Renewable and Sustainable Energy Reviews* 2019;112:775–787. <https://doi.org/10.1016/j.rser.2019.06.030>.
- [28] David M, Ocampo-Martínez C, Sánchez-Peña R. Advances in alkaline water electrolyzers: A review. *Journal of Energy Storage* 2019;23:392–403. <https://doi.org/10.1016/j.est.2019.03.001>.
- [29] Shi X, Liao X, Li Y. Quantification of fresh water consumption and scarcity footprints of hydrogen from water electrolysis: A methodology framework. *Renewable Energy* 2020;154:786–796. <https://doi.org/10.1016/j.renene.2020.03.026>.

- [30] Becker H, Murawski J, Shinde DV, Stephens IEL, Hinds G, Smith G. Impact of impurities on water electrolysis: a review. *Sustainable Energy & Fuels* 2023;7(7):1565–1603. <https://doi.org/10.1039/D2SE01517J>.
- [31] Voitic G, Nestl S, Lammer M, Wagner J, Hacker V. Pressurized hydrogen production by fixed-bed chemical looping. *Applied Energy* 2015;157:399–407. <https://doi.org/10.1016/j.apenergy.2015.03.095>.
- [32] Barbaresi A, Morini M, Gambarotta A. Review on the Status of the Research on Power-to-Gas Experimental Activities. *Energies* 2022;15(16):5942. <https://doi.org/10.3390/en15165942>.
- [33] Dahiru AR, Vuokila A, Huuhtanen M. Recent development in Power-to-X: Part I - A review on techno-economic analysis. *Journal of Energy Storage* 2022;56:105861. <https://doi.org/10.1016/j.est.2022.105861>.
- [34] Strübing D, Moeller AB, Mößnang B, Lebuhn M, Drewes JE, Koch K. Anaerobic thermophilic trickle bed reactor as a promising technology for flexible and demand-oriented H<sub>2</sub>/CO<sub>2</sub> biomethanation. *Applied Energy* 2018;232:543–554. <https://doi.org/10.1016/j.apenergy.2018.09.225>.
- [35] Strübing D. H<sub>2</sub>/CO<sub>2</sub> biomethanation in anaerobic thermophilic trickle bed reactors: Development of a flexible and efficient energy conversion technology; PhD thesis, Technical University of Munich, 2020.
- [36] Logroño W, Kleinstaub S, Kretschmar J, Harnisch F, Vrieze J de, Nikolausz M. The microbiology of Power-to-X applications. *FEMS microbiology reviews* 2023. <https://doi.org/10.1093/femsre/fuad013>.
- [37] Jensen MB, Ottosen L, Kofoed M. H<sub>2</sub> gas-liquid mass transfer: A key element in biological Power-to-Gas methanation. *Renewable and Sustainable Energy Reviews* 2021;147:111209. <https://doi.org/10.1016/j.rser.2021.111209>.
- [38] Feickert Fenske C, Kirzeder F, Strübing D, Koch K. Biogas upgrading in a pilot-scale trickle bed reactor – Long-term biological methanation under real application conditions. *Bioresource Technology* 2023;376:128868. <https://doi.org/10.1016/j.biortech.2023.128868>.
- [39] Savvas S, Donnelly J, Patterson T, Chong ZS, Esteves SR. Biological methanation of CO<sub>2</sub> in a novel biofilm plug-flow reactor: A high rate and low parasitic energy process. *Applied Energy* 2017;202:238–247. <https://doi.org/10.1016/j.apenergy.2017.05.134>.
- [40] Lecker B, Illi L, Lemmer A, Oechsner H. Biological hydrogen methanation – A review. *Bioresource Technology* 2017;245:1220–1228. <https://doi.org/10.1016/j.biortech.2017.08.176>.
- [41] Kimmel DE, Klasson KT, Clausen EC, Gaddy JL. Performance of trickle-bed bioreactors for converting synthesis gas to methane. *Applied Biochemistry and Biotechnology* 1991;28/29:457–469. <https://doi.org/10.1007/BF02922625>.
- [42] Angelidaki I, Treu L, Tsapekos P, Luo G, Campanaro S, Wenzel H, Kougias P. Biogas upgrading and utilization: Current status and perspectives. *Biotechnology Advances* 2018;36(2):452–466. <https://doi.org/10.1016/j.biotechadv.2018.01.011>.
- [43] Nashmin Elyasi S, He L, Tsapekos P, Rafiee S, Khoshnevisan B, Carbajales-Dale M, Saeid Mohtasebi S, Liu H, Angelidaki I. Could biological biogas upgrading be a sustainable substitution for water scrubbing technology? A case study in Denmark. *Energy Conversion and Management* 2021;245:114550. <https://doi.org/10.1016/j.enconman.2021.114550>.

- [44] Jønson BD, Tsapekos P, Tahir Ashraf M, Jeppesen M, Ejbye Schmidt J, Bastidas-Oyanedel J-R. Pilot-scale study of biomethanation in biological trickle bed reactors converting impure CO<sub>2</sub> from a Full-scale biogas plant. *Bioresource Technology* 2022;365:128160. <https://doi.org/10.1016/j.biortech.2022.128160>.
- [45] Jensen MB, Poulsen S, Jensen B, Feilberg A, Kofoed MVW. Selecting carrier material for efficient biomethanation of industrial biogas-CO<sub>2</sub> in a trickle-bed reactor. *Journal of CO<sub>2</sub> Utilization* 2021;51:101611. <https://doi.org/10.1016/j.jcou.2021.101611>.
- [46] Liu Y, Beer LL, Whitman WB. Methanogens: a window into ancient sulfur metabolism. *Trends in Microbiology* 2012;20(5):251–258. <https://doi.org/10.1016/j.tim.2012.02.002>.
- [47] Federal Ministry of Food and Agriculture. Biogas 2022. <https://www.bmel.de/DE/themen/landwirtschaft/bioeconomie-nachwachsende-rohstoffe/biogas.html>.
- [48] Cummins Inc. Cummins-Enbridge project brings large-scale hydrogen blending to North America 2020. <https://www.cummins.com/news/2020/12/22/cummins-enbridge-project-brings-large-scale-hydrogen-blending-north-america>.
- [49] Cummins Inc. Enbridge Gas announces the launch of the first-of-its-kind hydrogen-blending project in North America 2022. <https://www.cummins.com/news/releases/2022/01/13/enbridge-gas-announces-launch-first-its-kind-hydrogen-blending-project>.
- [50] Air Liquide S.A. Inauguration of the world's largest PEM electrolyzer to produce decarbonized hydrogen 2021. <https://www.airliquide.com/stories/industry/inauguration-worlds-largest-pem-electrolyzer-produce-decarbonized-hydrogen>.
- [51] Air Liquide S.A. Air Liquide receives support from French State to its 200 MW electrolyzer project in Normandy and accelerates the development of the hydrogen sector in Europe 2022. <https://www.airliquide.com/group/press-releases-news/2022-03-08/air-liquide-receives-support-french-state-its-200-mw-electrolyzer-project-normandy-and-accelerates>.
- [52] Salzgitter AG. GrInHy2.0: Green Hydrogen for Green Steel 2022. <https://www.salzgitter-flachstahl.de/en/news/details/grinhy20-green-hydrogen-for-green-steel-20194.html>.
- [53] Zavarkó M, Imre AR, Pörzse G, Csedő Z. Past, Present and Near Future: An Overview of Closed, Running and Planned Biomethanation Facilities in Europe. *Energies* 2021. <https://doi.org/10.3390/en14185591>.
- [54] Limeco. Limeco Power-to-Gas Facility 2022. [https://www.powertogas.ch/wp-content/uploads/Limeco\\_Power-to-Gas-Factsheet\\_Englisch.pdf](https://www.powertogas.ch/wp-content/uploads/Limeco_Power-to-Gas-Factsheet_Englisch.pdf).
- [55] Bittante A, García-Serna J, Biasi P, Sobrón F, Salmi T. Residence time and axial dispersion of liquids in Trickle Bed Reactors at laboratory scale. *Chemical Engineering Journal* 2014;250:99–111. <https://doi.org/10.1016/j.cej.2014.03.062>.
- [56] Levenspiel O. *Tracer technology: Modeling the flow of fluids*. New York: Springer, 2014.
- [57] Rachbauer L, Voitl G, Bochmann G, Fuchs W. Biological biogas upgrading capacity of a hydrogenotrophic community in a trickle-bed reactor. *Applied Energy* 2016;180:483–490. <https://doi.org/10.1016/j.apenergy.2016.07.109>.
- [58] Burkhardt M, Jordan I, Heinrich S, Behrens J, Ziesche A, Busch G. Long term and demand-oriented biocatalytic synthesis of highly concentrated methane in a trickle bed reactor. *Applied Energy* 2019;240:818–826. <https://doi.org/10.1016/j.apenergy.2019.02.076>.



- [59] Thema M, Weidlich T, Kaul A, Böllmann A, Huber H, Bellack A, Karl J, Sterner M. Optimized biological CO<sub>2</sub>-methanation with a pure culture of thermophilic methanogenic archaea in a trickle-bed reactor. *Bioresource Technology* 2021;333:125135. <https://doi.org/10.1016/j.biortech.2021.125135>.
- [60] Burkhardt M, Koschack T, Busch G. Biocatalytic methanation of hydrogen and carbon dioxide in an anaerobic three-phase system. *Bioresource Technology* 2015;178:330–333. <https://doi.org/10.1016/j.biortech.2014.08.023>.
- [61] Sposob M, Wahid R, Fischer K. Ex-situ biological CO<sub>2</sub> methanation using trickle bed reactor: review and recent advances. *Reviews in Environmental Science and Bio/Technology* 2021;20(4):1087–1102. <https://doi.org/10.1007/s11157-021-09589-7>.
- [62] Dupnock TL, Deshusses MA. Detailed investigations of dissolved hydrogen and hydrogen mass transfer in a biotrickling filter for upgrading biogas. *Bioresource Technology* 2019;290:121780. <https://doi.org/10.1016/j.biortech.2019.121780>.
- [63] Dupnock TL, Deshusses MA. Biological Co-treatment of H<sub>2</sub>S and reduction of CO<sub>2</sub> to methane in an anoxic biological trickling filter upgrading biogas. *Chemosphere* 2020;256:127078. <https://doi.org/10.1016/j.chemosphere.2020.127078>.
- [64] Asimakopoulos K, Łężyk M, Grimalt-Alemany A, Melas A, Wen Z, Gavala HN, Skiadas IV. Temperature effects on syngas biomethanation performed in a trickle bed reactor. *Chemical Engineering Journal* 2020;393:124739. <https://doi.org/10.1016/j.cej.2020.124739>.
- [65] Tsapekos P, Treu L, Campanaro S, Centurion VB, Zhu X, Peprah M, Zhang Z, Kougias PG, Angelidaki I. Pilot-scale biomethanation in a trickle bed reactor: Process performance and microbiome functional reconstruction. *Energy Conversion and Management* 2021;244:114491. <https://doi.org/10.1016/j.enconman.2021.114491>.
- [66] Asimakopoulos K, Gavala HN, Skiadas IV. Biomethanation of Syngas by Enriched Mixed Anaerobic Consortia in Trickle Bed Reactors. *Waste and Biomass Valorization* 2020;11(2):495–512. <https://doi.org/10.1007/s12649-019-00649-2>.
- [67] Markthaler S, Plankenbühler T, Weidlich T, Neubert M, Karl J. Numerical simulation of trickle bed reactors for biological methanation. *Chemical Engineering Science* 2020;226:115847. <https://doi.org/10.1016/j.ces.2020.115847>.
- [68] Markthaler S, Plankenbühler T, Miederer J, Kolb S, Herkendell K, Karl J. Combined Two-Model CFD Simulation of Trickle Bed Reactors with Head-Sump Extension: Case Study on Hydrodynamics and Biological Methanation. *Industrial & Engineering Chemistry Research* 2022;61(11):4134–4152. <https://doi.org/10.1021/acs.iecr.1c04262>.
- [69] Dupnock TL, Deshusses MA. High-performance biogas upgrading using a biotrickling filter and hydrogenotrophic methanogens. *Applied Biochemistry and Biotechnology* 2017;183(2):488–502. <https://doi.org/10.1007/s12010-017-2569-2>.
- [70] Strübing D, Moeller AB, Mößnang B, Lebuhn M, Drewes JE, Koch K. Load change capability of an anaerobic thermophilic trickle bed reactor for dynamic H<sub>2</sub>/CO<sub>2</sub> biomethanation. *Bioresource Technology* 2019;289:121735. <https://doi.org/10.1016/j.biortech.2019.121735>.
- [71] Porté H, Kougias PG, Alfaro N, Treu L, Campanaro S, Angelidaki I. Process performance and microbial community structure in thermophilic trickling biofilter reactors for biogas upgrading. *Science of The Total Environment* 2019;655:529–538. <https://doi.org/10.1016/j.scitotenv.2018.11.289>.

- [72] Dupnock TL, Deshusses MA. Development and validation of a comprehensive model for biotrickling filters upgrading biogas. *Chemical Engineering Journal* 2021;407:126614. <https://doi.org/10.1016/j.cej.2020.126614>.
- [73] Tchobanoglous G, Burton FL, Tsuchihashi R, Stensel HD. *Wastewater Engineering: Treatment and Resource Recovery*. 4th ed. Boston: McGraw-Hill, 2013.
- [74] Ashraf MT, Yde L, Triolo JM, Wenzel H. Optimizing the dosing and trickling of nutrient media for thermophilic biomethanation in a biotrickling filter. *Biochemical Engineering Journal* 2021;176:108220. <https://doi.org/10.1016/j.bej.2021.108220>.
- [75] Ashraf MT, Sieborg MU, Yde L, Rhee C, Shin SG, Triolo JM. Biomethanation in a thermophilic biotrickling filter — pH control and lessons from long-term operation. *Bioresource Technology Reports* 2020;11:100525. <https://doi.org/10.1016/j.biteb.2020.100525>.
- [76] Jensen MB, Strübing D, Jonge N de, Nielsen JL, Ottosen LDM, Koch K, Kofoed MVW. Stick or leave - Pushing methanogens to biofilm formation for ex situ biomethanation. *Bioresource Technology* 2019;291:121784. <https://doi.org/10.1016/j.biortech.2019.121784>.
- [77] Veiga MC, Jain MK, Wu W, Hollingsworth RI, Zeikus JG. Composition and role of extracellular polymers in methanogenic granules. *Applied and Environmental Microbiology* 1997;63(2):403–407. <https://doi.org/10.1128/aem.63.2.403-407.1997>.
- [78] Jamali NS, Jahim JM, Isahak WNRW, Abdul PM. Particle size variations of activated carbon on biofilm formation in thermophilic biohydrogen production from palm oil mill effluent. *Energy Conversion and Management* 2017;141:354–366. <https://doi.org/10.1016/j.enconman.2016.09.067>.
- [79] Sander R. Compilation of Henry's law constants (version 5.0.0) for water as solvent. *Atmospheric Chemistry and Physics* 2023;23(19):10901–12440. <https://doi.org/10.5194/acp-23-10901-2023>.
- [80] Feickert Fenske C, Md Y, Strübing D, Koch K. Preliminary gas flow experiments identify improved gas flow conditions in a pilot-scale trickle bed reactor for H<sub>2</sub> and CO<sub>2</sub> biological methanation. *Bioresource Technology* 2023;371:128648. <https://doi.org/10.1016/j.biortech.2023.128648>.
- [81] Taubner R-S, Rittmann SK-MR. Method for Indirect Quantification of CH<sub>4</sub> Production via H<sub>2</sub>O Production Using Hydrogenotrophic Methanogens. *Frontiers in Microbiology* 2016;7:532. <https://doi.org/10.3389/fmicb.2016.00532>.
- [82] Baird RB, Eaton AD, Rice EW, editors. *Standard methods for the examination of water and wastewater*. 23rd ed. Washington, DC: American Public Health Association, 2017.
- [83] Cheng G, Gabler F, Pizzul L, Olsson H, Nordberg Å, Schnürer A. Microbial community development during syngas methanation in a trickle bed reactor with various nutrient sources. *Biochemical Engineering Journal* 2022;106(13):5317–5333. <https://doi.org/10.1007/s00253-022-12035-5>.
- [84] Tsapekos P, Alvarado-Morales M, Angelidaki I. H<sub>2</sub> competition between homoacetogenic bacteria and methanogenic archaea during biomethanation from a combined experimental-modelling approach. *Journal of Environmental Chemical Engineering* 2022;10(2):107281. <https://doi.org/10.1016/j.jece.2022.107281>.

- [85] Sun M, Liu B, Yanagawa K, Ha NT, Goel R, Terashima M, Yasui H. Effects of low pH conditions on decay of methanogenic biomass. *Water Research* 2020;179:115883. <https://doi.org/10.1016/j.watres.2020.115883>.
- [86] Laguillaumie L, Rafrafi Y, Moya-Leclair E, Delagnes D, Dubos S, Spérandio M, Paul E, Dumas C. Stability of ex situ biological methanation of H<sub>2</sub>/CO<sub>2</sub> with a mixed microbial culture in a pilot scale bubble column reactor. *Bioresource Technology* 2022;354:127180. <https://doi.org/10.1016/j.biortech.2022.127180>.
- [87] Weißbach M, Thiel P, Drewes JE, Koch K. Nitrogen removal and intentional nitrous oxide production from reject water in a coupled nitrification/nitrous denitrification system under real feed-stream conditions. *Bioresource Technology* 2018;255:58–66. <https://doi.org/10.1016/j.biortech.2018.01.080>.
- [88] Inanc B, Matsui S, Ide S. Propionic acid accumulation and controlling factors in anaerobic treatment of carbohydrate: effects of H<sub>2</sub> and pH. *Water Science and Technology* 1996;34(5-6):317–325. <https://doi.org/10.2166/wst.1996.0566>.
- [89] Mulat DG, Mosbæk F, Ward AJ, Polag D, Greule M, Keppler F, Nielsen JL, Feilberg A. Exogenous addition of H<sub>2</sub> for an in situ biogas upgrading through biological reduction of carbon dioxide into methane. *Waste Management* 2017;68:146–156. <https://doi.org/10.1016/j.wasman.2017.05.054>.
- [90] Appels L, Baeyens J, Degreè J, Dewil R. Principles and potential of the anaerobic digestion of waste-activated sludge. *Progress in Energy and Combustion Science* 2008;34(6):755–781. <https://doi.org/10.1016/j.pecs.2008.06.002>.
- [91] Ripley LE, Boyle WC, Converse JC. Improved Alkalimetric Monitoring for Anaerobic Digestion of High-Strength Wastes. *Water Pollution Control Federation* 1986;58:406–411. <https://doi.org/10.2307/25042933>.
- [92] Kamravamanesh D, Rinta Kanto JM, Ali-Loytty H, Myllärinen A, Saalasti M, Rintala J, Kokko M. Ex-situ biological hydrogen methanation in trickle bed reactors: Integration into biogas production facilities. *Chemical Engineering Science* 2023;269:118498. <https://doi.org/10.1016/j.ces.2023.118498>.
- [93] Ghofrani-Isfahani P, Tsapekos P, Peprah M, Kougiass P, Zervas A, Zhu X, Yang Z, Jacobsen CS, Angelidaki I. Ex-situ biogas upgrading in thermophilic trickle bed reactors packed with micro-porous packing materials. *Chemosphere* 2022;296:133987. <https://doi.org/10.1016/j.chemosphere.2022.133987>.
- [94] Jønson B, Mortensen L, Schmidt J, Jeppesen M, Bastidas-Oyanedel J-R. Flexibility as the Key to Stability: Optimization of Temperature and Gas Feed during Downtime towards Effective Integration of Biomethanation in an Intermittent Energy System. *Energies* 2022;15(16):5827. <https://doi.org/10.3390/en15165827>.
- [95] Hadjipaschalis I, Poullikkas A, Efthimiou V. Overview of current and future energy storage technologies for electric power applications. *Renewable and Sustainable Energy Reviews* 2009;13(6-7):1513–1522. <https://doi.org/10.1016/j.rser.2008.09.028>.
- [96] Bailera M, Lisbona P, Romeo LM, Espatolero S. Power to Gas projects review: Lab, pilot and demo plants for storing renewable energy and CO<sub>2</sub>. *Renewable and Sustainable Energy Reviews* 2017;69:292–312. <https://doi.org/10.1016/j.rser.2016.11.130>.
- [97] Fendt S, Buttler A, Gaderer M, Spliethoff H. Comparison of synthetic natural gas production pathways for the storage of renewable energy. *Wiley Interdisciplinary Reviews: Energy and Environment* 2016;5(3):327–350. <https://doi.org/10.1002/wene.189>.

- [98] Sieborg MU, Jønson BD, Ashraf MT, Yde L, Triolo JM. Biomethanation in a thermophilic biotrickling filter using cattle manure as nutrient media. *Bioresource Technology Reports* 2020;9:100391. <https://doi.org/10.1016/j.biteb.2020.100391>.
- [99] Dahl Jønson B, Ujarak Sieborg M, Tahir Ashraf M, Yde L, Shin J, Shin SG, Mi Triolo J. Direct inoculation of a biotrickling filter for hydrogenotrophic methanogenesis. *Bioresource Technology* 2020;318:124098. <https://doi.org/10.1016/j.biortech.2020.124098>.
- [100] Aryal N, Odde M, Bøgeholdt Petersen C, Ditlev Mørck Ottosen L, Vedel Wegener Kofoed M. Methane production from syngas using a trickle-bed reactor setup. *Bioresource Technology* 2021;333:125183. <https://doi.org/10.1016/j.biortech.2021.125183>.
- [101] Ullrich T, Lemmer A. Performance enhancement of biological methanation with trickle bed reactors by liquid flow modulation. *GCB Bioenergy* 2019;11(1):63–71. <https://doi.org/10.1111/gcbb.12547>.
- [102] Tauber J, Möstl D, Vierheilig J, Saracevic E, Svardal K, Krampe J. Biological Methanation in an Anaerobic Biofilm Reactor—Trace Element and Mineral Requirements for Stable Operation. *Processes* 2023;11(4):1013. <https://doi.org/10.3390/pr11041013>.
- [103] Ebrahimian F, Bernardini N de, Tsapekos P, Treu L, Zhu X, Campanaro S, Karimi K, Angelidaki I. Effect of pressure on biomethanation process and spatial stratification of microbial communities in trickle bed reactors under decreasing gas retention time. *Bioresource Technology* 2022;361:127701. <https://doi.org/10.1016/j.biortech.2022.127701>.
- [104] Mauerhofer L-M, Zwirtnayr S, Pappenreiter P, Bernacchi S, Seifert AH, Reischl B, Schmider T, Taubner R-S, Paulik C, Rittmann SK-MR. Hyperthermophilic methanogenic archaea act as high-pressure CH<sub>4</sub> cell factories. *Communications Biology* 2021;4(1):289. <https://doi.org/10.1038/s42003-021-01828-5>.
- [105] Pan X, Zhao L, Li C, Angelidaki I, Lv N, Ning J, Cai G, Zhu G. Deep insights into the network of acetate metabolism in anaerobic digestion: focusing on syntrophic acetate oxidation and homoacetogenesis. *Water Research* 2021;190:116774. <https://doi.org/10.1016/j.watres.2020.116774>.
- [106] Angenent LT, Usack JG, Sun T, Fink C, Molitor B, Labatut R, Posmanik R, Hörl M, Hafenbradl D. Upgrading anaerobic digestion within the energy economy – the methane platform. In: Pikaar I, Guest J, Ganigué R, Jensen P, Rabaey K, Seviour T, et al., editors. *Resource Recovery from Water: IWA Publishing*, 2022. p. 141–158. [https://doi.org/10.2166/9781780409566\\_0141](https://doi.org/10.2166/9781780409566_0141).
- [107] Schill NA, Liu J-S, Stockar U von. Thermodynamic analysis of growth of *Methanobacterium thermoautotrophicum*. *Biotechnology and Bioengineering* 1999;64(1):74–81. [https://doi.org/10.1002/\(SICI\)1097-0290\(19990705\)64:1<74::AID-BIT8>3.0.CO;2-3](https://doi.org/10.1002/(SICI)1097-0290(19990705)64:1<74::AID-BIT8>3.0.CO;2-3).
- [108] Muñoz R, Meier L, Diaz I, Jeison D. A review on the state-of-the-art of physical/chemical and biological technologies for biogas upgrading. *Reviews in Environmental Science and Bio/Technology* 2015;14(4):727–759. <https://doi.org/10.1007/s11157-015-9379-1>.
- [109] Choi O, Kim M, Go Y, Hong M-G, Kim B, Shin Y, Lee S, Kim YG, Joo JS, Jeon BS, Sang B-I. Selective Removal of Water Generated during Hydrogenotrophic Methanation from Culture Medium Using Membrane Distillation. *Energies* 2019;12(21):4130. <https://doi.org/10.3390/en12214130>.

- [110] Weiland P. Biogas production: current state and perspectives. *Applied Microbiology and Biotechnology* 2010;85(4):849–860. <https://doi.org/10.1007/s00253-009-2246-7>.
- [111] Spirito CM, Richter H, Rabaey K, Stams AJM, Angenent LT. Chain elongation in anaerobic reactor microbiomes to recover resources from waste. *Current Opinion in Biotechnology* 2014;27:115–122. <https://doi.org/10.1016/j.copbio.2014.01.003>.
- [112] German Gas and Water Association (DVGW). DWA-M 361. 2022nd ed. Hennef, 2022.
- [113] Rittmann BE, McCarty PL. *Environmental Biotechnology: Principles and Applications*. New York, N.Y.: McGraw-Hill Education; McGraw Hill, 2018.
- [114] Hirano S, Matsumoto N, Morita M, Sasaki K, Ohmura N. Electrochemical control of redox potential affects methanogenesis of the hydrogenotrophic methanogen *Methanothermobacter thermoautotrophicus*. *Letters in Applied Microbiology* 2013;56(5):315–321. <https://doi.org/10.1111/lam.12059>.
- [115] Batstone DJ, Takacs I, Flores-Alsina X. Chemical oxidation and reduction. In: Batstone DJ, editor. *Generalised physicochemical model no. 1 (PCM1) for water and wastewater treatment*. London: IWA Publishing, 2022. p. 55–60. [https://doi.org/10.2166/9781780409832\\_0055](https://doi.org/10.2166/9781780409832_0055).
- [116] Chen B, Rupani PF, Azman S, Dewil R, Appels L. A redox-based strategy to enhance propionic and butyric acid production during anaerobic fermentation. *Bioresource Technology* 2022;361:127672. <https://doi.org/10.1016/j.biortech.2022.127672>.
- [117] Angelidaki I, Alves M, Bolzonella D, Borzacconi L, Campos JL, Guwy AJ, Kalyuzhnyi S, Jenicek P, van Lier JB. Defining the biomethane potential (BMP) of solid organic wastes and energy crops: a proposed protocol for batch assays. *Water Science and Technology* 2009;59(5):927–934. <https://doi.org/10.2166/wst.2009.040>.
- [118] Vintiloiu A, Boxriker M, Lemmer A, Oechsner H, Jungbluth T, Mathies E, Ramhold D. Effect of ethylenediaminetetraacetic acid (EDTA) on the bioavailability of trace elements during anaerobic digestion. *Chemical Engineering Journal* 2013;223:436–441. <https://doi.org/10.1016/j.cej.2013.02.104>.
- [119] Glass JB, Orphan VJ. Trace metal requirements for microbial enzymes involved in the production and consumption of methane and nitrous oxide. *Frontiers in Microbiology* 2012;3:61. <https://doi.org/10.3389/fmicb.2012.00061>.
- [120] Bellini R, Bassani I, Vizzarro A, Abdel Azim A, Vasile N, Pirri C, Verga F, Menin B. Biological Aspects, Advancements and Techno-Economical Evaluation of Biological Methanation for the Recycling and Valorization of CO<sub>2</sub>. *Energies* 2022;15(11):4064. <https://doi.org/10.3390/en15114064>.
- [121] Peillex J-P, Fardeau M-L, Belaich J-P. Growth of *Methanobacterium thermoautotrophicum* on H<sub>2</sub>CO<sub>2</sub>: High CH<sub>4</sub> productivities in continuous culture. *Biomass* 1990;21(4):315–321. [https://doi.org/10.1016/0144-4565\(90\)90080-4](https://doi.org/10.1016/0144-4565(90)90080-4).
- [122] Gantenbein A, Kröcher O, Biollaz SMA, Schildhauer TJ. Techno-Economic Evaluation of Biological and Fluidised-Bed Based Methanation Process Chains for Grid-Ready Biomethane Production. *Frontiers in Energy Research* 2022;9:775259. <https://doi.org/10.3389/fenrg.2021.775259>.